Investigating the molecular mechanisms involved in the developmental assembly of the mushroom body calyx in *Drosophila melanogaster*

Dissertation

zur

Erlangung des Doktorgrades (Dr. rer. nat.)

der

Mathematisch-Naturwissenschaftlichen Fakultät

der

Rheinischen Friedrich-Wilhelms-Universität Bonn

vorgelegt von

Komal B. Patil

aus

Mumbai, India

Bonn 2024

Angefertigt mit Genehmigung der Mathematisch-Naturwissenschaftlichen Fakultät

der Rheinischen Friedrich-Wilhelms-Universität Bonn

Gutachter/Betreuerin: Prof. Dr. Gaia Tavosanis

Gutachter: Prof. Dr. Dietmar Schmucker

Tag der Promotion: 22 January 2025

Erscheinungsjahr: 2025

TABLE OF CONTENTS

LIST OF FIGURES V

LIST OF TABLES VI

LIST OF ABBREVIATIONS VII

SUMMARY 1

1 INTRODUCTION 2

1.1 Neuronal wiring 2

1.2 Investigating wiring logic and synaptic specificity in non-stereotypical circuits 7

1.3 Mushroom body calyx: a non-stereotypical circuit 12

1.4 Developmental wiring of the calyx 14

1.5 PN – KC interactions in the adult calyx 17

1.6 Implication of CAMs in PN-KC synaptic matching 19

1.7 Role of Anaplastic lymphoma kinase (Alk) - Jelly-Belly (Jeb) signalling in *Drosophila* 20

2 AIMS OF THE THESIS 23

2.1 Determining whether KCs express unique cell surface markers that may help in KC-PN partner matching. 23

2.2 Investigating the role of differentially expressed CAMs in PN - KC wiring. 23

2.3 Exploring the role of Alk-Jeb signalling in the calyx. 24

2.4 Developing an *in vivo* longitudinal imaging method. 24

3 MATERIALS AND METHODS 25

3.1 Fly Husbandry 25

3.2 Reagents 27

3.3 Antibodies 27

3.4 Software 28

3.5 Lab equipment 29

3.6 Single cell RNA sequencing analysis 29
3.7 RNAi screen 30
3.8 Immunocytochemistry 30
3.9 Confocal imaging 30
3.10 3-Photon (3P) imaging 31
3.11 Image analysis 31
4 RESULTS 33
4.1 Transcriptomic analysis of pupal γKCs identifies differentially expressed CAMs 33
4.2 Investigation of role of candidate molecules in calyx wiring via pan-neuronal RNAi genetic screen 36
4.3 Effect of *alk* or *jeb* knockdown in the calyx 47
4.4 Expression and localization of Alk-Jeb 51
4.5 Interdependence of Alk and Jeb localization 55
4.6 Effect of Alk or Jeb loss on the cell viability 62
4.7 Development of an *in vivo* longitudinal imaging method of developing pupae 66
5 DISCUSSION 70
5.1 Investigating wiring logic of mushroom body calyx as a non-stereotypical circuit 70
5.2 Alk-Jeb signalling is implicated in KCs and PNs 72
5.3 Alk and Jeb localization in the calyx 73
5.4 Role of Alk-jeb signalling on neuronal health and survival 74
5.5 Development of an *in vivo* longitudinal imaging method of developing pupae 76
6 SUPPLEMENTARY INFORMATION 77
7 REFERENCES 84
ACKNOWLEDGEMENTS 118

List of Figures

Figure 1. Mechanisms that promote the establishment of synaptic specificity. 3
Figure 2. Olfactory system and information flow in *Drosophila*. 10
Figure 3. Mushroom body calyx and the microglomerulus. 12
Figure 4. Temporal specification of KCs and termination of MB-NBs during development. . 14
Figure 5. Maturation of PN and KC neurites in the calyx during pupal development. 17
Figure 6. Schematic of Alk and Jeb regulatory elements. 22
Figure 7. Mounting setup of intact pupa for 3P microscopy. 31
Figure 8. Volcano plot of differentially expressed cell surface molecules in γKCs. 34
Figure 9. Characterization of the fly line used to carry out pan-neuronal RNAi screen. 39
Figure 10. Phenotypes observed with respect to calyx and postsynaptic organization. 41
Figure 11. Phenotypes observed with respect to presynaptic bouton formation. 42
Figure 12. Change in number of boutons in response to knockdown of alk or jeb. 51
Figure 13. Localization of Alk and Jeb in the MB calyx. 52
Figure 14. Validation of anti-Alk Ab specificity in the calyx and AL. 53
Figure 15. : Validation of anti-Jeb Ab specificity in the calyx and AL. 54
Figure 16. Change in localization of Alk in response to presynaptic knockdown of *alk* or *jeb*. 56
Figure 17. Change in localization of Jeb in response to presynaptic knockdown of *alk* or *jeb*. 57
Figure 18. Change in localization of Alk in response to postsynaptic knockdown of *alk* or *jeb*. 59
Figure 19. Change in localization of Jeb in response to postsynaptic knockdown of *alk* or *jeb*. 60
Figure 20. Change in PN and KC cell numbers in response to knockdown of alk or jeb. 63
Figure 21. Change in cell number of VC3, VM5v, Dl2v PNs in response to knockdown of *alk* or *jeb*..... 65
Figure 22. In vivo imaging of pupal calyx development from immature neurites to mature MG structures. 69

List of Tables

Table 1. List of 215 molecule candidate resulting from the transcriptomic analysis. 36
Table 2. Molecules and their interaction partners shortlisted after phenotype analysis of the RNAi screen..... 43
Table 3. Qualitative summary of Alk or Jeb localization in calyx and AL in response to knockdown of *alk* or *jeb*..... 61
Table 4. Genotypes used for figures in the results section 77
Table 5. RNAi lines used in this study. 79

List of Abbreviations

αβ KC…….alpha beta Kenyon cells
α'β' KC….alpha prime beta prime Kenyon cells
γ KC…….gamma Kenyon cells
2P……2 Photon
3P……3 Photon
Ab……..Antibody
adPN……..antero-dorsal PN
Alk……..Anaplastic lymphoma kinase
AL……Antennal lobe
APF……...After puparium formation
APL……...Anterior paired lateral neuron
BDSC…...Bloomington drosophila stock centre
Brp……..Bruchpilot
CAM……Cell adhesion molecule
DN……...Dominant negative
EM……Electron microscopy
GMC……..Granule mother cell
GFP…….Green-fluorescent protein
HU……..Hydroxyurea
IgSF……Immunoglobulin superfamily
Jeb……..Jelly-Belly
KC……Kenyon cell
LDLa……..Low density lipoprotein class a
LH……Lateral horn
LexA……. ……DNA binding protein
LexAop……LexA DNA-binding sequence
lPN……Lateral PN
iALT……Inner antennal lobe tract
mALT……Medial antennal lobe tract
oALT……..……Outer antennal lobe tract
MB……..Mushroom body
MBC…….Mushroom body calyx
MG…….Microglomerulus
NB……Neuroblast
NLS……Nuclear localization sequence
Ole……....Octavolateralis efferent
ORN……..Olfactory receptor neuron
PBS……..Phosphate buffered saline
PF…….Puparium formation
PN……Projection neuron
PTK……Protein tyrosine kinase
RNA……...Ribonucleic acid
RNAi……Ribonucleic acid (RNA) interference
RTK…….Receptor tyrosine kinase
SCAPE.Swept confocally-aligned planar excitation
TF……..Transcription factor
TRiP…….Transgenic RNAi project
UAS……..Upstream activating sequence
VDRC……Vienna drosophila resource centre
vPN……..Ventral PN
VST……Variance stabilising transformation

Summary

How a circuit functions can be investigated by examining the organisation of the circuit to be able to decipher the connectivity logic and the logic of information flow within that circuit. Hence, to understand how the sparse coding of the Kenyon cells (KCs) is wired into the circuit, the organisational logic must be resolved. To that effect, a major question emerges - how do KCs find their synaptic partners during development?

This thesis aims to answer that question by taking advantage of available transcriptomic datasets (Alyagor et al., 2018; Li et al., 2020; Li et al., 2017; Xie et al., 2021) and focusing on the possible role of cell surface molecules in circuit assembly by means of RNAi-mediated knockdown in the PNs and KC. The effect of the knockdown was analysed by measuring number and distribution of PN boutons, calyx organisation and synapse formation. Based on this primary RNAi screen, candidate molecules that displayed circuit defects in the calyx were isolated and examined for the pattern of expression, the mutant phenotype and its cell autonomy in order to elucidate the role the molecules play in the development of the calyx. In addition, a method for *in vivo* imaging of the pupa was developed to be able to image developmental milestones in the context of normal development as well as mutants.

With this work, we hope to shed light in understanding how the non-stereotypical circuit of the calyx is assembled during development.

1 Introduction

1.1 Neuronal wiring

Developmental neuronal wiring is an incredibly elaborate process essential for establishing functional neural networks. Neurons navigate the complex milieu of the developing nervous system with the help of axon guidance and dendrite targeting cues to extend their axons and dendrites to the appropriate target regions (Araújo and Tear, 2003; Kolodkin and Tessier-Lavigne, 2011; Yogev and Shen, 2014). Having reached the target neuropil, the neurites then form synapses with their appropriate synaptic partners with cellular and sub-cellular specificity (Eichler et al., 2017; Gerhard et al., 2017; Jovanic et al., 2016; Lee et al., 2016), How this synaptic specificity is achieved is an interesting as well as complex question that became even more evident since recent 3D EM datasets have confirmed the intricacies of neuropiles packed with processes of neuronal and non-neuronal populations (Blockus and Polleux, 2021; Briggman and Bock, 2012; Scheffer and Meinertzhagen, 2019; Xu et al., 2020; Zheng et al., 2018).

Extensive research using model organisms such as *Caenorhabditis elegans*, *Drosophila melanogaster*, and *Mus musculus* has been pivotal in elucidating the mechanisms underlying neuronal wiring and synaptic specificity. These organisms have well characterized neuroanatomies, fully sequenced genomes, and a variety of genetic tools available that enable investigation of different aspects of circuit assembly (White et al., 1986; Eichler et al., 2017; Gerhard et al., 2017; Mark et al., 2021; Witvliet et al., 2021; Valdes-Aleman et al., 2021).Neuronal circuit assembly during development is a multistep process (Figure 1). Newly differentiated neurons grow and target the accurate neuropils while segregating their axons/dendrites into appropriate target regions. At the target regions, the axons/dendrites must navigate the synaptic partners present to make the correct connections/synapses via cell surface and/or secreted molecules. Synaptic connections may also be refined later with the help of neuronal activity patterns (Figure 1D). All of these steps are spatiotemporally controlled during development to acieve accurate circuit assembly. These key mechanisms are further elaborated below.

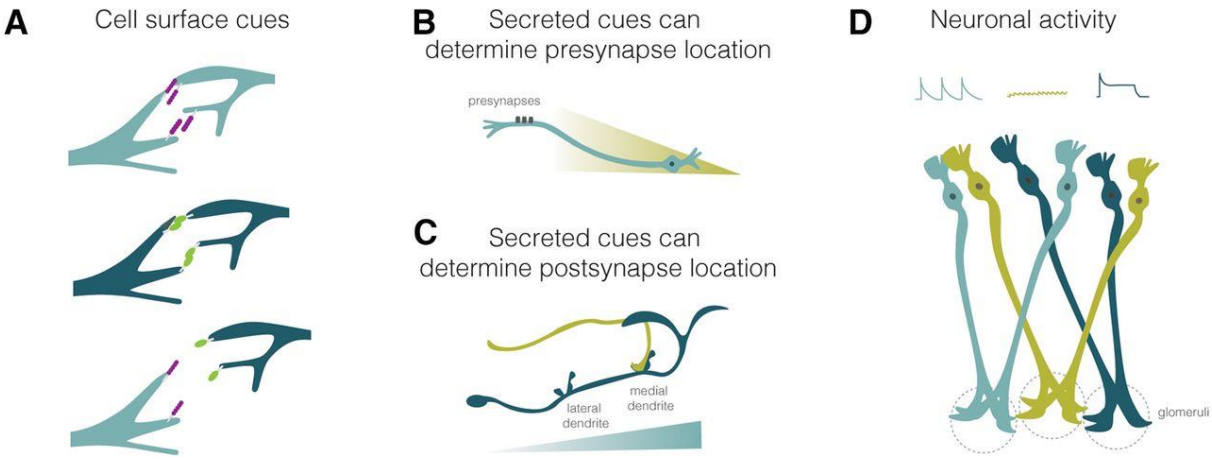

Figure 1. Mechanisms that promote the establishment of synaptic specificity.

(A) Cell surface cues can promote the proper matching of presynaptic and postsynaptic partners. (B) Secreted cues can specify the subcellular location of pre-synapses. (C) Secreted cues can specify the subcellular location of postsynaptic sites. (D) Patterns of spontaneous neuronal activity influence the organisation of olfactory sensory neurons into discrete glomeruli. Figure from Heckman and Doe, 2021.

1.1.1 Role of genetically encoded coordinates in synaptic specificity

Transcription factors (TF) and/or secreted molecules play a role in establishing the neuronal structure of a neuron, which in turn allows it to be located in proximity of its synaptic partner. The Lin B TF expressing leg motor neurons in *Drosophila* exhibits combinatorial transcriptional programs that specify unique dendritic and axonal morphologies (Enriquez et al., 2015). TFs have also been shown to regulate gene expression of molecules that regulate wiring, in turn determining synaptic specificity (Morey et al., 2008; Lie et al., 2018). In the *Drosophila* olfactory and visual systems, single cell RNA sequencing data suggests an important role of TFs in regulating neuronal diversity and driving expression of specific cell surface molecules to determine patterns of synaptic connectivity (Li et al., 2017; Kurmangaliyev et al., 2019).

Gradients of secreted molecules have been reported to organize neural connections into topological maps. The earliest reports were of the complimentary gradients of Eph kinases and their ligands, Ephrins, in the establishment of the retinotectal maps (Drescher et al., 1995; Cheng et al., 1995). Since then, axon guidance studies in

vertebrate and invertebrate systems have revealed more such molecules that form gradients along the neuronal growth path, helping in neuronal targeting. In *Drosophila*, Semaphorin1a gradients in the antennal lobe directs dendritic targeting of olfactory projection neurons (Komiyama et al., 2007). The Slit and Robo interaction in vertebrate and invertebrate models indicate a conserved role as repellent guidance cues for commissural axons away from the midline (Hummel et al., 1999; Kidd et al., 1999; Long et al., 2004; Hao et al., 2001; Sabatier et al., 2004). Conversely, the interaction of Netrin and Frazzled promotes midline crossing of dendrites in zebrafish octavolateralis efferent (OLe) neurons and in *Drosophila* motoneurons (Furrer et al., 2003; Ou et al., 2008).

It is interesting how these guidance cues can direct axon and dendrites of different neurons to distinct neuropil regions. There is some evidence that this may be achieved either by the temporal regulation of the expression of guidance cue and receptors during development or the differential localization of downstream signalling pathways (Godenschwege et al., 2002; Polleux et al., 2000).

1.1.2 Role of cell surface molecules in synaptic specificity

The chemoaffinity hypothesis put forth by Langley and Sperry posits that neurons exhibit unique molecular tags that allow them to recognize and be recognized by their synaptic partners (Figure 1A) (Langley, 1895; Sperry, 1963). Subsequently, many such molecules have been identified from a variety of model organisms and these molecules are broadly classified as cell adhesion molecules (CAMs). CAMs are generally transmembrane proteins that are involved in cell adhesion and local signalling via physical hetero- or homophilic interactions (Williams et al., 2010; de Wit and Ghosh, 2016). In *Drosophila*, postsynaptic dendrites of basin interneurons have been shown to perform extensive exploration for the presynaptic mechanosensory neuron axons and are able to find and synapse with each other even when present in aberrant location. (Valdes-Aleman et al., 2021). This indicates an important contribution of partner-derived cues in determining synaptic partner matching.

With the advent of high-throughput methods, comprehension of these molecules has vastly expanded. In *Drosophila*, an extracellular interactome of 202 CAMs was

generated, which included immunoglobulin superfamily (IgSF) proteins, leucine-rich repeat proteins, and proteins containing Fibronectin type III domains (Özkan et al., 2013). Despite the moniker, CAMs do not exclusively regulate cell adhesion but have also been implicated in different functions that include axon targeting, dendrite arborization, synaptogenesis, synapse maintenance, thereby determining not only cellular but also subcellular specificity (Huber et al., 2003; Kurusu et al., 2008; Barish et al., 2018; Sanes and Zipursky, 2020).

The implication of CAMs in diverse functions depending on the context of the cell type and its developmental stage, indicates a dynamic and complex regulation of expression and localization. How a neuron and its synaptic partner employ these molecules to be able to synapse with each other is essential to elucidate wiring mechanisms at a molecular resolution. Recent transcriptomic analysis of the projection neurons and olfactory receptor neurons in the *Drosophila* antennal lobe reveal temporally controlled expression of unique combinations of CAMs and TFs during circuit wiring (Xie et al., 2021; Wong et al., 2023). The *Drosophila* visual system circuit assembly in its different layers is also driven by the cell-type specific expression of specific CAMs to some extent (Plazaola-Sasieta et al., 2017). It is interesting how different CAMs regulate wiring mechanisms in the context of neurons as well as the circuits they comprise of.

1.1.3 Role of secreted molecules in subcellular synaptic specificity

In murine cortical and cerebellar circuits, excitatory neurons are innervated by different interneuron subtypes at specific subcellular locations indicating a role of subcellular specificity of synapses in circuit function (Favuzzi et al., 2019; Tai et al., 2019). Modelling studies analysing the function of such circuits suggest that subcellular specificity of synapses is vital for a number of processes that include regulation of action potential generation, integration of dendritic spiking, and also, coincidence detection (Hao et al., 2009; Pouille et al., 2013; Bloss et al., 2016; Wang et al., 2020). Diverse studies have been carried out in vertebrate as well as invertebrate model organisms in order to reveal the mechanisms that not only regulate but also establish subcellular synaptic targeting (Figure 1B,1C). In *Drosophila* ventral nerve cord, the

segmentally repeated A08a interneuron displays a medial and a lateral dendritic arbour and the presynaptic partners of this neuron selectively form synapses either with the medial or the lateral branch with the help of specific secreted axon guidance cues (Schneider-Mizell et al., 2016; Sales et al., 2019). In *C.elegans,* the Da9 neuron forms *en passant* synapses with dorsal muscles and motor neurons along the anterior-posterior axis in the tail, where secreted signals guide the clustering of presynaptic sites, and local inhibitory cues refine the connectivity (Colón-Ramos et al., 2007; Poon et al., 2008).

1.1.4 Role of neuronal activity in synaptic specificity

The Hebbian cell assembly theory suggests that neurons that are active together, preferentially synapse with each other (Hebb, 1949; McLaughlin et al., 2003). Developmental work in mice indicates a role of spontaneous neuronal activity patterns in expression of guidance molecules that regulate and direct the initial organisation of circuit connectivity in the olfactory bulb (Serizawa et al., 2006; Nakashima et al., 2019). The vertebrate visual system also displays spontaneous bursts of action potentials in individual retinal ganglion cells during development in a stimulus-independent manner (Masland, 1977). This developmental retinal activity pattern is required for organizing the visual pathway and circuits before the onset of visual stimulus (Welicky and Katz, 1999; Ackman and Crair, 2014; Arroyo and Feller, 2016). Recent work in the *Drosophila* visual system has revealed the presence of cell-type specific spontaneous neuronal activity patterns during synaptogenesis in pupal stages (Akin et al., 2019). Spontaneous patterned neural activity in *Drosophila* embryo also plays a crucial role in the larval mechanosensory circuit formation (Carreira-Rosario et al., 2022).

In addition to circuit development, neuronal activity is also implicated in the refinement and maintenance of circuits (Figure 1D). Mammalian studies indicate a role of stimulus-dependent sensory-evoked activity in the organisation and refinement of circuits within a defined critical period of development of the visual system (Shatz and Stryker, 1978; LeVay et al., 1980; McLaughlin et al., 2003). This is consistent with similar findings in *Drosophila* for circuits of the visual system and the mushroom body (Jarecki and Keshishian, 1995; Pech et al., 2015; Doll et al., 2017; Akin et al., 2019).

1.2 Investigating wiring logic and synaptic specificity in non-stereotypical circuits

To understand how different stimuli are processed by different circuits to produce distinct behaviours, it is important to understand how circuits are wired and assembled. The mechanisms regulating neuronal circuit wiring and establishment have been extensively studied across diverse model organisms with the help of stereotypic circuits such as the retinotectal circuit and olfactory bulb in mice, as well as the antennal and optic lobe circuits in flies (Fischbach and Hiesinger, 2008; Cho et al., 2009; Feldheim and O'Leary, 2010; Plazaola-Sasieta et al., 2017; Wong et al., 2023).

Stereotypical circuits are defined by their precise and consistent connectivity pattern across individuals. This provides an ideal framework to dissect the mechanisms driving circuit assembly within a species and also to compare how similar circuits across different species are wired (Feldheim and O'Leary, 2010; Yogev and Shen, 2014; Sanes and Yamagata, 2009; Sanes and Zipursky, 2020; Dunn and Wong, 2012). However, not all circuits exhibit such robust connectivity patterns. Some circuits display stochastic wiring that results in behavioural variability within a population (Linneweber et al., 2020). In the *Drosophila* visual system, the dorsal cluster neurons display non-heritable, inter-individual variation in right/left wiring asymmetry (Linneweber et al., 2020). Enhancing this wiring asymmetry led to an improvement in the individual's orientation towards visual objects, indicating that wiring asymmetry is an advantageous wiring decision (Linneweber et al., 2020).

Theoretical studies have suggested that random synaptic connections in cerebrocortical neurons enhance the ability of the neurons to make and learn associations (Hansel and van Vreeswijk, 2012, Rigotti et al., 2013, Barak et al., 2013, Babadi and Sompolinsky, 2014). This is also consistent with computational modelling of the synaptic connections of the mushroom body calyx in *Drosophila* (Litwin-Kumar et al., 2017). These findings indicate that the presence of some random connections in a circuit strengthen overall circuit function (Litwin-Kumar et al., 2017). How such non-stereotypical circuits are wired and what molecular mechanisms are implemented during circuit wiring has not been studied extensively.

1.2.1 Drosophila melanogaster as a model organism

Drosophila melanogaster is an exemplary model organism in the field of neuroscience since the 1960's when Seymour Benzer used the fruit fly in the field of neurogenetics to reveal that unique genetic loci regulated complex behavioural traits (Benzer, 1967; Quinn et al., 1974; Dudai et al., 1976). In the 1980s and 1990s, the genetic toolkit was expanded immensely to generate transgenic animals, transposon-mediated mutants, mosaic analysis, and tissue specific control of gene expression (Rubin and Spradling, 1982; Bellen et al., 1989; Golic and Lindquist, 1989; Fischer et al., 1988; Brand and Perrimon, 1993). In more recent years, fruit flies offer the possibility of labelling distinct neuronal populations and lineages, inducing specific genetic mutations, and the ability to knockdown, knockout or overexpress individual genes in virtually any neuronal population (Lee and Luo, 2001; Rong and Golic, 2000; Dietzl et al., 2007; Ni et al., 2008; Meltzer et al., 2019). Equipped with such a vast and powerful genetic toolset, EM datasets with synaptic resolution, and a fully sequenced and mapped genome, neuroscience research with *Drosophila* as a model has contributed immensely to diverse fields such as synaptic transmission, axon guidance, dendrite branching dynamics, circuit development, processing of visual or olfactory stimuli and associative learning and memory (Thomas and Wassarman, 1999; Davis, 2005; Schwarz, 2006; Fiala 2007; Dickson and Zou, 2010; Evans and Bashaw, 2010; Stürner et al., 2019; Zheng et al., 2018).

In addition, synaptic proteins in *Drosophila* bear >70% similarity to the corresponding synaptic proteins in mammalian systems, and 60% of mammalian proteins have a fruit fly ortholog (Littleton and Ganetzky, 2000; Littleton, 2000; Lloyd et al., 2000; Ugur et al., 2016). Across insects and vertebrates, studies have shown patterning mechanisms to be evolutionarily conserved at the genetic level and investigation of developmental mechanisms in insects have facilitated the discovery of similar mechanisms in vertebrates (Lichtneckert and Reichert, 2005; Pearson et al., 2005). Hence, the *Drosophila* brain with ~100,000 neurons as compared to the ~15 million neurons in mice and ~86 billion neurons in humans, offers a tractable model that is yet capable of complex brain wiring and behaviours (Zheng et al., 2018; Erö et al., 2018; Azevedo et al., 2009).

1.2.1.1 Olfactory system in Drosophila melanogaster

The olfactory nervous system of *Drosophila* shows significant homology in structure as well as function to the olfactory system in vertebrates (Davis, 2004; Ache and Young, 2005; Kaupp, 2010). In *Drosophila*, olfactory stimuli are important for carrying out basic functions like food detection and mating. The presence of odours is detected by sensilla, present on the antennae and the maxillary palps (Figure 2). The odour molecules are taken up and transported to olfactory receptors expressed by the dendritic branches of olfactory receptor neurons (ORNs) (Shanbhag et al., 2000). Each sensillium exhibits the presence of 2-4 ORNs but each ORN only expresses one distinct olfactory receptor type (Stocker, 1994).

In total ~1200 ORNs and ~50 distinct receptor types are expressed, such that one receptor type is expressed by ~10-100 ORNs (Vosshall et al., 2000; Couto et al., 2005). The ORNs extend their axons and transport odour information to the first odour processing centre called the antennal lobe (AL) (Figure 2, in red), where ORNs expressing the same receptor type project to the same distinct glomeruli (Vosshall and Stocker 2007). There are ~50 glomeruli in the antennal lobe and each glomerulus has a stereotypic position such that individual glomeruli can be identified across different flies (Laissue et al., 1999; Grabe et al., 2015).

In each glomerulus, the ORN axons arborize and form excitatory synapses with second order projection neurons (PNs). The PNs that innervate only one glomerulus are excitatory and are called uniglomerular PNs, and PNs that innervate multiple glomeruli are inhibitory and are called multiglomerular PNs (Stocker et al., 1990; Lai et al., 2008; Tanaka et al., 2012). In addition to PNs and ORNs, the AL also consists of a network of local interneurons which can either be glomerulus specific or capable of connecting multiple glomeruli together (Stocker et al., 1997; Seki et al., 2010).

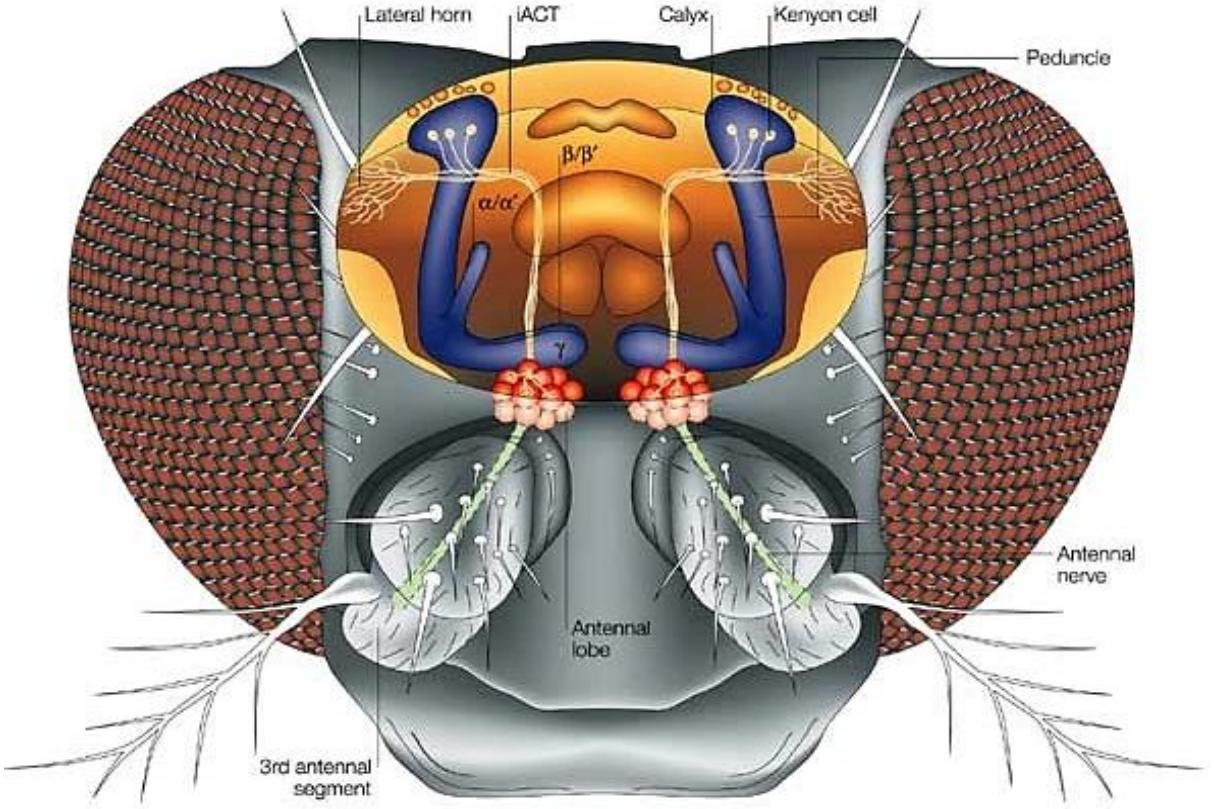

Figure 2. Olfactory system and information flow in *Drosophila*.

Olfactory information is taken up by olfactory receptor neurons located at the antenna and maxillary palp. Odour information is transferred along the antennal nerve (in green) towards the antennal lobe (in red), where it is relayed on to olfactory second order projection neurons. Projection neurons extend their axons via the iACT towards the lateral horn and the mushroom body calyx. The calyx is the dendritic input area of Kenyon Cells, which are tertiary neurons forming the mushroom body (shown in blue). Figure adapted from Heisenberg 2003.

The olfactory information is further transferred by the PNs from the AL to two higher order brain centres - the mushroom body (MB) (Figure 2, in blue) and the lateral horn (LH), via 3 major tracts (Figure 2). The inner antennal lobe tract (iALT) innervates the MB calyx and then the LH, the medial antennal lobe tract (mALT) innervates the LH predominantly but also has been shown to have some MB calyx projections, and lastly, the outer antennal lobe tract (oALT) consists of very few PNs that only project to the LH (Wong et al., 2002; Marin et al., 2002; Lin et al., 2013). The MB has been implicated in transforming olfactory sensory information into learned behavioural responses and the LH is associated with mediating innate behaviours (Heisenberg et al., 1985; Davis, 1993; Jefferis et al., 2007; Schultzhaus et al., 2017).

1.2.1.2 Mushroom body

Lesion and ablation experiments along with classical conditioning experimental paradigms in the 1990s indicated that the mushroom body is involved in olfactory associative learning and memory in *Drosophila* (Heisenberg et al., 1985; de Belle and Heisenberg, 1994; De Belle and Heisenberg, 1996; Crittenden et al., 1998; Tully and Quinn, 1985). More recent research has revealed evidence for sparse representation of olfactory responses and multimodal integration of sensory input in the MB (Honegger et al., 2011; Lin et al., 2014; Vogt et al., 2014). The MB is structurally similar to the hippocampus and cerebellum, and functionally analogous to piriform cortex. The MB displays an expansion layer motif that is also seen in other brain regions such as the cerebellum and hippocampus, to amplify information processing capability (Olshausen and Field, 2004; Farris, 2011; Cayco-Gajic and Silver, 2019). In addition, the mammalian and fly olfactory systems show similar overall circuit features (Ache and Young, 2005).

The MB consists of bilateral neuropils in the central brain, and each hemisphere exhibits the presence of ~2200 intrinsic neurons called Kenyon cells (KCs) (Aso et al., 2009). The cell bodies form quadruple clusters at the dorsal posterior brain and the KCs extend their dendrites into a globular structure called the calyx where they interact with the axonal projections of olfactory PNs (Stocker et al., 1990). The axons of the KCs project anteriorly as a bundle called the peduncle to eventually bifurcate and terminate in the dorsal anterior brain as tripartite MB lobes, which are the main output regions of the MB (Technau, 1984; Ito et al., 1997). The MB lobes extend vertically and medially to give rise to two vertical lobes (α and α') and three horizontal lobes (β, β' and γ) (Ito et al., 1998; Crittenden et al., 1998).

The KCs can be broadly categorised into three types based on their gene expression pattern, birth order and the lobes in which their axons terminate. The axons of γ KCs innervate the most anterior medial γ lobe; the axons of α'β' KCs bifurcate at the anterior end of the peduncle to form the α' vertical lobe and the β' medial lobe; and similarly, the axons of αβ KCs also bifurcate and form the vertical α and medial β lobe (Crittenden et al., 1998; Tanaka et al., 2008). Each KC subset also expresses marker genes such that γ KCs express *Imp*, *sNPF*, *trio*; the αβ KCs express *sNPF*, *Fas2*; and

the α'β' KCs express *DAT* and *trio* (Davie et al., 2018; Shih et al., 2019). Later in-depth studies and more recent connectomic analysis of the fly brain revealed that KCs can be further divided into seven subtypes, based on their morphology and gene expression patterns, which are: αβ core, αβ surface, αβ posterior, α'β' middle, α'β' anterior-posterior, γ main, and γ dorsal (Aso et al., 2009; Aso et al., 2014; Butcher et al., 2012; Strausfeld et al., 2003; Zheng et al., 2018; Li et al., 2020; Shih et al., 2019).

1.3 Mushroom body calyx: a non-stereotypical circuit

In the mushroom body calyx (MBC) combinatorial olfactory input from the ~50 types of projection neurons, converges onto ~2200 mushroom body intrinsic Kenyon cells (Li et al., 2020). In the calyx region, the axonal projections of the PNs form collateral branches that innervate the calyx and produce multisynaptic boutons (Stocker, 1994). The KCs extend into the calyx with their dendritic branches terminating in a claw-like structure, such that each KC has ~3-7 clawed branches (γKCs - ~7 claws, αβKCs - ~5 claws and α'β'KCs – 3 claws) each interacting with a single bouton (Leiss et al., 2009; Caron et al., 2013; Gruntman and Turner, 2013). Each PN forms 1-20 boutons and each bouton is ensheathed by 12-14 claws on average of different KCs, forming the characteristic microcircuit within the calyx, called a microglomerulus (MG) (Figure 3) (Yasuyama et al., 2002; Leiss et al., 2009; Butcher et al., 2012; Zheng et al., 2020).

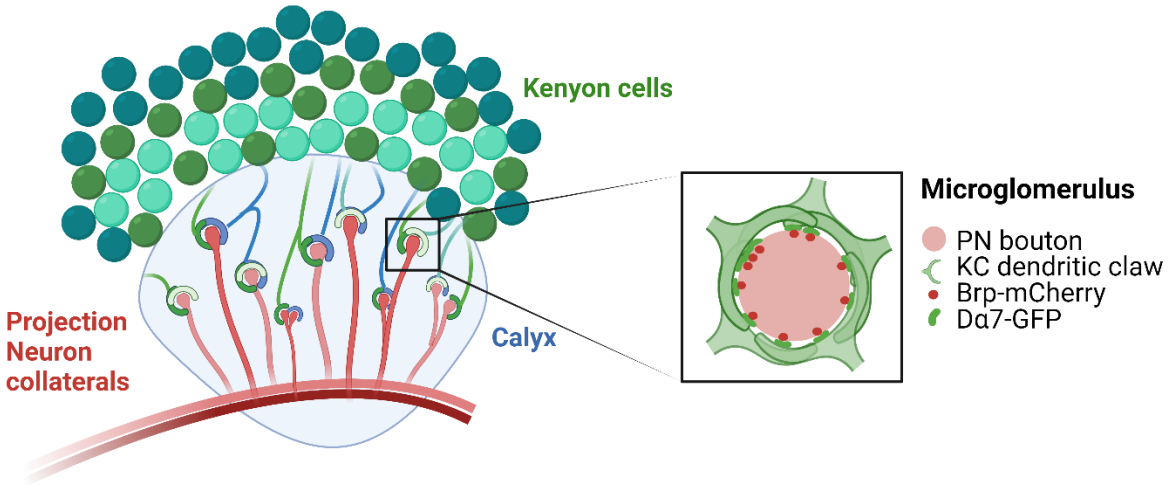

Figure 3. Mushroom body calyx and the microglomerulus.

The MB calyx is the site of interaction of PN axonal collaterals (in red) terminating in boutons and KC dendrites (in green) that end in claws; giving rise to a microcircuit called the microglomerulus (in inset). MG cross-section shows different over-lapping KC claws on the same PN bouton. The MG synaptic

complex can be visualized by expressing pre-synaptic active zone molecule Bruchpilot with mCherry tag in the PNs and by expressing the post-synaptic acetyl choline receptor subunit Dα7 tagged with GFP in the KCs.

The stereotypy of neural architecture and functional odour coding seen in the AL is largely lost in the MBC. The AL shows very stereotypical connections such that an ORN only interacts with its complementary PN type, and together they consistently innervate the same glomerulus across flies (Laissue et al., 1999; Grabe et al., 2016). Theoretical modelling and photoconversion studies on PN-KC interactions hypothesized that KCs may receive input from a combination of glomeruli that are randomly chosen from the non-uniformly distributed PN types in the MB (Murthy et al., 2008; Caron et al., 2013; Litwin-Kumar et al., 2017). However, developmental light microscopy data for the PNs shows that some PNs preferentially innervate specific regions in the calyx and this has been confirmed with the recent EM datasets (Zheng et al., 2020; Jeffris et al., 2007; Lin et al., 2007). In addition, KCs show a NB specific quadripartite innervation of the calyx, with regions of enrichment for dendritic claws of particular KC subtypes (Zhu et al., 2003; Lin et al., 2007; Leiss et al., 2009; Zheng et al., 2020). These findings along with the EM data analyses suggests that the calyx is a non-stereotypical circuit and that PN and KCs might display some bias in connectivity and are not connected fully randomly (Zheng et al., 2018; Zheng et al., 2020; Li et al., 2020).

Functionally, the convergence of ~50 PN types onto ~2000 KCs creates an expansion layer motif where there is a 40 fold expansion between olfactory input and the postsynaptic cells (Laurent, 2002; Litwin-Kumar et al., 2017). The presence of an expansion layer plays an important role in optimizing the ability of an organism to discriminate between stimuli by reducing the overlap between their sensory representations (Rolls and Treves, 1990; Fiete et al., 2004; Cayco-Gajic and Silver, 2019). The KCs also exhibit a functional constraint whereby a KC only responds on the coincident activation of more than half of its connected PN boutons (Gruntman and Turner, 2013). The inhibitory input provided by the anterior paired lateral (APL) neuron, in each MG also guarantees the capacity of KCs to encode complex sensory information input with a sparse response (Prisco et al., 2021; Perez-Orive et al., 2002; Honegger et al., 2011; Lin et al., 2014). These properties together allow only ~10% of

KCs to be responsive on odour presentation, despite ~50% of the PN population showing a response (Perez-Orive et al., 2002; Wang et al., 2004; Turner et al., 2008; Honegger et al., 2011; Lin et al., 2014).

How such a non-stereotypical circuit with its functional and structural constraints is wired and assembled during development is a fascinating question that remains unresolved.

1.4 Developmental wiring of the calyx

During development, the calyx is wired twice, such that the functional larval calyx is disassembled during metamorphosis and re-assembled during pupal development to produce the functional adult calyx (Armstrong et al., 1998; Lee et al., 1999; Eichler et al., 2017; Li et al., 2020).

1.4.1 KC neurogenesis and wiring of larval calyx

All KCs are born from the sequential division of four neuroblasts (NB) that ~~continuously~~ divide throughout development, producing the different KCs types at different developmental stages (Truman and Bate, 1988; Ito and Hotta, 1992). At each division, the MB-NB divides to form a ganglion mother cell (GMC) and a self-renewed MB-NB, and each GMC divides again to produce 2 KCs (Figure 4) (Lee et al., 1999).

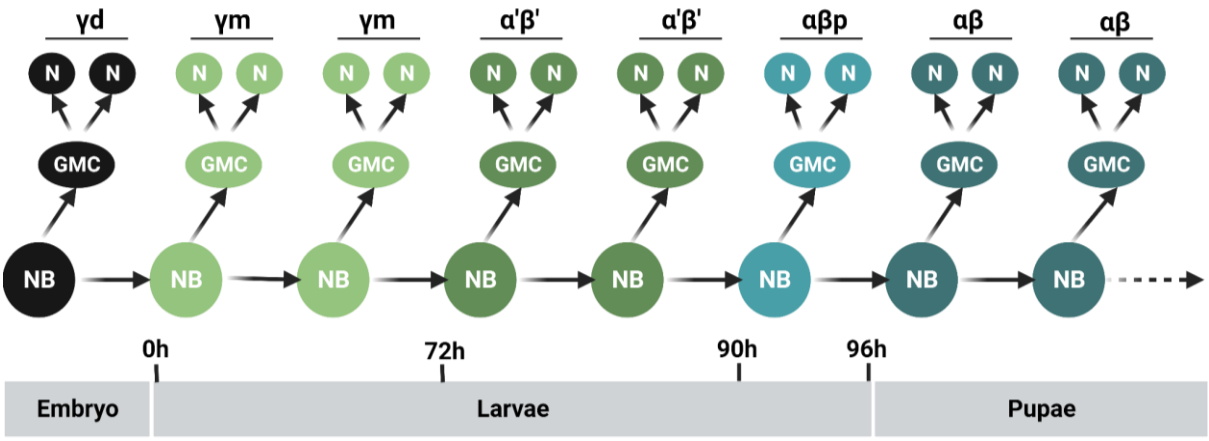

Figure 4. Temporal specification of KCs and termination of MB-NBs during development.

During embryonic development, the first 8-15 cells produced by the MB-NBs are not KCs and these cells project their neurites to other brain regions (Kunz et al., 2012).

Subsequently, the MB-NBs produce ~95 γKCs, and since they project consistently to the dorsal layer of the adult γ lobe, are γd KCs (Kunz et al., 2012; Armstrong et al., 1998; Pauls et al., 2010). All the KCs produced after larval hatching to the mid-third instar larval stage are γ KCs that are likely to be γm subset; KCs born from mid-third instar larval stage to ~6hr before puparium formation (PF) are α'β' KCs; KCs generated in the 6hr till PF are αβ pioneer (αβp) KCs and the KCs produced during the pupal stages are all αβ KCs (Figure 4) (Lee et al., 1999; Zhu et al., 2006). Similarly, the PN-NBs also generate different PN subsets depending on different developmental stages. During embryo development, 21 embryonic olfactory PNs are generated that each receive input from a single glomerulus in the larval antennal lobe (Ramaekers et al., 2005; Eichler et al., 2017). After larval hatching, from the L1 larval stage to PF the PN-NBs generate the rest of the total 150 PNs seen in the adult AL, these PNs are also referred to as larval PNs (Jefferis et al., 2001; Marin et al., 2005).

The larval calyx only sees the interaction of embryonic born PNs and KCs, and the larval born PNs and KCs do not integrate into this circuit (Jefferis et al., 2004; Pauls et al., 2010; Punal et al., 2023;). The larval calyx shows a glomerular organisation where PNs innervate calyx glomeruli in a stereotypical manner, and the KCs although showing a subset-specific bias for certain regions of the calyx, in general, innervate ~6 glomeruli in a seemingly random manner (Masuda-Nakagawa et al., 2005; Ramaekers et al., 2005).

1.4.2 Metamorphosis and wiring of adult calyx

The olfactory repertoire required by a larva and an adult fly is not equivalent and hence, during metamorphosis the larval calyx is disassembled and the larval born PNs and KCs are integrated to form the adult specific calyx (Lee et al., 1999; Jefferis et al., 2004; Marin et al., 2005).

During pupation, only the MB-NBs actively divide to produce pupal born αβ KCs, a subset that is not subject to pruning and instead extends its dendrites unhindered into the calyx (Lee et al., 1999; Zhu et al., 2006). The onset of pupation initiates differential pruning and regrowth programs for the embryonic and larval born KC and PN subsets. Between 4-18h APF the γ KC dendrites undergo extensive pruning and α'β' dendrites

show slight pruning (Lee et al., 1999). By 24h APF, the immature dendrites of α'β' and of αβ KCs are present in the calyx while γ KC dendrites are only observed in the calyx after 36h APF (Lee et al., 1999).

The PN-NBs have generated all the PNs before pupation begins, with the embryonic PNs integrated into the larval calyx and the larval PNs having extended towards the calyx but without any collaterals innervating the calyx (Jefferis et al., 2004). The boutons and axons of embryonic PNs are completely pruned away from 4-12h APF and the larval PNs start sprouting collaterals in the region of the calyx from 6-18h APF (Jeffris et al., 2004; Marin et al., 2005). By 18h APF larval PN collaterals are observed in the calyx and the embryonic born PNs start to re-extend into the calyx (Marin et al., 2005). By 24-30h APF, all PNs have extended immature collaterals in the calyx (Marin et al., 2002; Marin et al., 2005).

By 30-40h APF, the calyx is populated by immature PN and KC neurites and these neurites start maturing and displaying complexity of structure by 40-50h APF (Marchetti and Tavosanis, unpublished). MARCM clones of PNs and KCs show the neurites becoming more precisely defined such that by 50-60h APF PN collaterals show bouton like structures and KC dendrites terminating in maturing claws (Figure 5; Marchetti and Tavosanis, unpublished). 40-50h APF also shows initial recruitment and localization of synaptic proteins, suggesting an initiation of synaptic interactions and by 50-60h APF onwards synaptic connections have started to form (Figure 5; Marchetti and Tavosanis, unpublished).

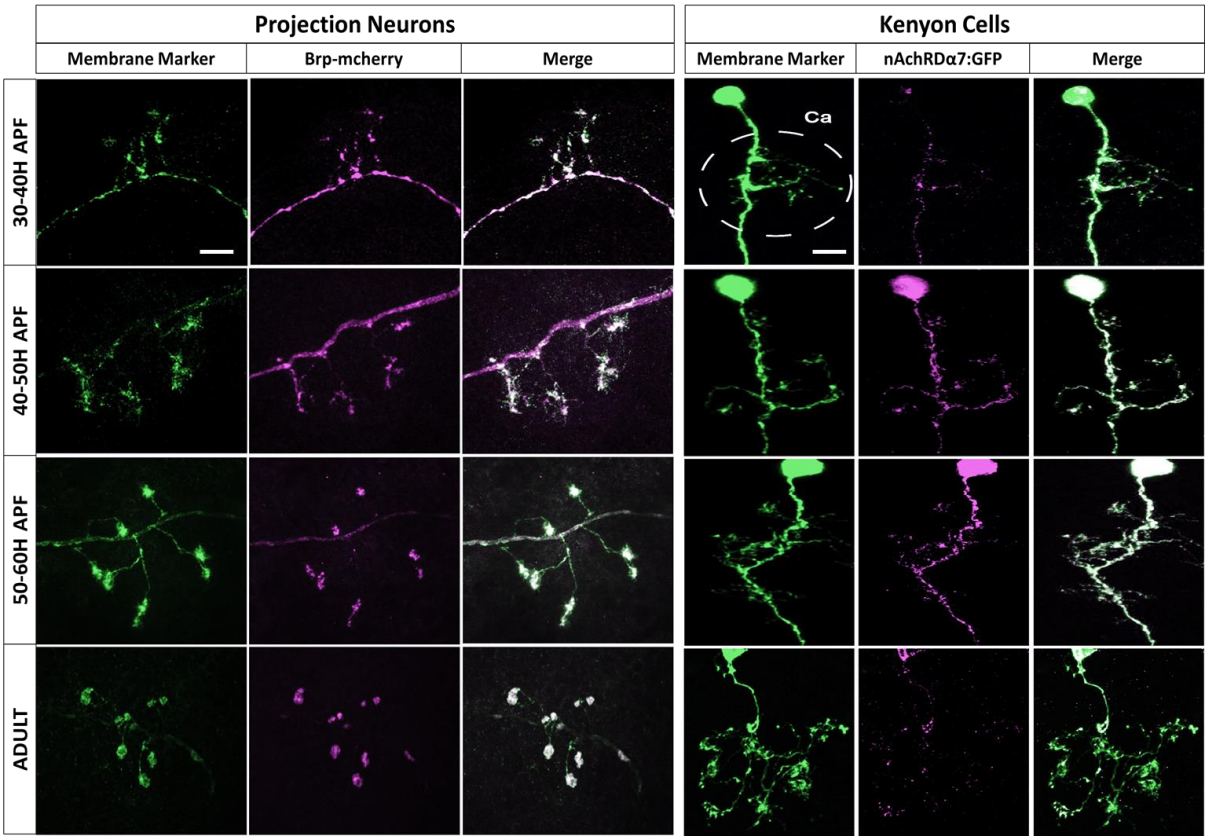

Figure 5. Maturation of PN and KC neurites in the calyx during pupal development.
Individual PN and KC clones obtained by MARCM expressing membrane marker (*mCD8-GFP* or *tdTomato* respectively) (in green) and pre- or post- synaptic proteins (*Brp-mCherry* or *Dα7-GFP* respectively) (in magenta) imaged at 3 time points during pupal development and in the adult. Image from Marchetti and Tavosanis, unpublished. Scale bar = 10µm.

1.5 PN – KC interactions in the adult calyx

Hydroxyurea (HU) mediated ablation studies have been useful in investigating the role of neurons and their synaptic partners in different brain functions. HU inhibits DNA synthesis in actively dividing cells, hence any proliferating neuroblasts at the time of HU treatment are terminated (Brandt et al., 1972; de Belle and Heisenberg, 1994; Sweeney et al., 2012). In the first 8hr after larval hatching, the KC neuroblasts continue to divide while other neuroblasts pause their divisions (de Belle and Heisenberg, 1994). Feeding the larvae HU in this time period, hence, specifically ablates KC neuroblasts (de Belle and Heisenberg, 1994). These animals lack all larval KCs that receive olfactory inputs, and therefore have abrogated olfactory learning (de Belle and Heisenberg, 1994).

In the calyx, ablation of KCs during development leads to a directly proportional loss of PN axonal arborisation in the calyx region, but this loss of arborisation is not reflected in the LH, indicating that the loss of PN collaterals is a calyx-specific effect and does not affect the PNs ability to innervate other brain regions (Elkahlah et al., 2020; Marchetti and Tavosanis, unpublished). This suggests that the presence of KCs might be required to induce PN collateral sprouting and innervation in the calyx. On the other hand, ablation of majority of PNs does not have a profound effect on the PN collaterals in the calyx region, as the surviving PNs are seen to expand their collaterals and boutons to interact with the unaffected KC claws innervating the calyx (Elkahlah et al., 2020). Expansion of KC cell population shows a proportional expansion of calyx size and PN bouton repertoire (Elkahlah et al., 2020). Similarly, increasing the number of claws formed by the KCs also reiterates a similar increase in calyx size and number of PN boutons (Elkahlah et al., 2020). Taken together, these findings suggest that KCs play an important role in not only determining the calyx size and connections but also in influencing the PN axons to sprout collaterals and innervate the calyx. How the KCs induce the PNs to sprout and/or maintain collaterals in the calyx region is not known.

Studies focusing on KC dendrite organization in the calyx show that KC dendrites are not uniformly distributed across the calyx. The dendrites of different subtypes occupy loosely defined overlapping regions such that γ KC dendrites are present at the calyx core, while α/β and α′/β′ KCs are present mostly at the periphery (Zhu et al., 2003; Leiss et al., 2009; Aso et al., 2014; Zheng et al., 2018). Despite this, a single PN bouton can be contacted by claws of different KC types, indicating that calycal regions are enriched for KC subtypes but are not exclusive (Caron et al., 2013; Leiss et al., 2009; Baltruschat et al., 2020). Specific KC subsets (γd, α′/β′ap1, and α/βp) innervate the ventral, lateral and dorsal accessory calyces, respectively, and receive primarily non-olfactory sensory information (Tanaka et al., 2008; Aso et al., 2014; Vogt et al., 2016; Zheng et al., 2018; Li et al., 2020a, b). How this network architecture is set up and what molecular mechanisms may be employed to drive accurate PN and KC synaptic matching are interesting avenues of further research.

1.6 Implication of CAMs in PN-KC synaptic matching

Cell surface and secreted molecules have been shown to be essential for layer specific synaptic partner recognition in the fly visual system (Tan et al., 2015). Genetic screens have also helped in identifying different molecules required for wiring in the MB. Transcription factors like *lola* are shown to be required for accurate wiring and targeting of axons as well as dendrites of PNs (Spletter et al., 2007). In the KCs, RhoA is required for NB proliferation and normal dendritic morphogenesis (Lee et al., 2000). Similarly, *trio* is essential for proper extension patterning of the KC axons in the MB lobe (Awasaki et al., 2000).

Investigation of wiring determinants in the developmental assembly of the antennal lobe have shown the temporal expression of “wiring molecules” in developing vs mature PNs, indicating that cell surface molecules may be involved in synaptic partner matching between ORNs and PNs (Li et al., 2020). From these studies, the endocytic receptor LRP1 was found to be a cell-autonomous regulator of dendrite targeting of PNs in the antennal lobe (Li et al., 2020). Fili was also recognized as a molecule involved in ORN and PN wiring such that it mediated repulsion between non-synaptic partners to ensure precise synaptic partner matching (Xie et al., 2019).

Further transcriptomic analysis of the PNs at different pupal time points, has revealed the occurrence of a “wiring -phase” from 24-48h APF where each class of PNs is distinct from other PN subtypes on the basis of their unique expression pattern of transcription factors and cell surface molecules (Xie et al., 2021; Li et al., 2020). RNA single cell sequencing data for the γ KCs reveals dramatic changes in the global gene expression patterns at each stage of pupation (Alyagor et al., 2018). Between 24-30h APF, the γ KCs show an upregulation of genes associated with not only cellular growth but also of axon guidance molecules (Alyagor et al., 2018). This raises the possibility that the KCs may also express cell surface tags specifically in this wiring phase. Whether this expression of CAMs is similar to that of PNs, remains to be investigated. It would be highly interesting if the KC - PN interaction also employ wiring strategies involving CAMs like those used in the AL by the ORNs and PNs.

1.7 Role of Anaplastic lymphoma kinase (Alk) - Jelly-Belly (Jeb) signalling in *Drosophila*

Receptor tyrosine kinase (RTK) signalling is an evolutionarily conserved mechanism for cells to transduce extracellular cues present in their environment (Sopko and Perrimon, 2013). RTKs play essential roles in the development of metazoans, including differentiation and tissue patterning, morphogenesis, cell growth, and proliferation (Mele and Johnson, 2020). Alk, one of the ~20 RTKs expressed in *Drosophila*, is highly conserved in vertebrates, *Caenorhabditis elegans* and *Drosophila melanogaster,* and plays a major role in development of the CNS (Lorén et al., 2001; Hallberg and Palmer 2013). In addition, *alk* has been intensively studied in the context of embryonic development of visceral muscles, where, by binding to its secreted ligand Jeb, it activates the Ras-Raf-MAPK pathway and facilitates founder cell fate specification (Englund et al., 2003; Lee et al., 2003; Lorén et al., 2003; Stute et al., 2004). Alk is strongly expressed in the CNS and plays a role in diverse functions. During nutrient restrictions, Alk-Jeb signalling acts as a neuroprotectant by suppressing amino acid sensing pathways and also by activating PI3-kinase signalling (Cheng et al., 2011). These regulatory features are consistent with the starvation-resistant growth programs seen in mammalian tumors (Kalaany and Sabatini, 2009). Recently, oncogenic *alk* mutations were found to affect the levels of apoptosis and neuronal fate specification in MB-NB lineages that persist into adulthood (Pfeifer et al., 2022).

Mutations in Alk were shown to also affect circadian rhythm by increasing the period of locomotor activity behaviour (Kumar et al., 2021). In the *Drosophila* visual system, Alk-Jeb signalling regulates layer-specific expression of cell-adhesion molecules, Dumbfounded/Kirre, Roughest/IrreC, and Flamingo (Bazigou et al., 2007). Jeb expressed by photoreceptor neurons also interacts with the Alk expressed by L3 neuron dendrites to promote survival of L3 neurons in the lamina (Pecot et al 2014). This suggests that Alk-Jeb signalling is involved in layer-specific target recognition, and neuronal survival in the visual system. In the developing motor circuit of Drosophila larvae, trans-synaptic Alk-Jeb signalling was shown to play a key role in establishment of functional synapses (Rohrbough and Broadie, 2010). Additionally,

this trans-synaptic signalling negatively regulates neurotransmission and activates Ras-MAP kinase cascades in both pre- and post- synaptic partners (Rohrbough et al., 2013). Taken together, Alk-Jeb signalling is suggested to be an upstream regulator of synaptic structure and function. Alk is also implicated in learning and memory. In the α/β KCs, reduced Alk expression during conditioning enhanced LTM, whereas its overexpression impaired LTM (Gouzi et al., 2018). Alk has been suggested to be present on the KC claws, while its ligand Jeb would be localized on the PN boutons (Bai and Sehgal, 2015; Gouzi et al., 2011; Gouzi et al., 2018).

Although Alk signalling is implicated in a diverse range of physiological processes across vertebrate and invertebrates, the underlying molecular mechanisms have not been fully elucidated. In particular, very little is known about Alk-interacting molecules, other than Jeb. How these interactions may occur in different tissues and what pathways they might regulate is an open field of investigation. Recent proximitome and transcriptional profiling studies have suggested a few candidates such as Corkscrew, Rugose, Kahuli, as possible interactors and/or modulators of Alk signalling in the nervous system (Uckun et al., 2021; Mendoza-Garcia et al., 2021). However, their tissue specific functions and downstream pathways still need to be resolved.

The Alk receptor is a 200kD protein that contains two MAM-domains, one low density lipoprotein class a (LDLa) domain, a glycine rich region and an intracellular protein tyrosine kinase (PTK) (Figure 6) (Loren et al., 2003). The MAM domains are important for receptor activity in *Drosophila*, as a single point mutation in this domain results in a loss of function phenotype (Lorén et al., 2003). The function of the LDLa domain is important for binding of Alk to its ligand Jeb (Lee et al.,, 2003). The glycine rich region consists of three consecutive glycine residues, and mutations in this region result in non-functional Alk receptors (Lorén et al., 2003). The intracellular part contains a PTK domain, a juxtamembrane segment and a carboxy-terminal region (Lorén et al., 2003). Alk receptors occur as dimers and binding to Jeb activates a signalling cascade resulting in activation of the PTK domains via cross phosphorylation, which in turn activates different downstream kinase signalling cascades (Lee et al., 2003; Englund et al., 2003).

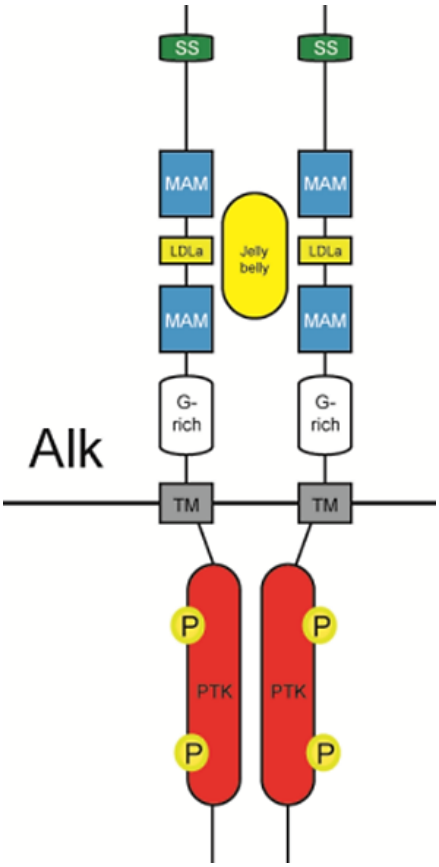

Figure 6. Schematic of Alk and Jeb regulatory elements.

The extracellular domain of Alk consists of a Signal Sequence (SS) (in green), an LDLa motif (yellow) flanked by two MAM domains (in blue), and a glycine rich region (G-rich). A transmembrane domain (TM) (in grey) localizes the receptor to the membrane. The intracellular domain contains a Protein Tyrosine Kinase (PTK) domain (in red). Alk is activated by the LDL domain binding protein Jeb (in yellow). Image from Hugosson 2015.

2 Aims of the thesis

Building complex functional circuits requires the matching of appropriate partners during development. Several molecular wiring mechanisms have been identified through genetic screens carried out in *Drosophila* taking advantage of stereotypic circuits of the visual system and the antennal lobe. However, very little is known about how non-stereotypical circuits are wired. This thesis focuses on attempting to resolve the developmental wiring of the non-stereotypical circuit of the mushroom body calyx. In this context, the the thesis investigated the following questions:

2.1 Determining whether KCs express unique cell surface markers that may help in KC-PN partner matching.

Transcriptomic analysis of the PNs reveals a distinct difference in the expression of cell surface molecules in developing vs mature PNs (Li et al., 2020). Available transcriptomic datasets (Alyagor et al., 2018; Li et al., 2020; Li et al., 2017; Xie et al., 2021) were analysed to investigate whether KCs also exhibit such a differential expression of cell surface molecules in pupal stages compared to adult KCs.

2.2 Investigating the role of differentially expressed CAMs in PN - KC wiring.

Pan-neuronal genetic screens have been used successfully in the antennal lobe to identify molecular mechanisms involved in the synaptic partner matching of ORNS and PNs (Xie et al., 2019). A similar strategy was employed to investigate the role of the differentially expressed cell surface molecules, from the transcriptomic analysis, in PN-KC wiring. The observed phenotypes were analysed for any change in MG shape, and PN bouton size and distribution.

2.3 Exploring the role of Alk-Jeb signalling in the calyx.

From the shortlisted candidates obtained from the screen, Alk and Jeb were selected for further analysis in the context of calyx wiring based on their phenotype and their published role in neuronal axon targeting, cell survival, synaptogenesis, memory and learning (Bazigou et al., 2007; Gouzi et al., 2018; Pecot et al., 2014; Rohrbough and Broadie, 2010; Rohrbough et al., 2013; Woodling et al., 2020). Alk-Jeb localization was investigated in KCs and PNs, along with the pre- and/or post- synaptic requirement of Alk-Jeb signalling in the calyx assembly.

2.4 Developing an *in vivo* longitudinal imaging method.

To investigate the dynamics involved in pupal wiring of the calyx, a 3P based *in vivo* longitudinal imaging method was established. This method will also be useful in exploring the dynamics of KC and PNs in the context of normal development as well as mutants.

.

3 Materials and methods

3.1 Fly Husbandry

Drosophila melanogaster was raised at 25°C, at 60% relative humidity under a 12/12h light-dark cycle on a standard cornmeal-based diet. Stock lines were maintained at 18°C, at 60% relative humidity under a 12/12h light-dark and experimental lines were moved to 25°C incubators for at least one generation before experimental use.

3.1.1 Fly food

To prepare 25 l of fly food, the following recipe was followed:

Ingredient	Quantity
Agar Agar	234g
Malt syrup	800g
Brewer's yeast	370g
Corn flour	2000g
Methyl-4-hydroxybenzoate	50g
10% Phosphoric acid	200ml
Soybean flour	200g
Sugar syrup	800g

Agar agar was soaked in 1l water overnight at 4°C. The pre-soaked agar alongwith malt syrup, sugar syrup, brewer's yeast, soybean flour and corn flour was mixed thoroughly with the help of an immersion blender. Water was added to the mixture to make up the volume to 30ml and was cooked with constant stirring for 2h. The food mix is allowed to cool to 60°C, and then 50g Methyl-4-hydroxybenzoate dissolved in warm (60°C) water as well as 10% phosphoric acid is added to the mixture while stirring. When the temperature reaches 55°C, the food is distributed in standard fly

culture vials. When the food has cooled and solidified, the vials are plugged and stored at 4°C.

3.1.2 Fly strains

Genotype	Source	Identifier
Elav^{C155}-GAL4, UAS-Dicer2; P{GMR68D02-lexA}, 8xlexAop2-brp-mCherry, MB247-Dα7-GFP	Line established in the Lab; *8xlexAop2-brp-mCherry* (Berger-Mueller et al.,, 2013); *MB247-Dα7-GFP* (Kremer et al.,, 2010)	Bloomington ID: 25750, 54923 FlyBase ID: FBti0002575, FBti0100275,FBti0156266, FBal0297300, FBal0264825
;P{GMR68D02-lexA}, 8xlexAop2-brp-mCherry, MB247-Dα7-GFP/CKG;;OK107-GAl4	Line established in the lab;*8xlexAop2-brp-mCherry* (Berger-Mueller et al., 2013); *MB247-Dα7-GFP* (Christiansen et al., 2011); *OK107-Gal4* (Connolly et al.,, 1996)	Bloomington ID: 854; 54923 FlyBase ID: FBti0156266, FBal0297300, FBal0264825, FBti0004170
Acj6-GAl4/FM7i; P{GMR68D02-lexA}, 8xlexAop2-brp-mCherry, MB247-Dα7-GFP/CKG;;	Line established in the lab; *Acj6-GAl4* (Bourbon et al.,, 2002); *8xlexAop2-brp-mCherry* (Berger-Mueller et al.,, 2013); *MB247-Dα7-GFP* (Christiansen et al.,, 2011)	Bloomington ID: 54923, 30025 FlyBase ID: FBti0022324, FBti0156266,FBal0297300, FBal0264825
;UAS-mCD8-GFP/CyO;;OK107-Gal4	Line established in the lab; *UASmCD8GFP* (Lee and Luo, 1999), *OK107-Gal4* (Connolly et al., 1996)	Bloomington ID: 5137, 854; FlyBase ID: FBti0012685, FBti0004170
;;UAS-Alk-RNAi;	*UAS-Alk-RNAi* (Perkins et al., 2015)	Bloomington ID: 27518 FlyBase ID:FBti0128777
;UAS-Jeb-RNAi;;	*UAS-Jeb-RNAi* (Perkins et al., 2015)	Bloomington ID: 56022 FlyBase ID: FBti0163424
UAS-Alk-DN;;;	*UAS-Alk-DN* (Lee et al., 2003)	Bloomington ID:92968 FlyBase ID: FBti0216632
;UAS-nls-mCherry;;		Bloomington ID: 38425 FlyBase ID: FBti0147459

Acj6-Gal4/FM7i;;;	*Acj6-Gal4* (Bourbon et al., 2002)	Bloomington ID: 30025 FlyBase ID:FBti0022324
;;;OK107-Gal4	*OK107-Gal4* (Connolly et al., 1996)	Bloomington ID: 854 FlyBase ID: FBti0004170
;;GMR68D02-Gal4;	*GMR68D02-Gal4* (Jenett et al., 2012)	Bloomington ID: 39471 FlyBase ID: FBti0137719

3.2 Reagents

Reagent	**Company**
Phosphate buffered saline (PBS)	Gibco, Thermo Fisher Scientific Inc.
16% Paraformaldehyde (PFA)	Thermo Fisher Scientific Inc.
Triton X-100	Th. Geyer GmbH & Co.
Swine serum	Histoprime, Biozol Diagnostics Inc.
Vectashield	Vector Laboratories, Inc.

3.3 Antibodies

Antibody	**Host**	**Dilution**	**Source**
Anti-RFP	Rabbit	1:200	Rockland Immunochemicals, Inc.
Anti- Alk	Rabbit	1:1000	Gift from Prof. Ruth Palmer, University of Gothenburg
Anti-Jeb	Guinea Pig	1:1000	Gift from Prof. Ruth Palmer, University of Gothenburg
Anti -Synapsin (3C11)	Mouse	1:200	Developmental Studies Hybridoma Bank
Anti-mouse 643 nm	Donkey	1:1000	Thermo Fisher Scientific Antibodies

Anti-rabbit 643nm	Donkey	1:1000	Thermo Fisher Scientific Antibodies
Anti-guinea pig 643nm	Donkey	1:1000	Thermo Fisher Scientific Antibodies

3.4 Software

Software	Source
Fiji/ imageJ (1.54f)	Wayne Rasband, National Institute of Health, USA
Imaris 9	Andor Technology, Oxford Instruments, UK
Graphpad Prism 8	GraphPad Software, USA
Biorender (online)	www.biorender.com
Galaxy (online)	www.usegalaxy.eu
Automated single-cell analysis portal (ASAP) (online)	www.asap.epfl.ch
SCope (online)	www.scope.aertslab.org

3.5 Lab equipment

Equipment	Source
25°C Incubator	Percival Scientific, Inc.
Dissecting microscope (Stemi 2000C)	Zeiss, Germany
Light source (CL 6000 LED)	Zeiss, Germany
Forceps (Dumont 55)	Fine Science Tools, Germany
Double sided adhesive tape (15mm)	Tesa, Germany
Hot plate stirrer (RH Basic2)	IKA, Germany
Macro fluorescence microscope MVX10	Olympus IMS
PS-3D platform rotator	Grant Instruments Ltd
800 LSM confocal microscope	Zeiss, Germany
980 LSM confocal microscope	Zeiss, Germany
3P microscope	ThorLabs, USA

3.6 Single cell RNA sequencing analysis

Single-cell RNA sequencing datasets were analysed using the public server of Galaxy (Afgan et al., 2016; Galaxy Community, 2022) and ASAP (Gardeux et al., 2017) web application. Datasets were variance stabilising transformation (VST)-normalised and developing pupal data was compared against adult data for differential gene expression for cell surface molecules. Genes that showed a more than 2-fold change in expression were used as candidate genes for an RNAi screen investigating role of cell surface molecules in the developmental wiring of the MB calyx.

3.7 RNAi screen

For RNAi experiments, F0 flies (parental cross) were maintained at 25°C and F1 embryos were raised at 29°C throughout development until 3 days' post eclosion. At 3 days' post eclosion, the progeny of the right genotype was dissected and stained against RFP Ab (to enhance Brp signal) and then imaged with a confocal microscope. RNAi fly lines against cell surface molecules (Supplementary Table 5) were obtained from Vienna Drosophila Resource Center (VDRC) and Transgenic RNAi Project (TRiP) collections from Bloomington Drosophila Stock Center (BDSC) (Dietzl et al., 2007; Ni et al., 2008; Perkins et al., 2015).

3.8 Immunocytochemistry

Fly brains were dissected in cold PBS with 0.1% Triton X-100 (0.1% PBST) and fixed in 4% formaldehyde in PBS for 40 min. They were washed in 0.1% PBST and then blocked for an hour at room temperature in 0.1% PBST and 10% swine serum and then incubated overnight at 4°C with the primary antibodies diluted in the blocking solution. Next day, brains were washed thrice in 0.1% PBST for 5 minutes each and then incubated for four hours with the secondary antibody diluted in 0.1% PBST. The brains were washed thrice in 0.1% PBST and mounted onto an objective slide. All washing and incubation steps were performed on a platform rotator. The brains were arranged on the slide using strips of double-sided adhesive tape as spacers between the slide and coverslip to avoid compressing the brain tissue and Vectashield was used as a mounting medium. Depending on the neuropil of interest, the anterior (for imaging AL / MB lobes) or the posterior side (for imaging the MB calyx) of the brain would face towards the coverslip to gain a good resolution and imaging depth with confocal imaging.

3.9 Confocal imaging

All images for ICC were acquired using a Zeiss 980 or Zeiss 800 Confocal Microscope (Zeiss, Jena, Germany). High resolution Z-scans of neuropils of interest were acquired using a C-Plan-Apochromat 63x/NA 1.4 oil immersion objective (Zeiss). For inter-image comparability and automated image quantification, standardised settings were used across an experimental dataset.

3.10 3-Photon (3P) imaging

The developmental stage for each *Drosophila* pupa was determined based on identifiable developmental landmarks (Bainbridge and Bownes, 1981). The pupae were then placed dorsal side up, on a slide in a tilted position using double sided tape to keep the head slightly elevated. The pupal case was partially removed from the head and thorax region to expose the head of the developing pupa. A coverslip was then slightly pressed to the posterior side of the head, allowing the brain structures to be imaged stably without signal scattering (Figure 7). The pupae were imaged through the coverslip using the 3P microscope setup (as described in Kaushalya et al., 2008) equipped with a 25× Olympus XLPlan N WMP2 (1.05 NA, 2.0 mm WD) water-immersion objective. mCD8GFP was excited at 1300 nm and the fluorescence was detected using bandpass filters for 510/520 nm.

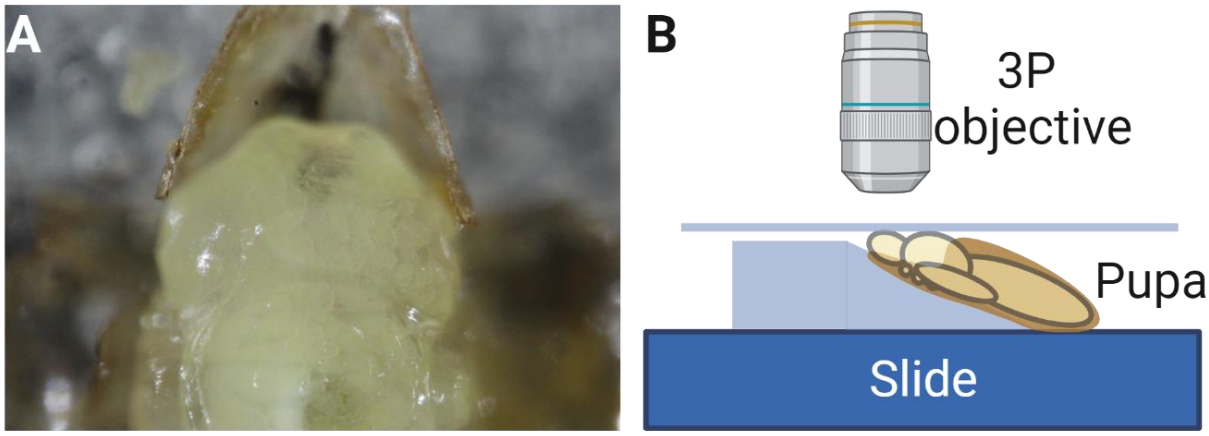

Figure 7. Mounting setup of intact pupa for 3P microscopy.

(A) View of exposed head of developing pupa at early pupal stage P6. (B) Positioning of the pupa on a sloped surface with a coverslip positioned on top to successfully image the developing pupa under an upright 3P microscope.

3.11 Image analysis

3.11.1 Bouton and cell counting with Fiji

Confocal acquired images were processed using the open source software Fiji (Schindelin et al., 2012). Bouton and cell numbers were counted manually using the cell counter plugin in FIJI.

3.11.2 Cell number counting with Imaris

Confocal acquired z-stacks were processed using the Imaris image analysis software (Oxford instruments). Labelled nuclei were marked by using the spot creation wizard in Imaris. The parameters for nuclei detection were kept constant across the images: they were nucleus diameter (2µm for KCs and 3.5µm for PNs) and quality threshold (2060). Numbers of nuclei identified were recorded and used for further statistical analysis with GraphPad Prism 8.

3.11.3 Statistical analysis

All statistical analysis was performed in GraphPad Prism 8. Data were tested for normality with a D'Agostino-Person omnibus K2 test. To compare differences between groups a two-sample t-test or a one-way analysis of variance (ANOVA) followed by pairwise multiple-comparison Bonferroni post hoc test. To compare the mean response of a group to a hypothetical value a one-sample t-test was performed. Statistical significance was defined as $p \leq 0.05$ = *, $p \leq 0.01$ = **, $p \leq 0.001$ = ***, $p \leq 0.0001$ = ****.

4 Results

4.1 Transcriptomic analysis of pupal γKCs identifies differentially expressed CAMs

The pupal stages between 24-48h APF have been shown to be a crucial wiring phase for the PNs, in which each PN subset distinctly expresses a unique pattern of cell surface molecules and transcription factors that allows PN and ORN partner matching in the antennal lobe (Xie et al., 2021). This distinctness in the gene expression pattern is lost as the PNs mature and start expressing genes generally required for cell function, maintenance and survival (Xie et al., 2021). This prompts the question of whether a similar wiring phase also occurs in the calyx between 24-48 h APF. Does the PN surface proteome show subset-specific distinct identities also on its axon collaterals that innervate the calyx? Do the KCs also exhibit unique cell surface molecules within this “wiring phase”?

To investigate these questions, I analysed published RNA single cell sequencing datasets for pupal KCs and PNs to identify differentially expressed cell surface molecules between 24-48h APF in comparison with the adult KCs (Figure 8). Based on the PN analysis (Xie et al., 2021; Wong et al., 2023), I postulated that molecules that showed an upregulation in the pupal stages as compared to the adult stages would be of particular interest. Datasets for the PNs and KCs were analysed using the public server of Galaxy and ASAP web applications (Afgan et al., 2016; Galaxy Community, 2022; Gardeux et al., 2017). Annotated and aligned reads were evaluated for differential gene expression using DESeq2 and then normalised using variance stabilising transformation (VST) (Love et al., 2014; Lin et al., 2008). Developing pupa data were compared against adult data, and the threshold for differential gene expression was set to a stringent 2-fold change between pupal vs adult stages (Figure 8).

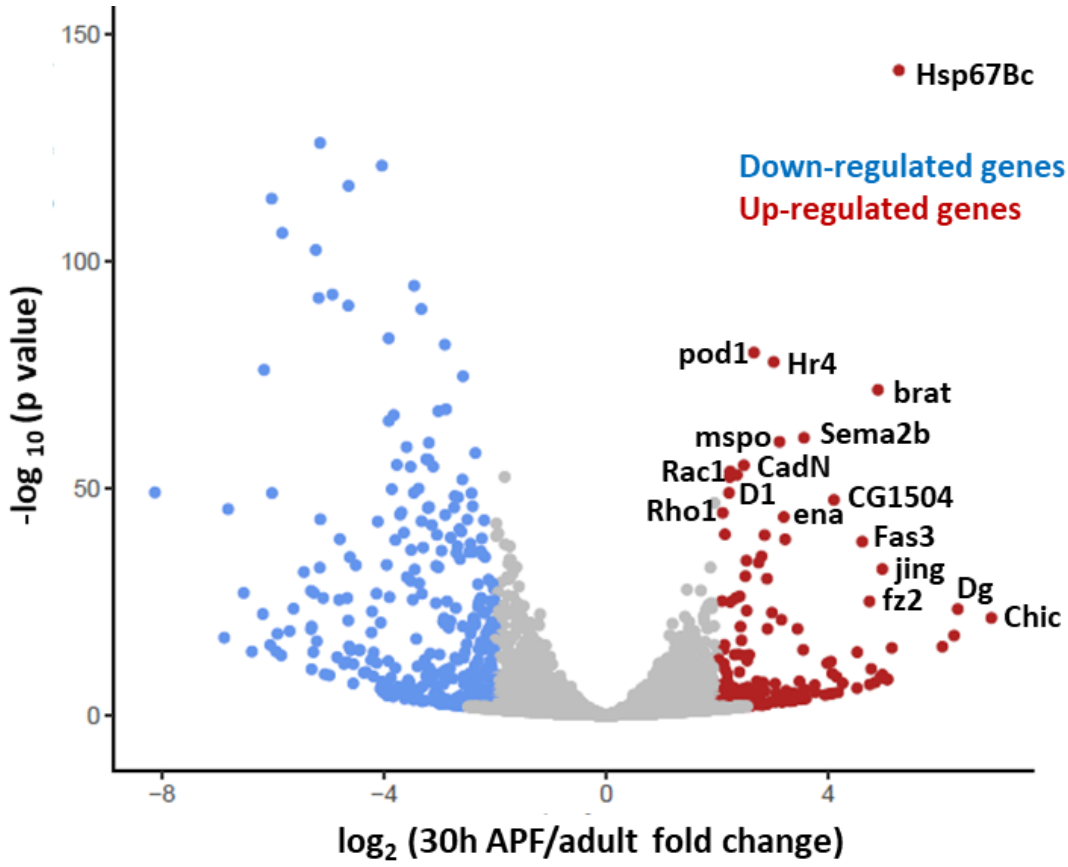

Figure 8. Volcano plot of differentially expressed cell surface molecules in γKCs.

Differential gene expression analysis for cell surface molecules expressed by γKCs in pupal stage 30h APF as compared to the adult. Upregulated genes (red) and downregulated genes (blue) are highlighted. The cut offs used were: log2 (30hAPF/adult fold change) > 2 and –log10 (p value) > 1. Highly upregulated genes are labelled.

The γ KCs show dramatic changes in global expression between larval and early pupal stages (L2 to 9 h APF) followed by more gradual, unidirectional, changes in global expression trends between 9 to 30 h APF (Alyagor et al., 2018). The latest pupal time point in the dataset is of 30h APF and since that is the closest to the wiring phase (24h-48h APF), it was chosen for further analysis and comparison with the adult. The γKCs showed very clear differential expression of cell surface molecules at 30h APF vs adult (Figure 8). Gene ontology analysis of the cell surface molecules that are expressed at more than 2 fold higher levels in 30h pupal γKCs in comparison to adult KCs revealed that these were enriched in axon guidance and synaptic target recognition ontologies and this is consistent with published findings (Alyagor et al., 2018). This suggests that a surface code may be involved to some extent in pupal

wiring of the calyx also for the KCs. I then asked whether the sets of surface molecules expressed by PNs and by KCs at 30h APF were complementary. I found a 30% overlap between known interaction partners expressed in in pupal PNs and pupal KCs (Table 1, in yellow). The upregulated molecules did not include some molecules that have been shown to affect KC-PN interaction in the calyx, such as *lola*, *RhoA* and *trio* (Spletter et al., 2007; Lee et al., 2000; Awasaki et al., 2000). This suggests that these molecules may not be selectively upregulated at pupal 30h stage compared to the adult.

To evaluate the role of these upregulated molecules in calyx wiring, a genetic knockdown screen approach was chosen. I hypothesized that if any of the molecules are vital for PN-KC wiring in the calyx, their knockdown would lead to a wiring defect in the calyx. It is important to note however that the analysed RNA sequencing datasets provide comprehensive information on only 12 subtypes out of the total 50 PN types and on only γ KCs out of the three KC subsets (Xie et al., 2021; Li et al., 2020; Alyagor et al., 2018), and hence not all PN and KCs populations are well represented in the analysis. To overcome this bias, not only individual upregulated molecules, but also other members of their protein family were included to cover the possibility that different molecules within the same gene family could be implicated in the cell types not covered by the RNA sequencing data (Table 1). With this list of 215 candidate molecules, an RNAi screen was planned to look for wiring defects in the calyx.

Candidate cell surface molecules for RNAi screen								
18w	capt	DIP-lambda	dpr5	fog	kek5	Nrg	robo1	sns
acj6	CD98hc	DIP-zeta	dpr6	fra	kek6	Nrk	robo2	spz
Alk	CdGAPr	DIP-α	dpr7	fru	kirre	Nrt	robo3	Sra-1
Arp6	Cdk8	DIP-β	dpr8	fz2	klg	Nrx	rst	Src64B
bdl	CG1504	DIP-ε	dpr9	Gat	ko	ome	scb	Ten-m
beat-Ia	CG1607	DIP-η	drl	Gfrl	Lac	otk	SelR	tey
beat-Ib	CG3036	DIP-θ	Drl-2	GILT1	LanA	PlexA	Sema1a	tinc
beat-Ic	CG31075	DIP-ι	Dscam1	GluRIA	LanB2	PlexB	Sema1b	Tl
beat-IIa	CG34353	DIP-κ	Dscam2	gogo	Lgr1	pod1	Sema2a	Toll-6
beat-IIb	CG42346	dlp	Dscam3	grn	Lola	pot	Sema2b	Toll-7
beat-IIIa	CG44153	dnt	Dscam4	gt	LRP1	Ppn	Sema5c	Tor
beat-IIIb	CG44837	dpr10	dysc	hbs	Ltl	Psc	Shc	trio
beat-IIIc	CG5758	dpr11	E(z)	hig	Meltrin	psidin	shf	trn
beat-IV	CG6218	dpr12	ed	Hsc70-3	mew	ptc	shg	tutl
beat-Va	CG6867	dpr13	Egfr	ImpL2	Mgstl	Ptp36E	side	uif
beat-Vb	CG7381	dpr14	eIF2beta	InR	Mical	Ptp4E	side-III	unc-104
beat-Vc	chb	dpr15	ena	ItgaPS4	mirr	Pvr	side-III	unc-5
beat-VI	chic	dpr17	eph	jbug	Mmp2	Rab6	side-IV	unc-51
beat-VII	Cht2	dpr18	ephrin	jeb	mspo	Rac1	side-IV	uzip
betaTub60D	ctp	dpr19	esn	jing	Mtl	Rac2	side-V	Vang
brat	D1	dpr2	eya	kek1	NetA	rdo	side-VIII	Vmat
Cad87A	Dfmr	dpr20	Fas1	kek2	NetB	rho	side-VIII	Wnt4
CadN	Dg	dpr3	Fas3	kek3	not	Rho1	sli	zfh1
CadN2	DIP-gamma	dpr4	Fdh	kek4	Npc2a	RhoGEF64C	smal	

Table 1. List of 215 molecule candidate resulting from the transcriptomic analysis.

The role of these CAMs in the PN-KC wiring was examined via a pan neuronal RNAi genetic screen. Molecules that show overlapping upregulation at ~30h APF in both PNs and KCs from the transcriptomic analysis are highlighted in yellow

4.2 Investigation of role of candidate molecules in calyx wiring via pan-neuronal RNAi genetic screen

4.2.1 Characterization of the genetic line used for the genetic screen

To verify which molecules from the list of candidates (Table 1) are truly implicated in the developmental assembly and wiring of the calyx, a pan-neuronal RNAi screen was planned and carried out. Knocking down the molecules in all neurons simultaneously allows examination of the role of the molecule irrespective of its required expression

on the pre- or post- synaptic side. This, hence, combines a pre and a post- synaptic screen in one and the exact synaptic role of a chosen molecule can be disentangled later. A similar pan-neuronal screening strategy has proved quite useful in the antennal lobe to elucidate the wiring logic of the ORNS and PNs (Xie et al., 2021). However, a pan-neuronal knockout could possibly lead to unspecific phenotypes in the calyx that are the result of global brain wide defects. The pan-neuronal *Elav^{C155}-Gal4* driver used by Xie et al (2021) in the antennal lobe wiring screen drives expression in post-mitotic neurons; it displays a strong expression in the MB and a slightly weaker but consistent expression in the PNs (Figure 9A, G). The level of expression in other regions of the central nervous system is lower. Based on this information and on the success of the antennal lobe screen (Hong et al., 2012; Xie et al., 2021) I chose to use the same *Elav^{C155}-Gal4* driver line to knock-down molecules pre- and post- synaptically in the calyx.

To visualize the effect of the knockdown of the molecules in the calyx, it was important to include readout elements in the genetic screen line that would help identify the wiring defects. *UAS-Dicer2* construct was utilized to enhance the efficiency of the RNAi mediated knockdown (Dietzl et al., 2007; Robinow and White, 1988; Brand and Perrimon, 1993). To observe general calyx defects as well as any post-synaptic defects a fusion construct *MB247-Dα7-GFP* was used (Kremer et al., 2010). This fusion construct consists of the promoter region MB247 (*mef2* gene) which drives expression in most KCs of a green fluorescent protein-tagged nicotinic acetylcholine receptor subunit *Dα7.* This construct hence expresses GFP at the KC dendritic claws in the calyx (Figure 9B, C) (Kremer et al., 2010). Using this fusion construct helps to distinguish not only all the MGs in the calyx but also the discrete KC post-synapses in each MG, hence any defect in MG size, shape, abundance as well as post synaptic specification would be identifiable.

On the corresponding PN side, a PN line was used that showed robust, specific, and consistent labelling patterns of a few PN subtypes to visualize any bouton distribution or morphology change. For this, the Gal4-independent lexA-lexAop system was utilised to mark the presynaptic active zones in the boutons by expressing *mCherry* tagged Bruchpilot (Brp) in a small subset of PNs using the *GMR68D02-lexA* driver

(Figure 9C, D) (Lai and Lee, 2006; Jenett et al., 2012; Kremer et al., 2010; Schmid et al., 2008). By marking the pre-synaptic active zones in the boutons, this construct not only identifies a reproducible subset of boutons but also helps in revealing pre-synaptic localisation defects. *GMR68D02-lexA* expression was mapped to three uniglomerular food-related subsets of PNs, namely VC3, DL2v, VM5v (Grabe et al., 2015; Laissue et al., 1999; Laissue and Vosshall, 2008; Mansourian and Stensmyr, 2015). This line labels 20 boutons on average, with a broad distribution within the calyx, thereby innervating most areas of the calyx (Figure 9E, F) (Grabe et al., 2015; Laissue et al., 1999). Hence, any alteration in global or local distribution can be isolated., Therefore, the genotype of the final assembled line was: *Elav^{C155}-GAL4, UAS-Dicer2; P{GMR68D02-lexA}, 8xlexAop2-brp-mCherry, MB247-Dα7-GFP*.

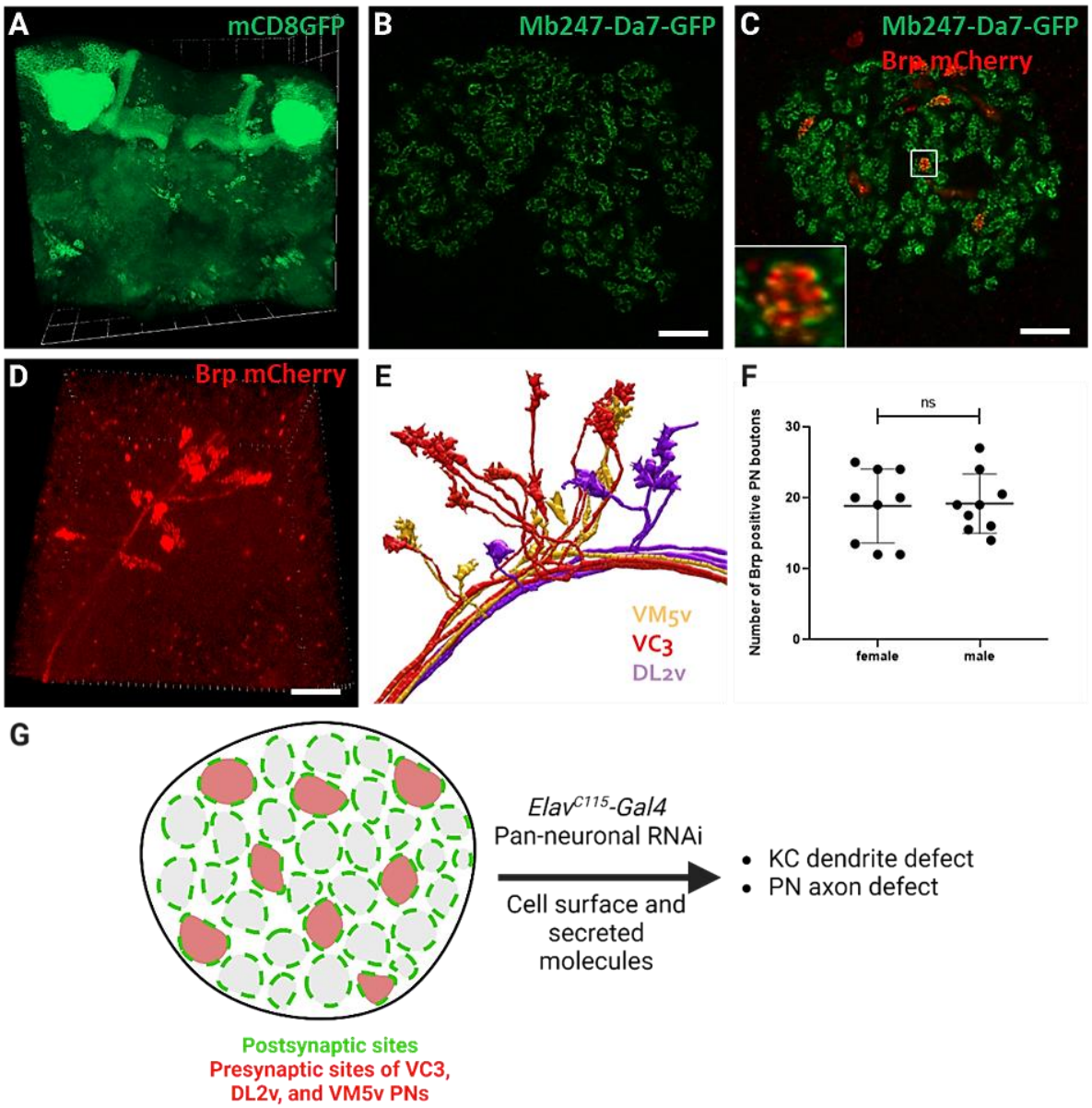

Figure 9. Characterization of the fly line used to carry out pan-neuronal RNAi screen.

(A) *Elav^{C155} - Gal4* driven expression of *mCD8-GFP* is enriched in the MB and AL. (B) Genetic labelling of MGs using *MB247-Dα7-GFP* fusion protein. (C) Synaptic labels visualising juxtaposition of the pre- and postsynaptic sites in the MG. Inset shows zoomed in MG. (D) PN bouton innervation pattern in the calyx for PNs labelled with *GMR68D02-LexA* driving *Brp-mCherry*. (E) Calyx-specific EM reconstruction of the PNs included in the *GMR68D02-LexA* line. (F) Quantification of Brp positive PN boutons in the calyx shows no sexual dimorphism and on average 20 boutons. Bouton counts are mean ± SD (ns, no statistical significance, n = 9 for each group, paired t-test). (G) Schematic representation of the strategy applied for pan-neuronal screening of cell surface molecules to investigate calyx wiring. Scale bar = 10 µm. Genotypes listed in Table 4.

4.2.2 Classification of phenotypes observed as a result of the pan-neuronal RNAi screen

For each of the 215 candidate cell surface molecules, 2 RNAi lines were used to test and confirm the phenotype resulting from the knockdown of a molecule. To avoid off-target effects, only candidates that produced similar phenotypes with both lines were considered for future analysis. For each RNAi cross, the progeny was dissected and analysed 3 days post-eclosion after completion of the refinement phase. This insured that observed changes in the circuit were due to the developmental knockdown and not an artefact of the refinement process. ~6 brains were analysed per RNAi condition. Each brain was dissected, imaged and analysed qualitatively to inspect for any gross changes in the calyx structure. MB lobes, LH and AL were not analysed since the focus was on a calyx specific defect. The calyx of each brain was evaluated for the number of Brp-positive boutons, change in calyx dimensions, change in arrangement of MGs or boutons, and morphology of MGs and the synaptic complexes. Taking these criteria into account, the phenotypes that were observed were:

- Synaptic organization defect (Figure 10B)
- Reduced calyx volume (Figure 10C)
- Gaps in calyx (Figure 10D)
- Altered bouton localization (Figure 11B)
- Decreased bouton number (boutons ≤ 10) (Figure 11C)
- Increased bouton number (boutons ≥ 30) (Figure 11D)

Of these phenotypes, the reduced calyx volume phenotype and gaps in calyx phenotype were seen to occur independently and also in combination with the other phenotypes and hence, were not considered as distinct categories for further analysis.

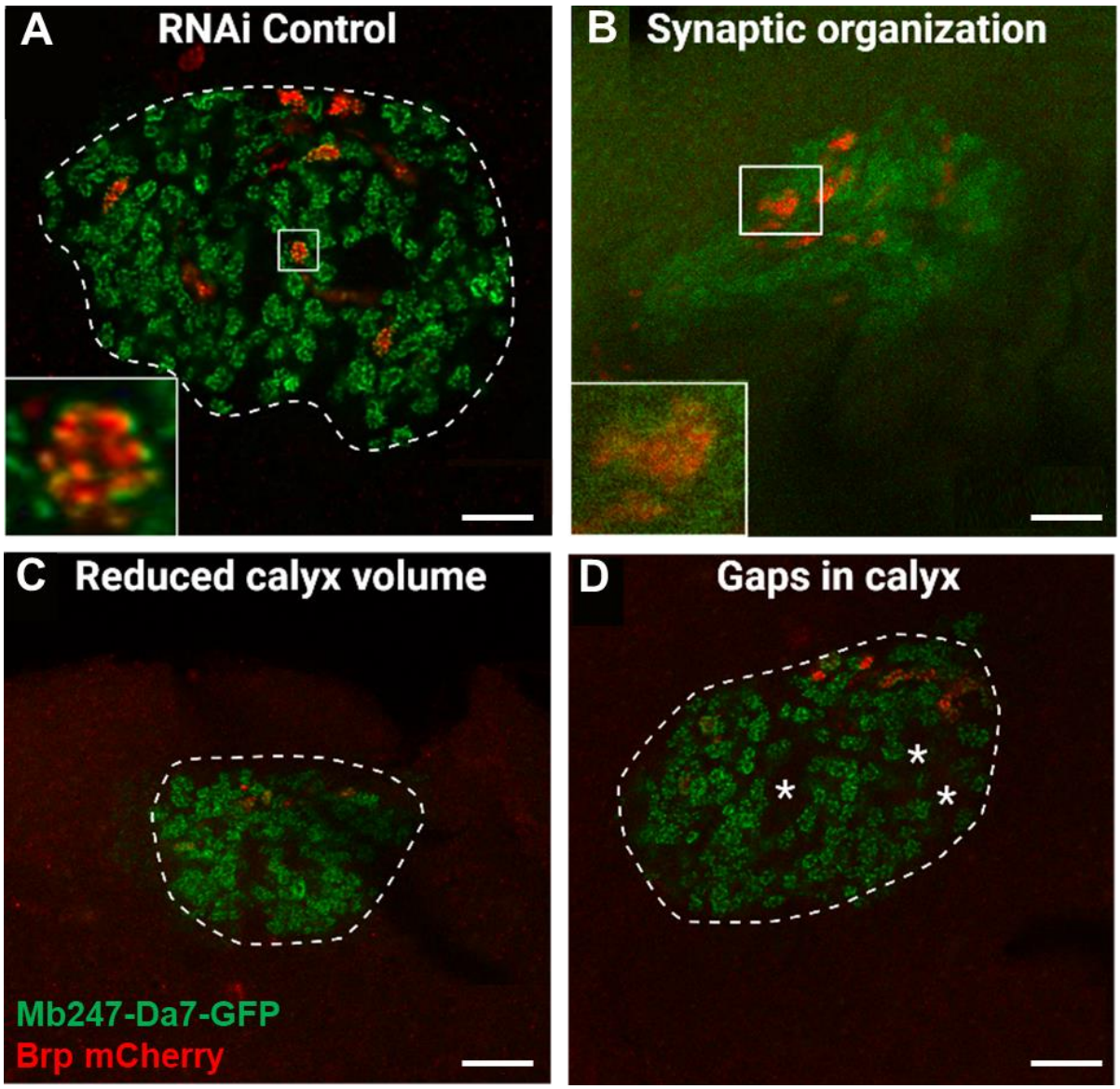

Figure 10. Phenotypes observed with respect to calyx and postsynaptic organization.

(A) RNAi control with synaptic labels visualising juxtaposition of the pre- (red) and post- (green) synaptic sites in the MGs. Inset shows zoomed-in MG. (B) Loss of localization of postsynaptic labelling. Inset shows overabundance of presynaptic labelling and diffuse postsynaptic labelling. (C) Overall reduction in calyx volume. (D) Calyx exhibits empty spaces or “gaps” in the calyx volume, as highlighted by the asterisks (✱). Scale bar = 10 µm. Genotypes listed in Table 4.

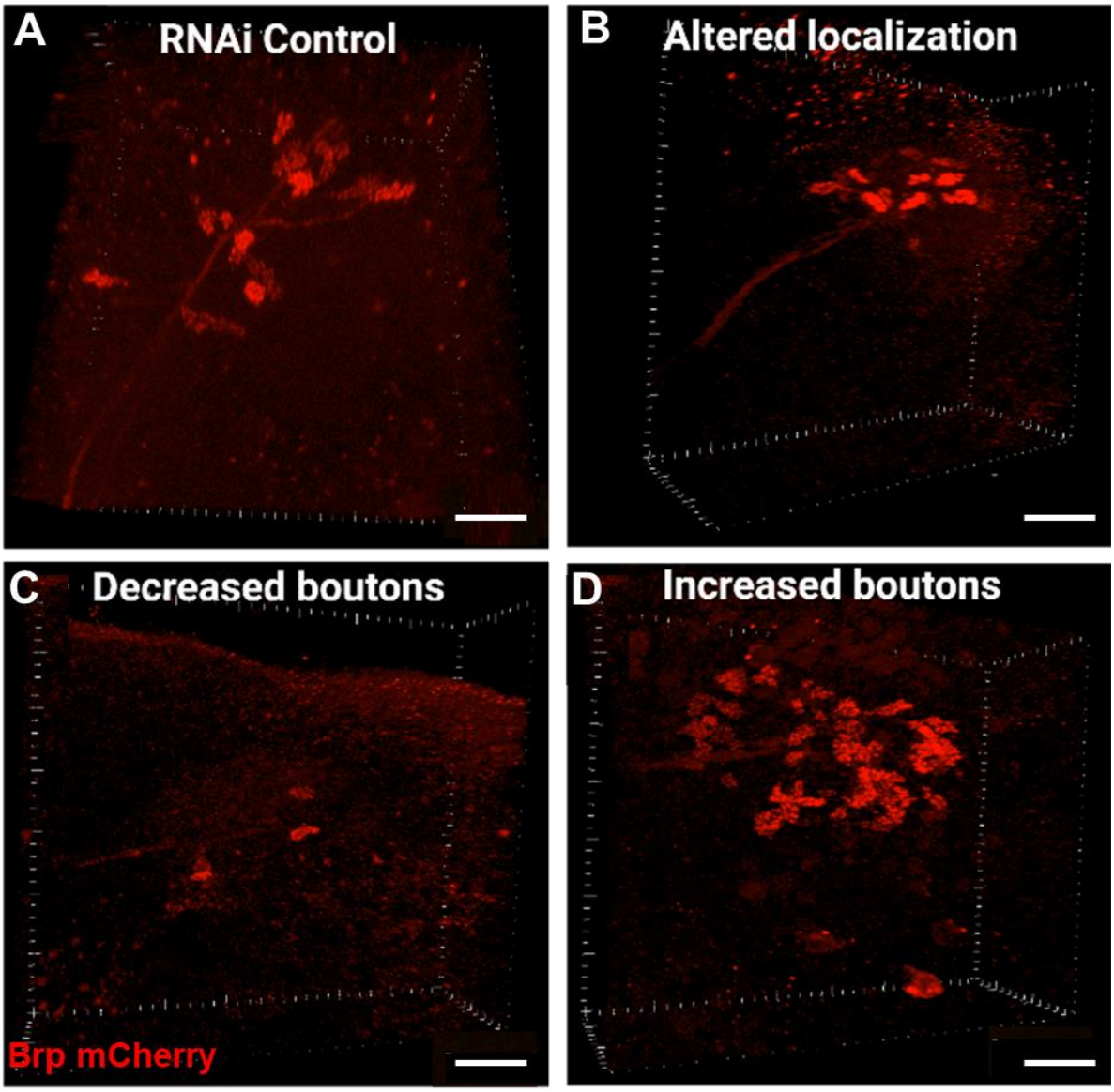

Figure 11. Phenotypes observed with respect to presynaptic bouton formation.

The pre-synaptic boutons of VC3, DL2v, and VM5v PNs were visualized by expressing lexAop-Brp-mCherry under the control of *GMR68D02-lexA* to highlight the PNs boutons and their presynaptic sites. (A) RNAi control shows presence of 20 boutons distributed within the calyx volume. (B) Bouton distribution pattern shows altered localization of boutons in only one area (here, dorsal) of the calyx. (C) Reduction in the number of boutons labelled by *GMR68D02-lexA*. Image shows presence of 4 boutons which is an 80% reduction from the average of 20 boutons in the control. (D) Stark increase in the number of boutons labelled by *GMR68D02-lexA*. Image shows presence of ~70 boutons, which is a 3.5-fold increase from the average of 20 boutons in the control. Scale bar = 10 µm. Genotypes listed in Table 4.

Molecules exhibiting the final phenotypes of interest, namely synaptic organization defect, altered bouton localization, decreased bouton number and increased bouton

number, were selected. I cross-referenced the known interaction partners (ligand/ receptor) for these molecules (Table 2). Each pair was evaluated based on type of interactions, published literature, and availability of tools. Eventually one pair was chosen for further analysis in this study.

Molecules of interest	
Altered bouton localization	**Synaptic organization defect**
Npc2a – Chb	Sema1a – PlexA, otk
DIP eta – DPR2, DPR3, DPR4, DPR7	Sli – Robo2, Robo3
Shc – Tor	
Decreased bouton number	**Increased bouton number**
Sns – hbs, rst, kirre, lar	DIP kappa – DPR2, DPR7
Cyfip – Dfmr1	Eph – Ephrin
DIP zeta – DPR19	Alk – Jeb

Table 2. Molecules and their interaction partners shortlisted after phenotype analysis of the RNAi screen

4.2.2.1 Altered bouton localization

Npc2a – Chb

Npc2a and Chb are both upregulated at 30h in γKCs. Knockdown of *npc2a* or *chb* both display an altered bouton localization. NPc2a is implicated in regulating sterol homeostasis and steroid biosynthesis (Huang et al., 2007). Npc2a was shown to selectively interact with Chb, a molecule associated with microtubule dynamics (Lowery et al., 2010; Inoue et al., 2000). However, Chb also interacts with various other molecules to regulate kinetochore-microtubule interaction (Lowery et al., 2010). Both molecules are implicated in regulating essential and fundamental growth programs, and are expressed only in the KCs at 30h APF. This suggests that the phenotype observed may be due to overall brain developmental defects not only altered PN-KC wiring.

DIP-eta – DPR2, DPR3, DPR4, DPR7

DIP/Dpr interaction pairs belong to Immunoglobulin superfamily of proteins, and have been shown to regulate patterns of synaptic connectivity in the *Drosophila* visual

system (Tan et al., 2015). They have also been shown to regulate self-adhesion and sorting of axons of the ORNs in the AL (Barish et al., 2018). In the current screen, *DIP-eta* knockdown leads to an altered localization effect. However, its interacting partners do not show the same phenotype but rather a reduction in bouton number. DIP-eta has also been shown to form homodimers as well as heterodimers to regulate cell adhesion (Cheng et al., 2019). Its interaction with its multiple interaction partners (Dprs) is regulated by the presence of other Dpr family members (Sergeeva et al., 2020). Taken together, this presents a fascinating yet complex interaction pattern to be employed for calyx wiring.

Shc – Tor

SHc and tor are both implicated in receptor tyrosine kinase signalling and regulate Torso and EGFR signalling pathways (Gayko et al., 1999; Luschnig et al., 2000). Hence, these molecules are required for essential growth programs in the cell. Additionally, only knockdown of Shc produces a phenotype but the knockdown of Tor does not produce any phenotype, indicating that the phenotype may be due to a gross developmental defect due to altered Shc signalling.

4.2.2.2 Synaptic organization defect

Sema1a – PlexA, Otk

Sema1a belongs to the semaphorin family of proteins and functions to regulate synapse formation, axon guidance and dendrite targeting (Kolodkin et al., 1993; Godenschwege et al., 2002; Cafferty et al., 2006). In the AL, Sema1a is distributed as a gradient and is used as landmarks by PNs for glomerular targeting of dendrites (Komiyama et al., 2007). Some PNs also depend on Sema1a to accurately target their axons in the calyx (Komiyama et al., 2007). In the MB, Serma1a and PlexinA interaction was observed to control axon outgrowth and guidance (Zwarts et al., 2016). However, in the current calyx-specific analysis, only synaptic organization was seen to be affected with no other organization defects. In addition, the interacting partners did not exhibit any phenotype. This suggests that due to reduction of Sema1a, the wiring is largely unaffected but the organization of the PN-KC synapses is severely affected.

Sli – robo2, robo3

During brain development, Sli was found to be enriched in the MB calyx and regulates axon growth in the vicinity of the calyx via Robo receptors (Oliva et al., 2016). From the current analysis, *sli* was indeed found to be upregulated in the KCs at 30h APF. However, pan-neuronal knockdown of *sli* affected synaptic organization but showed no other obvious wiring defects. Its interaction partners also displayed no phenotype.

4.2.2.3 Decreased bouton number

Sns – hbs, rst, kirre, lar

Sns belongs to an Immunoglobulin subfamily called Irre cell recognition module (IRM) proteins, which includes: Sns, Kirre, Roughest (Rst), and Hibris (Hbs) (Fischbach et al., 2009). These molecules function together in various processes such as myoblast fusion, cell sorting, axonal pathfinding, and target recognition in the optic neuropils of *Drosophila* (Fischbach et al., 2009). Recent work shows that the Lar and Sns interaction regulates morphogenesis of α/β and α′/β′ lobes of the adult MB and R7 photoreceptor axon targeting (Bali et al., 2022). In the current RNAi screen, Sns (~5 boutons), hbs (~7 boutons) and Lar (~10 boutons) showed a reduction of bouton numbers while kirre and rst did not show any observable phenotype. From the RNA sequencing analysis, the PNs expressed the different IRM molecules at similar levels but these molecules were not seen to be upregulated in the KCs at 30h APF. How these molecules interact to regulate PN bouton numbers in the calyx, is an interesting avenue for future studies.

Cyfip – Fmr1

The Cyfip-Fmr1 interaction shows a reduction in bouton number phenotype in the current pan-neuronal screen (~8 boutons in either knockdown). Cyfip is a molecule involved in the WAVE (WASP family Verprolin homolog) regulatory complex that controls actin cytoskeleton remodelling and interacts with Fmr1 (Schenk et al., 2003; Schenk et al., 2004). It also regulates synaptic organization (Galy et al., 2011). While both Cyfip and Fmr1 are not CAMs, they were included in the screen as they were found by Li et al (2020) to be wiring regulators in the AL via a surface proteomic screen. Since, these molecules regulate complex cellular regulatory pathways, it is difficult to ascertain the exact interaction leading to the observed reduced bouton number

phenotype. Hence, these molecules were not chosen for further analysis in the context of PN-KC wiring.

DIP zeta - DPR19

Upon pan-neuronal knockdown, DIP-zeta showed a slight reduction of bouton numbers (~14 boutons) while DPR19 knockdown did not produce any viable progeny. DIP-zeta was seen to be upregulated at 30h APF in KCs but not in PNs in my analysis. The lack of viable progeny after knocking down DPR19 suggests that it may play a vital role in neuronal development and/or survival. This needs further investigation before the role of the molecules can be tested in context of the calyx wiring and hence, these molecules were not analysed further.

4.2.2.4 Increased bouton number

DIP-kappa - DPR2, DPR7

Upon pan-neuronal knockdown, DIP-kappa (~40 boutons) showed an increase in bouton numbers while its interaction partners Dpr2 (~9 boutons) and Dpr7 (~7 boutons) showed an opposite phenotype of decreased bouton numbers. DIPs and Dprs exhibit complex interactions between each other, with some capable of exhibiting compensatory mechanisms (Xu et al., 2018; Bornstein et al., 2021). Hence, these moleclues were not analysed further.

Eph - Ephrin

Ephrin-Eph interaction is well documented to play a role in the development of nervous system in vertebrates as well as invertebrates (Kania and Klein 2016). In *Drosphila*, Eph and Ephrin instruct the dendrodendritic segregation during the glomerular olfactory map formation in the AL (Sakuma et al., 2014; Anzo et al., 2017). In the MB, this molecule pair acts to guide a subset of MB axons to their accurate synaptic target (Boyle et al., 2006). Eph or Ephrin, when knocked down pan –neuronally, both display an increase in bouton numbers (~37 boutons for each molecule). This interaction and its phenotype is an interesting avenue for future studies and was not analysed during this thesis.

Alk- Jeb

Alk is a transmembrane receptor tyrosine kinase that binds exclusively to the secreted ligand Jeb, regulating multiple conserved downstream kinase signalling cascades like the Ras/ERK and PI3K signalling pathways (Lorén et al., 2003; Englund et al., 2003). Alk expression in the mushroom body regulates long-term memory formation, and has been suggested to be present in the KC claws, while its ligand Jeb would be localized on the PN boutons (Bai and Sehgal, 2015; Gouzi et al., 2011; Gouzi et al., 2018). Disrupted Alk signalling also increased the levels of apoptosis and altered neuronal fate specification in MB-NB lineages that persisted into adulthood (Pfeifer et al., 2022). These findings along with the interesting increased bouton phenotype (~42 boutons) make Alk and Jeb a very interesting pair to study in the context of calyx wiring. In addition, the availability of useful genetic tools allows the possibility to investigate the genetic and functional aspects of Alk-Jeb interaction employed in the PNs and KCs. Hence, Alk and Jeb were chosen for further analysis.

4.3 Effect of *alk* or *jeb* knockdown in the calyx

On pan-neuronal knockdown of *alk*, the number of *Brp*-positive boutons was increased (~42 Boutons) (Figure 12 D-F, M). However, the pan neuronal knockdown of its ligand *jeb*, led to the opposite phenotype of a decrease in number of boutons (~15 boutons) (Figure 12 J-L, M). Other than Jeb no ligands have been reported for Alk yet. According to RNA single cell sequencing analysis, *alk* and *jeb* are both expressed at similar levels in both KCs and PNs. In the visual system as well as the visceral mesoderm, the Alk knockdown phenotype matches that of the phenotype of Jeb knockdown (Lorén et al., 2003; Englund et al., 2003; Bazigou et al., 2007). These studies also indicate a trans-interaction of Alk and Jeb. However, in the current pan-neuronal RNAi screen, Alk or Jeb knockdown display opposing phenotypes, indicating that the interaction in the calyx may not purely be a trans-interaction between the PNs and KCs.

In the MB, Alk acts as a negative regulator of olfactory learning, such that *alk* activation leads to learning defects (Gouzi et al., 2011). Studies indicate that *alk* acts as an upstream activator of Nf1-regulated neuronal Ras/ERK signalling cascades that contribute to organismal growth and learning (Gouzi et al., 2011). Disruption of Alk signalling also shows increased body size (Gouzi et al., 2011). Over activation of Alk

signalling led to ectopic expression of cell identity genes likes *Mamo* in γKCs (Pfeifer et al., 2022). In the context of this data, the Alk knockdown phenotype of increased boutons may be attributed to a loss of regulation of growth mechanisms that determine PN bouton and/or KC claw numbers in the calyx.

To understand the mechanisms resulting in the pan-neuronal knockdown phenotype, it is important to decipher what role *alk* or *jeb* play in KCs or PNS. To delineate the pre- or post- synaptic role of the Alk-Jeb molecule pair, I generated lines that included the elements necessary to define the postsynaptic densities on KCs and the presynaptic active zone of the VC3, DL2v and VM5v PNs. These elements (*P{GMR68D02-lexA}, 8xlexAop2-brp-mCherry, MB247-Dα7-GFP*), were the same elements used in the original pan-neuronal screen but here included Gal4 drivers specific only for PNs or only for KCs. The Gal4 driver line *OK107-Gal4 (eyeless* gene*)* was used to drive RNAi in all postsynaptic KCs, while the driver line *Acj6-Gal4* was (*acj6* gene) used to drive expression in 70% of all presynaptic PNs, including the *Brp*-positive PNs labelled by the screen line (Connolly et al., 1996; Bourbon et al., 2002). The pre- or post-synaptic knockdown of Alk or Jeb resulted in the same phenotype as seen in the pan neuronal knockdown of either Alk or Jeb. This suggested that both molecules might be required pre- as well as post-synaptically to some degree (Figure 12 D-F, N, J-K, O).

In addition to the RNAi constructs used to knockdown Alk or Jeb, a dominant negative (DN) construct was used (*UAS-Alk^{DN}*) which has been employed interchangeably with the Alk mutant allele (Lee et al., 2003; Gouzi et al., 2011; Georganta et al., 2021; Pfeifer et al., 2022; Durkin et al., 2023). The DN construct lacks the intracellular PTK domains and expresses a truncated protein that only possess the transmembrane and extracellular domain of Alk. The truncated DN construct dimerizes with the wild-type Alk, but does not allow downstream signalling in the absence of the PTK domain. Interestingly, expressing the *Alk^{DN}* construct in either the KCs or PNs, shows a similar phenotype of decreased bouton number that is seen with Jeb knockdown for pre- or post- synaptic manipulation (Figure 12, H-I, N, K-L, O).

Taken together, the data suggest that *alk* and *jeb* might be required both pre- and post-synaptically. The data obtained using the Alk^{DN} construct suggests a possible multifaceted role of the Alk and Jeb interaction where loss of function due to the truncated protein might disrupt cellular signalling pathways that may still be weakly activated in the case of the RNAi mediated knockdown. Hence, the phenotype observed needs verification with a loss of function mutant.

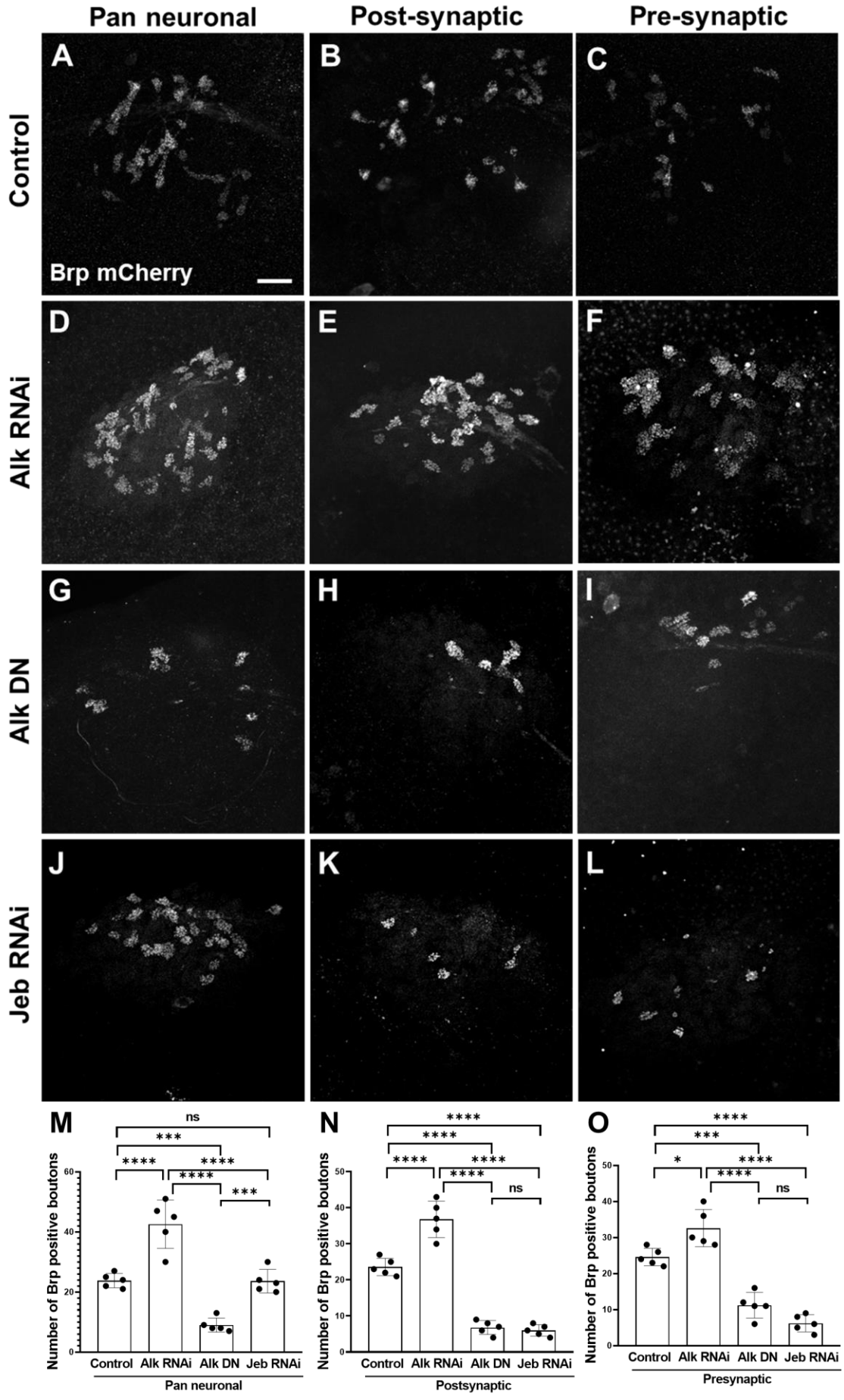
Pan neuronal
Post-synaptic
Pre-synaptic
Control
Alk RNAi
Alk DN
Jeb RNAi
A
B
C
D
E
F
G
H
I
J
K
L
Brp mCherry
M
N
O
Number of Brp positive boutons
Control
Alk RNAi
Alk DN
Jeb RNAi
Pan neuronal
Postsynaptic
Presynaptic
ns
****
***
*

Figure 12. Change in number of boutons in response to knockdown of *alk* or *jeb*.
(A, B, C) in controls, ~20 boutons on average are distributed throughout the calyx. (D, G, J, M) Change in bouton number in response to pan-neuronal *Elav^{C155}-Gal4* driven expression of *Alk-RNAI*, *Alk^{DN}*, and *Jeb-RNAi* constructs respectively. (E, H, K, N) Change in bouton number in response to postsynaptic *OK107-Gal4* driven expression of *Alk-RNAi*, *Alk^{DN}*, and *Jeb-RNAi* constructs respectively. (F, I, L, O) Change in bouton number in response to presynaptic *Acj6-Gal4* driven expression of *Alk-RNAi*, *Alk^{DN}*, and *Jeb-RNAi* constructs respectively. Scale bar = 10µm. Bouton numbers are represented as mean ± SD (n = 5 for each group, one-way ANOVA). Statistical significance was defined as p≤0.05 = *, p≤0.01 = **, p≤0.001 = ***, p≤0.0001 = ****. Genotypes listed in Table 4.

4.4 Expression and localization of Alk-Jeb

Published literature suggests the expression of Alk as well as of Jeb in the calyx using anti-Alk and anti-Jeb antibodies (Ab) (Gouzi et al., 2018). Analysis of RNAi-sequencing data indicated that Alk and Jeb are expressed in KCs as well as PNs. Therefore, to verify the actual localization of this receptor-ligand pair, Ab staining was carried out on dissected brain tissue from flies with the genotype: *;UAS-mCD8GFP;;OK107-Gal4.* In these flies, membrane bound GFP is expressed in all KCs under the *OK107* enhancer trap gal4 driver. Confocal images of the Ab staining suggest an enrichment of Alk in KC dendrites and enrichment of Jeb in PN boutons (Figure 13). However, the synaptic structures in the MGs are too compact to be easily resolved using confocal imaging and hence the localization of these proteins needs to be verified in the context of their knockdown to ascertain their localization.

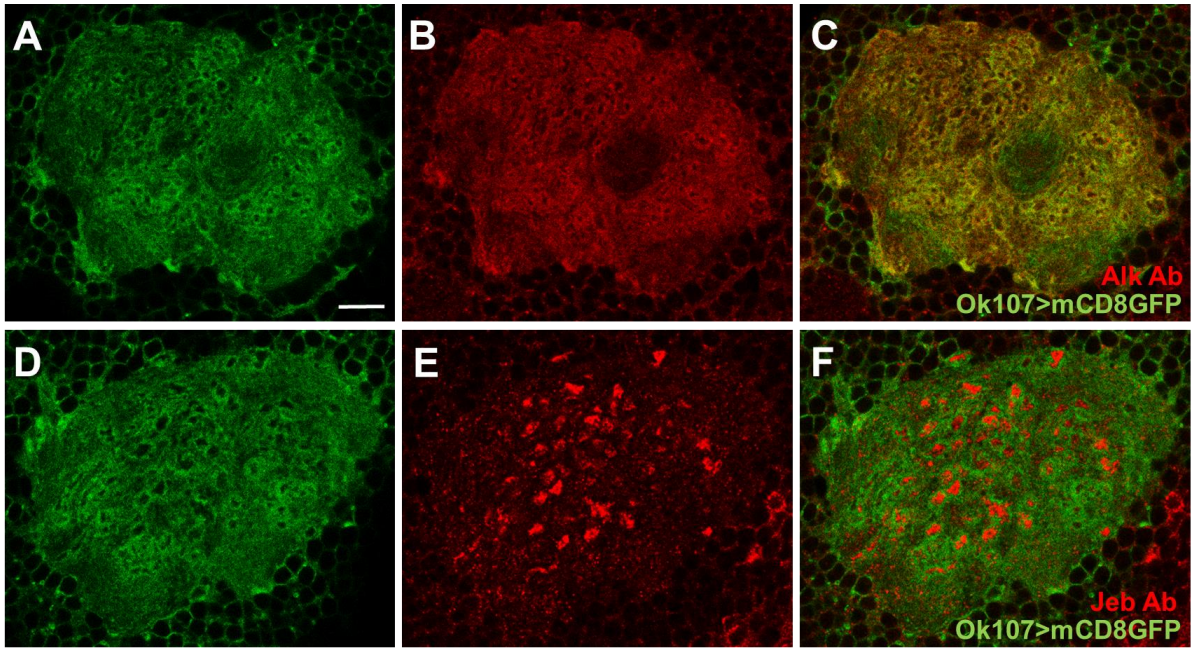

Figure 13. Localization of Alk and Jeb in the MB calyx.

(A, B, C) Alk Ab (in red) staining in brains expressing *mCD8-GFP* (in green) in KCs suggest dendritic localization of Alk in KCs in the calyx. (D, E, F) Jeb Ab (in red) staining in brains expressing *mCD8-GFP* (in green) in KCs suggest PN axonal bouton localization of Jeb. Scale bar = 10µm. Genotypes listed in Table 4.

4.4.1 Validation of Antibody specificity in the calyx

To confirm the cellular specificity of the antibodies in recognizing Alk and Jeb in the KCs and PNs, the antibodies were validated by carrying out Ab staining in an RNAi background. The pan-neuronal screen line with the genotype *Elav^{C155}-GAL4, UAS-Dicer2; P{GMR68D02-lexA}, 8xlexAop2-brp-mCherry, MB247-Dα7-GFP* was used to drive RNAi of Alk or Jeb and these brains were labelled with anti-Alk and anti-Jeb antibodies. In the control, the Alk Ab localization overlapped with the postsynaptic *MB247-Dα7-GFP* signal in the calyx and showed a very diffuse and low level of expression in the AL (Figure 14 A-D). Upon knockdown of *alk*, no Alk localization was observed in the calyx as well as the AL (Figure 14 E-H), supporting the fact that the antibody is specific and that the detected signal in the calyx derives from the endogenous Alk. Upon knockdown of *jeb*, the Alk expression pattern was similar to that seen in the control (Figure 14 I-L). This suggests that the localization of Alk in the calyx does not depend upon Jeb.

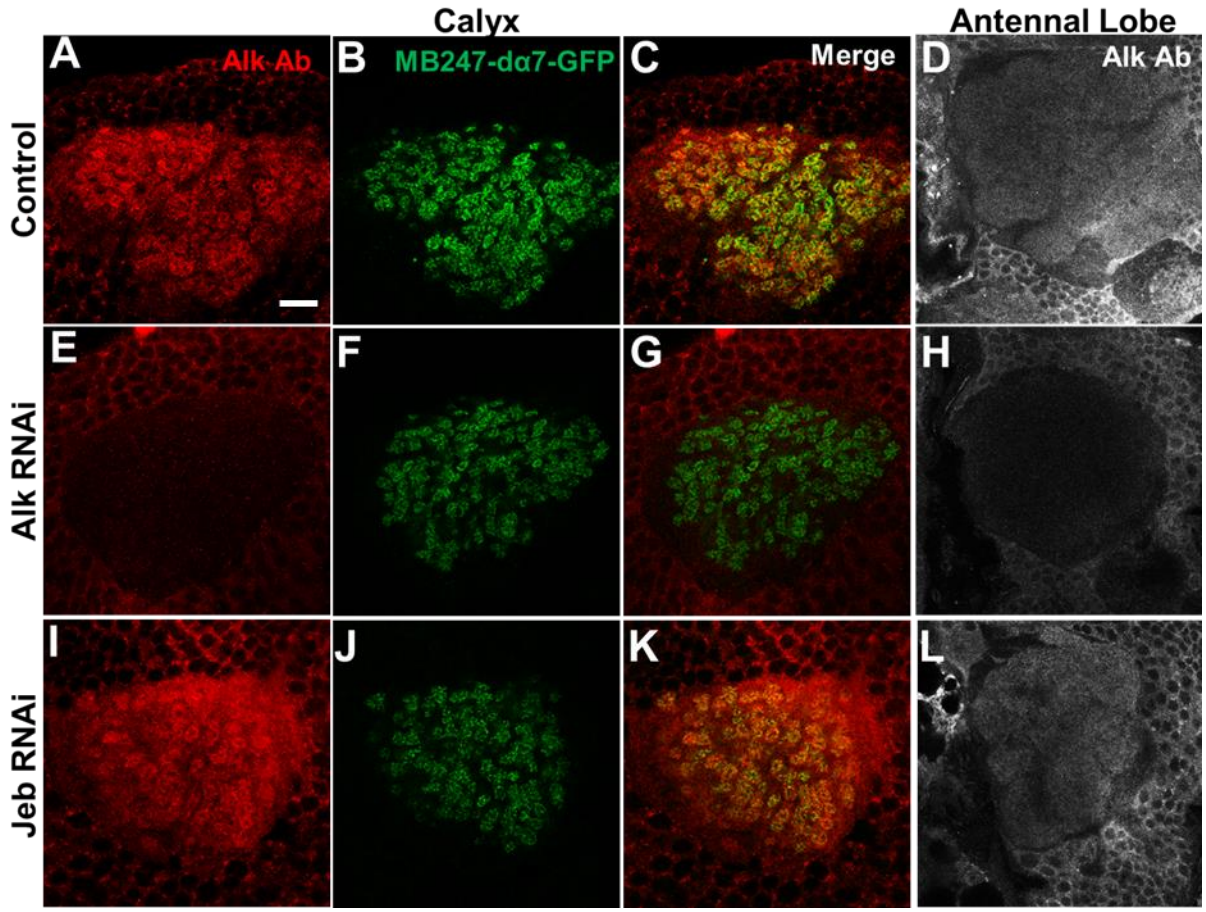

Figure 14. Validation of anti-Alk Ab specificity in the calyx and AL.

(A-D) Alk Ab (in red) in control condition shows KC dendritic localization in calyx and a diffuse localization in the AL. (E-H) Pan-neuronal *alk* knockdown with *Alk-RNAi* shows loss of Alk in the calyx and AL. (I-L) Pan-neuronal *jeb* knockdown with *Jeb-RNAi* shows no apparent effect on Alk localization in the calyx and AL. Scale bar = 10µm. Genotypes listed in Table 4.

Regarding the anti-Jeb antibody, in the control line Jeb localization was confined to the PN boutons in the calyx and, in the AL Jeb was detected in most PN glomeruli (Figure 15 A-D). Upon knockdown of *alk*, the Jeb expression pattern was similar to that seen in the control (Figure 15 E-H). Upon knockdown of *jeb*, no Jeb localization was observed in the calyx or in the AL (Figure 15 I-L). These data support that the anti-Jeb Ab is specific for the Jeb protein and that the signal detected with the anti-Jeb antibody in the calyx is primarily derived from the Jeb protein. They also suggest that the localization of Jeb in the calyx does not depend upon Alk.

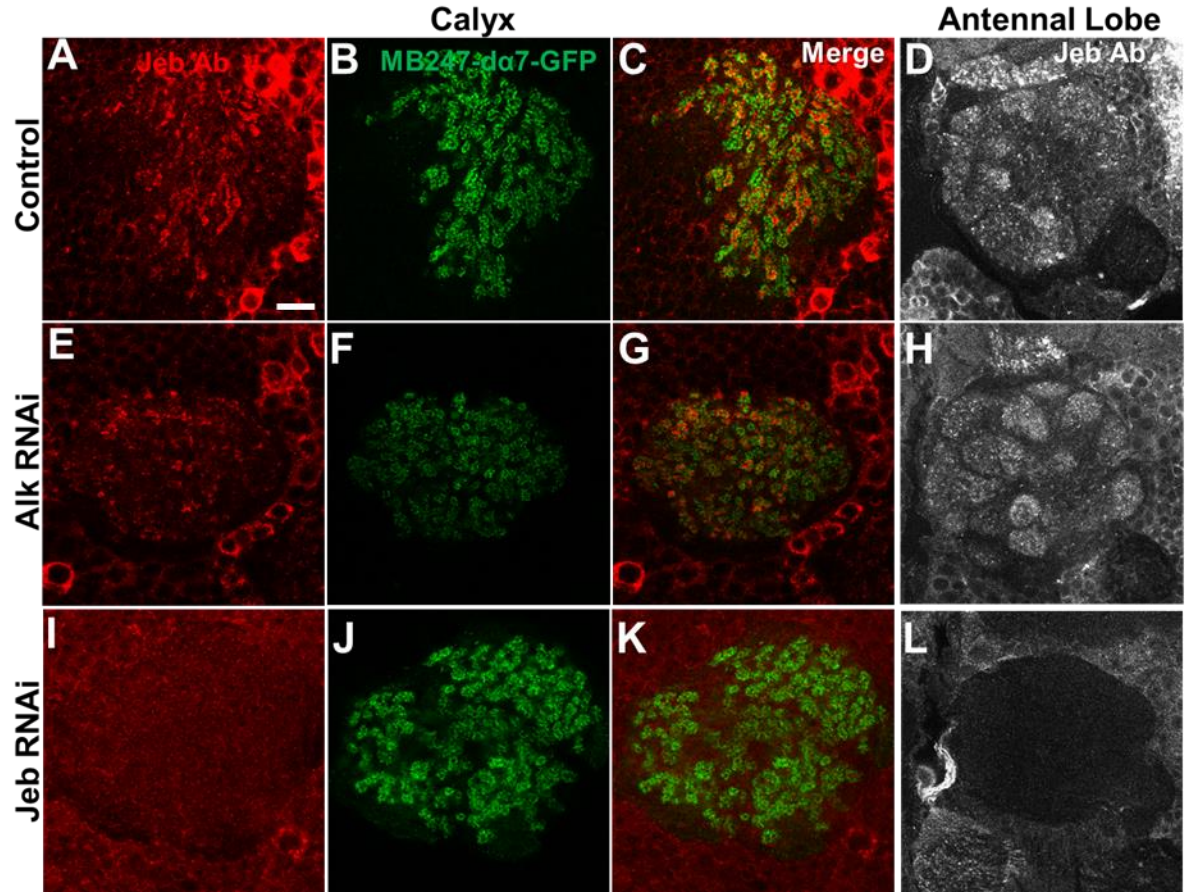

Figure 15. : Validation of anti-Jeb Ab specificity in the calyx and AL.

(A-D) Jeb Ab (in red) staining in control condition shows PN axonal bouton localization in calyx and a localization in distinct glomeruli in the AL. (E-H) Pan-neuronal *alk* knockdown with *Alk-RNAi* shows no apparent effect on Jeb localization in the calyx and AL. (I-L) Pan-neuronal *jeb* knockdown with *Jeb-RNAi* shows a loss of Jeb localization in the calyx and AL. Scale bar = 10µm. Genotypes listed in Table 4.

4.5 Interdependence of Alk and Jeb localization

To further investigate and verify whether Alk or Jeb are localised at pre- or post-synaptic structures and to determine if there is an interdependence in their localization patterns, antibody stainings were carried out in the background of presynaptic or postsynaptic knockdown of Alk and Jeb.

4.5.1 Presynaptic knockdown of *alk* or *jeb*

Alk localization

Knockdown of *alk* in the PNs using the *Acj6-Gal4* driver displayed a slightly diffuse localization of Alk in the calyx and no detectable specific signal in the AL. This suggests that not all the signal detected in the calyx derives from the KCs, in contrast to previous reports (Gouzi et al., 2018), but that part of Alk in the calyx is expressed in the PNs. In addition, this raises the possibility that the localization of Alk in the calyx depends on presynaptic Alk. The Alk Ab is generated against the amino acids 30-316 of the Alk molecule and recognizes the extracellular part of Alk. Hence, this antibody is capable of also recognizing the Alk^{DN} construct.

Expression of the Alk^{DN} construct in PNs showed ectopic expression of Alk in the AL and very diffuse localization of Alk in the calyx (Figure 16 A-D), again supporting the view that functional presynaptic Alk might be required for the discrete localization of Alk within MGs. Alternatively, the overexpression in the PNs of the Alk extracellular domain present in the Alk^{DN} might per se have an effect on Alk localization. When *jeb* was knocked down, the Alk localization was diffuse in the calyx but the Alk signal in the AL remained unaffected (Figure 16 I-L, compare with Figure 14 A-D). Therefore, Jeb is required presynaptically to localize Alk at the KC postsynaptic sites and potentially at the presynaptic PN membrane.

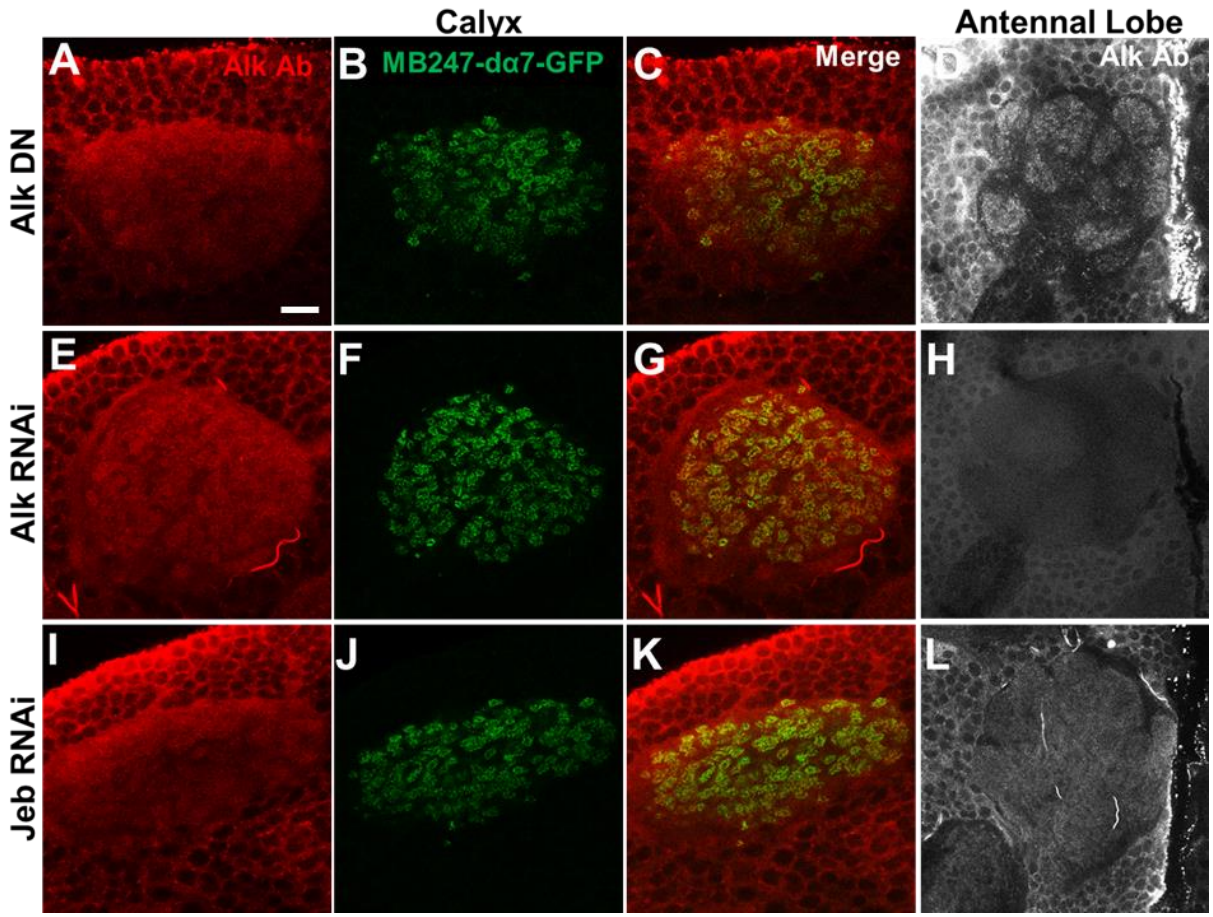

Figure 16. Change in localization of Alk in response to presynaptic knockdown of *alk* or *jeb*.
(A-D) *Alk*^{DN} shows a diffuse localization in calyx and an ectopic localization of Alk Ab (in red) in AL. (E-H) Knockdown of *alk* shows diffuse localization in calyx and no localization of Alk in the AL. (I-L) Knockdown of *jeb* shows diffuse localization of Alk in calyx, but the localization of Alk in AL is unaffected. Scale bar = 10µm. Genotypes listed in Table 4.

Jeb localization

Knockdown of *alk* in the PNs using the *Acj6-Gal4* driver did not affect the Jeb localization in the calyx or the AL (Figure 17 E-H, compare with Figure 15 A-D). This suggests that Jeb localization in the calyx and AL is independent of pre-synaptic Alk. Expression of the *Alk*^{DN} construct also did not show a significant effect on Jeb localization (Figure 17 A-D), supporting the claim that pre-synaptic Alk is not required for proper localization of Jeb. After knocking down *jeb* in the PNs, the calyx and the AL showed considerably reduced and diffuse expression of Jeb (Figure 17 I-L, compare with Figure 15 A-D). Since the Ab is specific, the presence of Jeb in the calyx can be due to the expression of Jeb in PNs that are *acj6* negative and therefore not affected in this experiment. It is also possible that KCs may express low levels of Jeb.

In the AL, the Jeb signal is probably derived from *acj6* negative PNs as well as from ORNs since RNA-sequencing data suggests that all ORNs express Jeb. Therefore, Jeb localization in the calyx and AL seem to be independent of pre-synaptic Alk. Taken together, most of the Jeb signal detected in the calyx appears to be derived from the PN boutons, but Jeb seems to also be expressed in KCs, albeit at low levels.

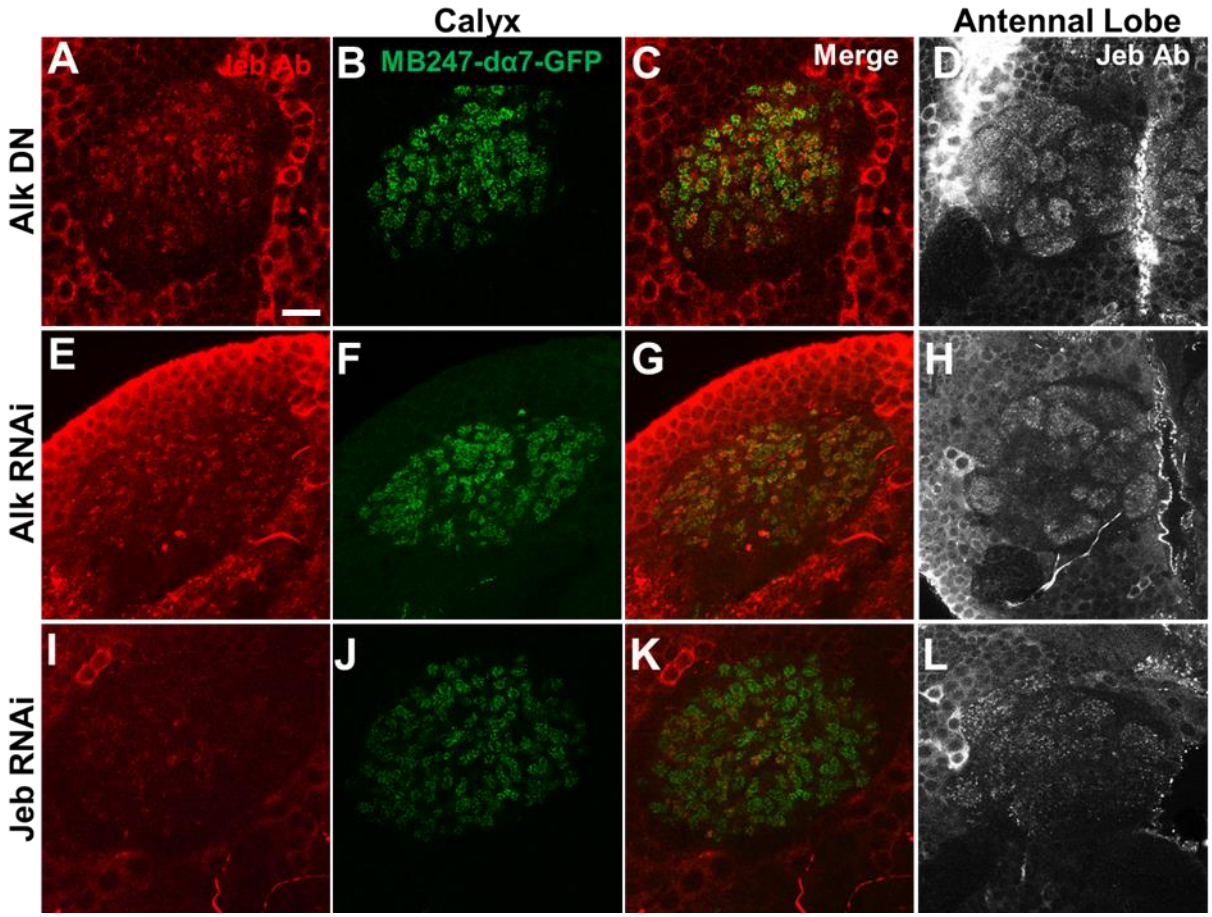

Figure 17. Change in localization of Jeb in response to presynaptic knockdown of *alk* or *jeb*.
(A-D) Alk^{DN} shows no significant effect on Jeb (in red) localization in calyx as well as AL. (E-H) Knockdown of *alk* shows no significant effect on Jeb localization in calyx as well as AL. (I-L) Knockdown of *jeb* shows significantly reduced localization of Jeb in the calyx and Jeb localization in the AL is likely due to the ORN-specific expression of Jeb. Scale bar = 10 µm. Genotypes listed in Table 4.

4.5.2 Postsynaptic knockdown of Alk or Jeb

Alk localization

Knockdown of *alk* in the KCs using the *OK107-Gal4* driver displayed an absence of Alk in the calyx and no change in the localization in the AL (Figure 18 E-H, compare with Figure 14 A-D). This indicates that Alk detected in the calyx is primarily associated with its expression in the post-synaptic KCs Expression of the Alk^{DN} construct showed a similar effect as the *alk* knockdown in the calyx (Figure 18 A-D). In addition, expression of the Alk^{DN} construct also showed an ectopic localization of Alk at the MB lobes, that are devoid of Alk localization in control conditions (data not shown). This suggests that the Alk^{DN} construct mislocalizes endogenous Alk. When *jeb* was knocked down, Alk expression was considerably reduced and showed diffuse expression in the calyx (Figure 18 I-L). This suggests that post-synaptic Jeb plays a role in Alk localization in the MGs. In the AL, no change was seen in Alk localization in response to *alk* or *jeb* knockdown or when Alk^{DN} construct was expressed. This indicates that Alk localization in the AL is independent of KC-specific expression of *alk* or *jeb*.

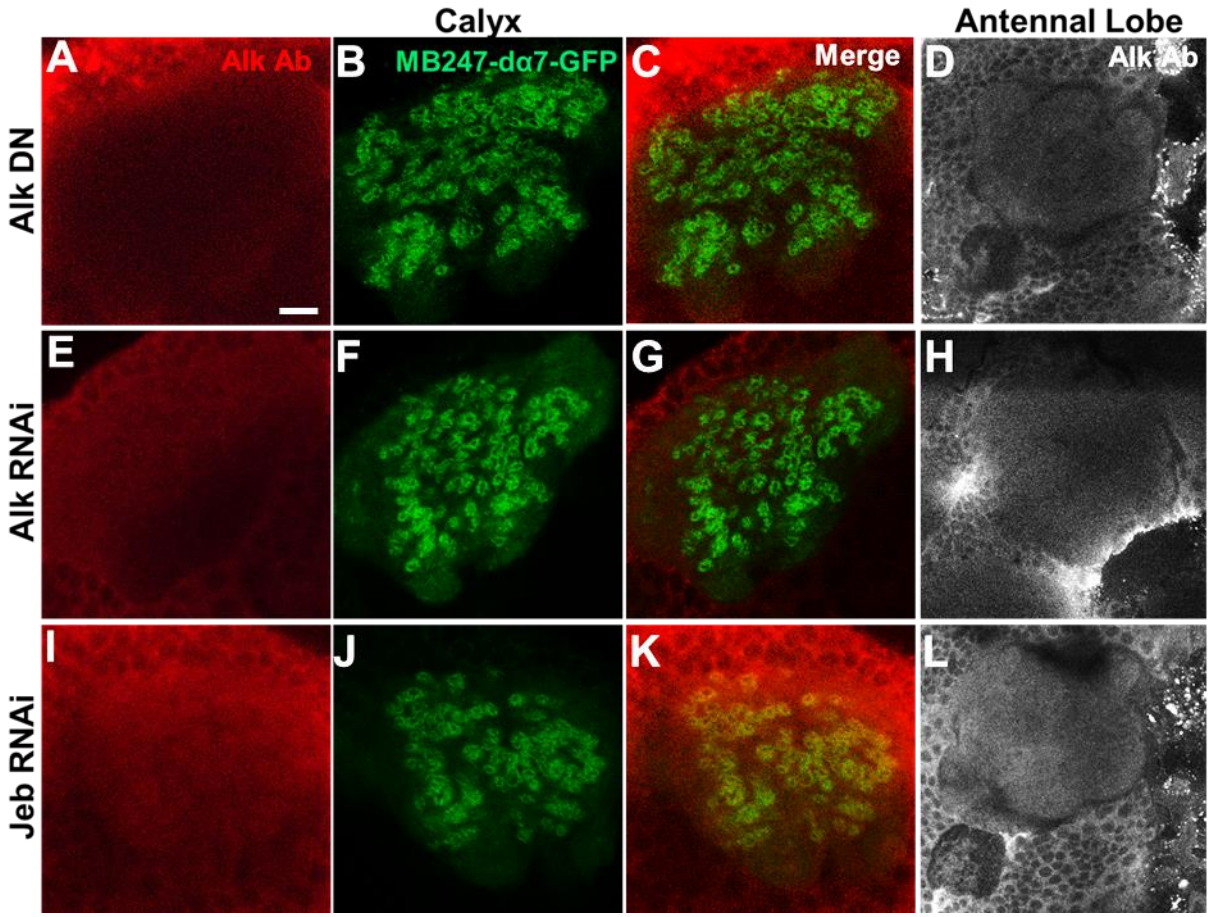

Figure 18. **Change in localization of Alk in response to postsynaptic knockdown of *alk* or *jeb*.** (A-D) *Alk^{DN}* shows an absence of Alk (in red) in the calyx and no effect on Alk localization in the AL. (E-H) Knockdown of *alk* shows an absence of Alk in the calyx and no effect on Alk localization in the AL. (I-L) Knockdown of *jeb* shows a reduction of Alk in the calyx, and the localization of Alk in AL is unaffected. Scale bar = 10 µm. Genotypes listed in Table 4.

Jeb localization

Knockdown of *alk* in the KCs using the *OK107-Gal4* driver reduced the amount of Jeb localised in the calyx, but did not affect Jeb expression or localization in the AL (Figure 19 E-H, compare to Figure 15 A-D). Expression of the *Alk^{DN}* construct also showed a similar effect as the *alk* knockdown on Jeb localization (Figure 19 A-D). These data suggest that functional post-synaptic Alk in the KCs is required for Jeb localization in MGs in the calyx. Upon *jeb* knockdown, the calyx showed reduced expression of Jeb but there was no change seen in the AL (Figure 19 I-L). Thus, the localization of Jeb in the calyx is associated to its expression in the KCs, as well as in the PNs.

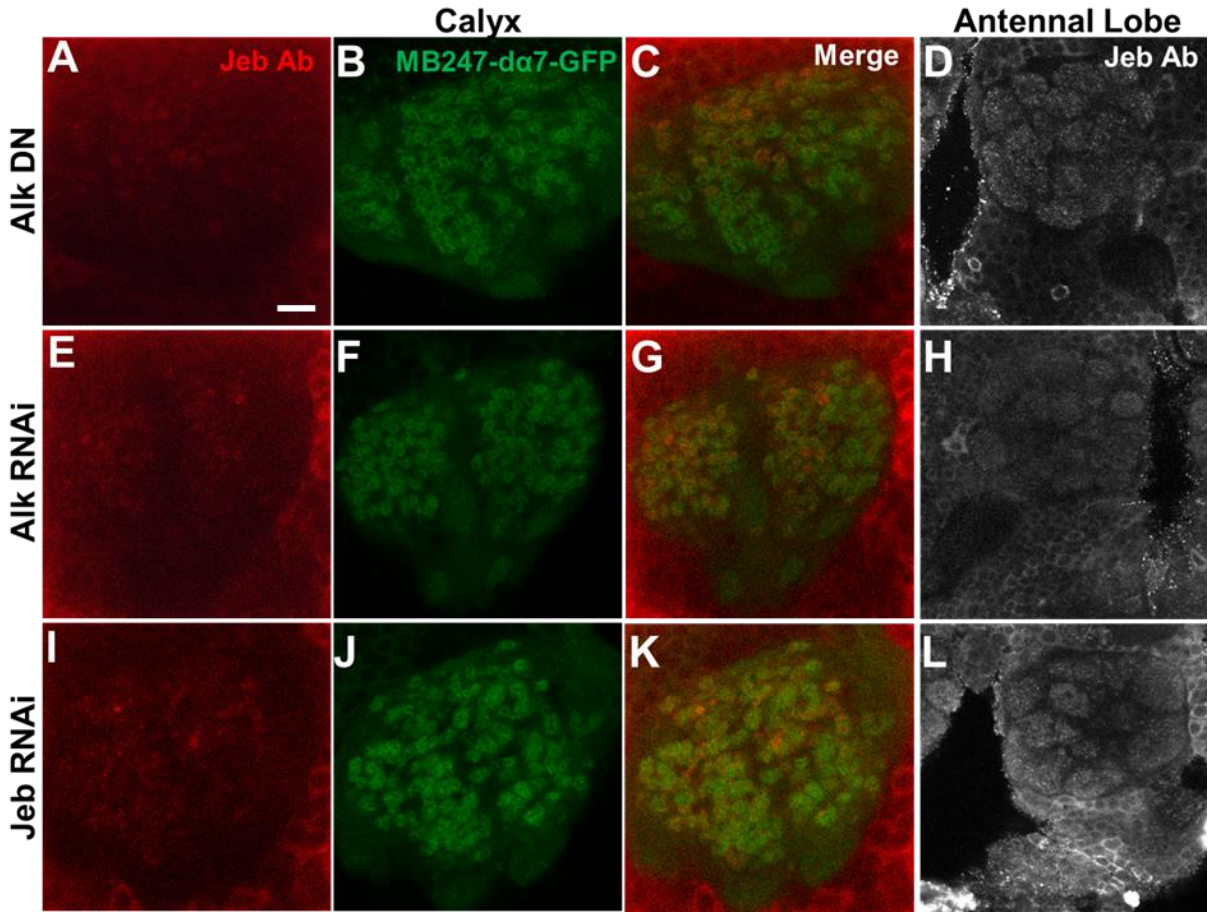

Figure 19. **Change in localization of Jeb in response to postsynaptic knockdown of *alk* or *jeb*.** (A-D) *Alk*^{DN} shows a reduction of Jeb (in red) in the calyx and no effect on Jeb localization in the AL. (E-H) Knockdown of *alk* shows a reduction of Jeb (red) in the calyx and no effect on Jeb localization in the AL. (I-L) Knockdown of *jeb* shows a reduction of Jeb in the calyx, but the localization of Jeb in AL is unaffected. Scale bar = 10 µm. Genotypes listed in Table 4.

Taken together, the localization changes of Alk or Jeb in response to pre- or post-synaptic knockdown suggests:

- In the calyx, Alk and Jeb are localized within the MG microcircuit.
- In the AL, Alk has a very low and diffused localization while Jeb shows a robust and distinct localization in all glomeruli.
- Alk is primarily expressed in the KCs. Alk localization in the MGs is dependent on pre-synaptic Alk and Jeb as well as post-synaptic Jeb.
- Jeb in the calyx is derived from both PNs and KCs. Jeb localization in the MGs is dependent on post-synaptic Alk and Jeb
- KC- specific manipulation of *alk* or *jeb* does not affect the localization of Alk or Jeb in the AL.

Driver	Construct	Alk localization		Jeb localization	
		MBC	AL	MBC	AL
Elav^{C155}-Gal4	Control	Localized in KC Claws	Diffuse localization	Localized in PN boutons	Localized in most glomeruli
	Alk RNAi	No signal	No signal	Similar to control	Similar to control
	Jeb RNAi	Similar to control	Similar to control	No signal	No signal
Acj6-Gal4	Alk^{DN}	Diffuse localization	Ectopic Alk in the lobes	Similar to control	Similar to control
	Alk RNAi	Diffuse localization	No signal	Similar to control	Similar to control
	Jeb RNAi	Very diffuse localization	Similar to control	Considerably reduced localization	Localized in ORNs and Acj6 negative PNs
OK107-Gal4	Alk^{DN}	Almost no signal	Similar to control	Considerably reduced localization	Similar to control
	Alk RNAi	No signal	Similar to control	Reduced localization	Similar to control
	Jeb RNAi	Reduced localization	Similar to control	Reduced localization	Similar to control

Table 3. Qualitative summary of Alk or Jeb localization in calyx and AL in response to knockdown of *alk* or *jeb*

4.6 Effect of Alk or Jeb loss on the cell viability

Alk-Jeb signalling has been implicated in neuronal cell survival. Experiments carried out in *Drosophila* ommatidia organisation reveal a role of Alk in non cell-autonomous induction of cell death in neighbouring cells implicating the signalling in cell fitness and competitive survival (Wolfstetter et al., 2020). Additionally, Alk promotes lamina neuron L3 development and survival in a cell autonomous manner (Pecot et al., 2014). Furthermore, a disruption of Alk-Jeb signalling via knockdown or inhibition of *alk* in zebrafish embryos led to increased apoptosis in the embryonic hindbrain (Yao et al., 2013). Recent work has also shown that a strong reduction of Alk-Jeb signalling increased the level of apoptosis and an overactivation of the signalling led to decreased apoptosis in NB progeny (Pfeifer et al., 2022).

To examine the effect of disruption in Alk-Jeb signalling on the KC and PN cell numbers, *alk* or *jeb* was knocked down in KCs or PNs. To visualize and count the nuclei, I used an *UAS-NLS-mCherry;;* construct in which red fluorescent *mCherry* is fused to a nuclear localization sequence (NLS). The number of nuclei revealed by driving the expression of this construct with *OK107-Gal4* or *Acj6-Gal4* was counted using the Imaris software (Figure 20 A-H). Knock down of *alk* or *jeb*, or expression of Alk^{DN} resulted in ~20% loss of total cell numbers in KCs or PNs, respectively (Figure 20I, K). Among the PNs, the reduction in cell number was evident in the lateral PN (lPN) and ventral PN (vPN) lineages but the antero-dorsal PN (adPN) lineage was less affected (Figure 20 J).

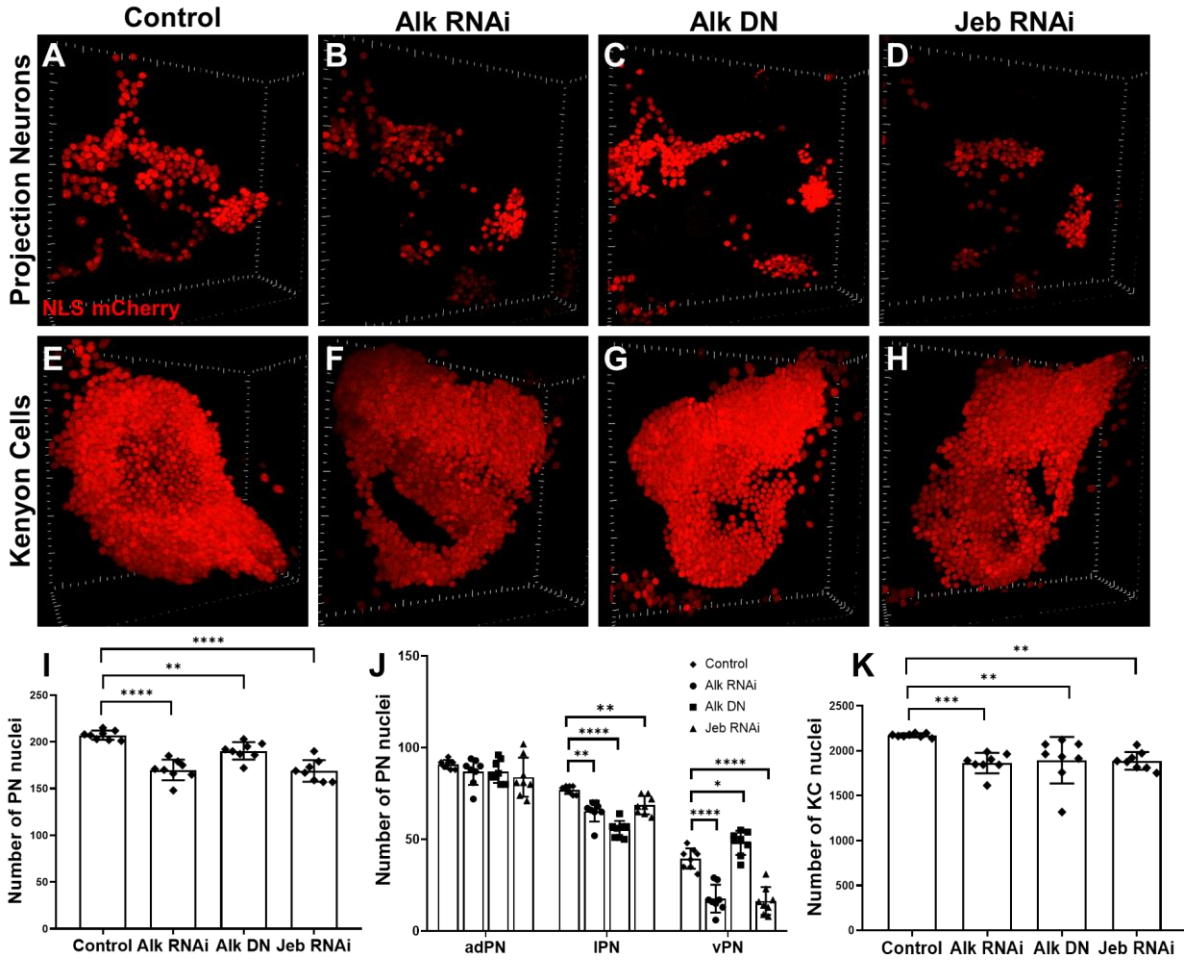

Figure 20. Change in PN and KC cell numbers in response to knockdown of alk or jeb.

(A-D) *Acj6* positive PN nuclei labelled with a nls-mCherry tag (in red) to evaluate cell numbers upon *Alk-RNAi*, *Alk^{DN}* or *Jeb-RNAi*, respectively, in PNs. (E-H) *OK107* positive KC nuclei labelled with a *nls-mCherry* tag to evaluate cell numbers upon *Alk-RNAi*, *Alk^{DN}* or *Jeb-RNAi*, respectively, in KCs. (I) PNs show 20% cell loss when Alk-Jeb signalling is disrupted. (J) Of the 3 PN lineages, lPN and vPN lineages are more vulnerable to cell death as a result of aberrant Alk-Jeb signalling. (K) KCs show 20% cell loss when Alk-Jeb signalling is disrupted. All cell counts are represented as mean ± SD (n = 9 for each group, one-way ANOVA). Statistical significance was defined as p≤0.05 = *, p≤0.01 = **, p≤0.001 = ***, p≤0.0001 = ****. Genotypes listed in Table 4.

4.6.1 Change in cell number and bouton number in a subset of PNs

Recent research suggests that PNs directly tune their bouton repertoire in response to the increase or decrease of number of KCs/ KC claws in the calyx. However, a reduction of PN cell population does not affect KCs and results in a compensatory expansion of PN bouton repertoire (Elkahlah et al., 2020). Therefore, to investigate the impact of *alk* or *jeb* knock-down on the PN number and on the number of boutons formed by the remaining PNs, I used the same *GMR68D02-Gal4* driver as above to visualize and manipulate only a small number of adPNs: subsets VC3, DL2v, and VM5v.

Upon *alk* or *jeb* knockdown or expression of Alk^{DN} construct, the total PN cell number showed a ~17% decrease and the boutons in the calyx showed a ~50% decrease (Figure 21). Interestingly, on altering Alk-Jeb signalling, the PN subset driver line was also seen to label a few KCs. These findings suggest that disrupting the Alk-Jeb signalling not only affects cell viability to some extent but also drastically affects the boutons produced by the surviving PNs in the calyx. This points to a multifaceted role of Alk-Jeb signalling in not only cell survival but also the ability of PNs to produce or maintain boutons in the calyx.

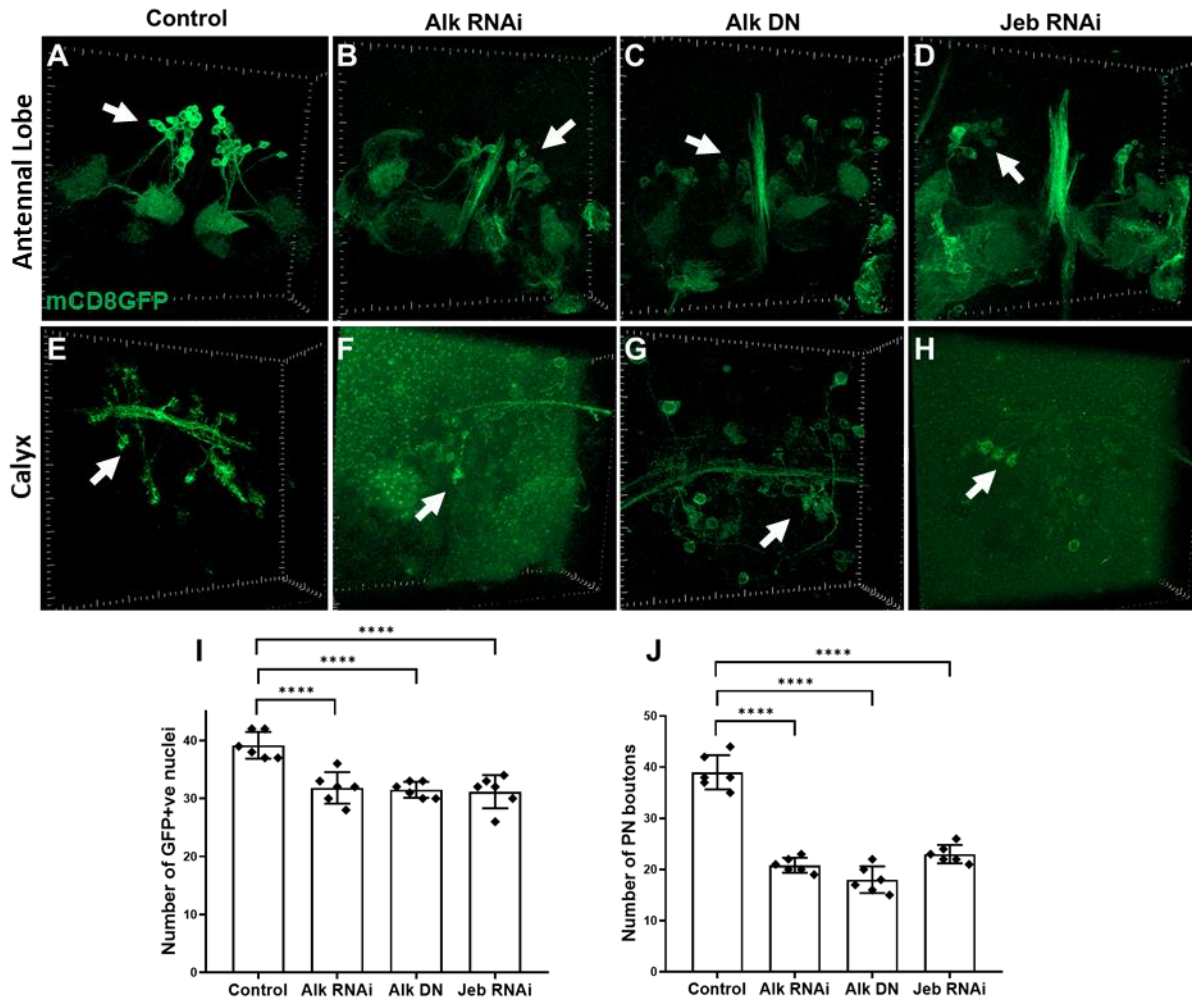

***Figure 21.* Change in cell number of VC3, VM5v, Dl2v PNs in response to knockdown of *alk* or *jeb*.**

(A-D) *GMR68D02-Gal4* positive PN nuclei labelled with *mCD8GFP* tag to evaluate cell numbers at the AL in the context of *Alk-RNAi*, *Alk^{DN}* and *Jeb-RNAi*, respectively. Arrows show cell nuclei clusters (E-H) *GMR68D02-Gal4* positive PN bouton labelled with *mCD8GFP* to evaluate bouton numbers in the calyx in the context of *Alk-RNAi*, *Alk^{DN}* and *Jeb-RNAi*, respectively. Arrows point to PN boutons (I) Aberrant Alk-Jeb signalling results in a 17% decrease in cell numbers. (J) Aberrant Alk-Jeb signalling results in a 50% decrease in boutons present in the calyx. All cell and boutons counts are represented as mean ± SD (n = 9 for each group, one-way ANOVA). Statistical significance was defined as p≤0.05 = *, p≤0.01 = **, p≤0.001 = ***, p≤0.0001 = ****. Genotypes listed in Table 4.

4.7 Development of an *in vivo* longitudinal imaging method of developing pupae

Alk-Jeb signalling has been implicated in multiple cellular pathways such as neuronal axon targeting, cell survival, proliferation of neuroblasts, neuronal differentiation as well as synaptogenesis (Bazigou et al., 2007; Cheng et al., 2011; Pecot et al., 2014; Rohrbough and Broadie, 2010; Rohrbough et al., 2013; Weiss et al., 2017; Wolfstetter et al., 2020; Pfeifer et al., 2022). In the context of these reports and the observations made in this study, it is highly probable that the observed effect of disrupted Alk-Jeb signalling may be a combinatorial culmination of various affected developmental pathways. Hence, it is vital to investigate the effect of acute disruption of Alk-Jeb signalling, during the pupal stages when the adult calyx is assembled and wired.

In order to investigate pupal wiring dynamics, the obvious approach would be staging and dissecting pupae, however this method yields a static snapshot of a very dynamic process. The alternative has been to carry out *ex vivo* brain cultures. However, long term cultures do not fully replicate the well-controlled environment of a developing brain and the culture conditions may affect the developmental processes (Rabinovich et al., 2015). Using the published brain ex-vivo culture protocols, I cultured pupal brains and imaged them at 4hr intervals till 16hrs post culture (Rabinovich et al., 2105). However, the normal brain development was seen to be disrupted with a very high incidence of apoptotic KCs. Hence, proving to be an unsuitable approach to investigate calyx development. In order to accurately investigate the temporal dynamics that occur during calyx assembly and the effect any signalling disruption may have on these dynamics, the logical approach was to attempt *in vivo* time-lapse imaging of the developing pupal brain.

In *Drosophila, in vivo* imaging during pupal stages has generally been carried out for superficial structures like the retina, dorsal thorax/pupal notum, and epithelium (Keroles et al., 2014; Hellerman et al., 2015; O'Connor et al., 2022). However, for deep brain circuits, explant systems and *ex vivo* cultures have been predominantly used in combination with 2P imaging and light-sheet microscopy (Rabinovich et al., 2015; Li

and Luo, 2021). I evaluated multiple imaging modalities including SCAPE microsocpy, lightsheet imaging, 2-photon imaging and 3-Photon imaging to visualize the calycal assembly and development in an *in vivo* set up. SCAPE and lightsheet imaging are capable of imaging deep brain structures but require an orthogonal angle of the illumination path and the detection path (Bouchard et al., 2015). This presented a major problem since the location of the calyx is such that there are highly auto fluorescent structures of the eyes or the ocelli at orthogonal angles from the calyx. Hence the tissue could not be imaged successfully. 2-Photon imaging, on the other hand, while able to visualize the gross structure, did not allow to image at the depth and resolution required to visualize and distinguish MG structure. To overcome this caveat, 3P microscopy was tested.

3P microscopy is a high resolution fluorescence microscopy technique that uses 1300 nm or longer wavelength lasers to excite the fluorescent dyes with three almost simultaneously absorbed photons (Hell et al., 1996). The use of longer wavelengths reduces the effects of light scattering and increases the penetration depth of the illumination beam into the sample (Montalban et al., 2018). 3P microscopy confines the excitation beam to a small volume in the sample and thereby reduces out-of-focus light (Montalban et al., 2018). It also minimizes photobleaching of the biological sample (Montalban et al., 2018; Sanderson, 2023; Xiao et al., 2023). Recent advancements in the 3P microscopy allow for the possibility to image intact pupal *Drosophila* brains and an intact mouse brain (Chen et al., 2018; Horton et al., 2013). Indeed, using 3P microscopy, I was able to visualize the calyx and MG structures at pupal stages.

To image the developing calyx at a high resolution, I developed and optimized a mounting procedure to expose the developing pupal head while keeping the cuticle intact (Figure 7). Combining this mounting method with 3P microscopy, it was possible to image through the intact cuticle of the developing pupa to visualise the KC soma, calyx and the mushroom body lobes (Figure 22A). The method was also used in proof-of-principle experiments to carry out reiterative imaging of the same pupa, allowing for the possibility to follow the developmental assembly of the MGs in the calyx. The pupae did not exhibit any observable cell death and tissue damage during reiterative imaging. Thus, the emergence of immature MGs at early pupal stages (~40 h APF)

and their consolidation into mature functional MGs at late pupal stages (~70h APF) was visualised in the same pupa (Figure 22B, C). Hence, this method is a first step in investigating the detailed dynamics occurring in the calyx during disassembling and re-assembly of the calyx, and can be used to verify the effect of acutely disrupted cellular signalling on developmental programs.

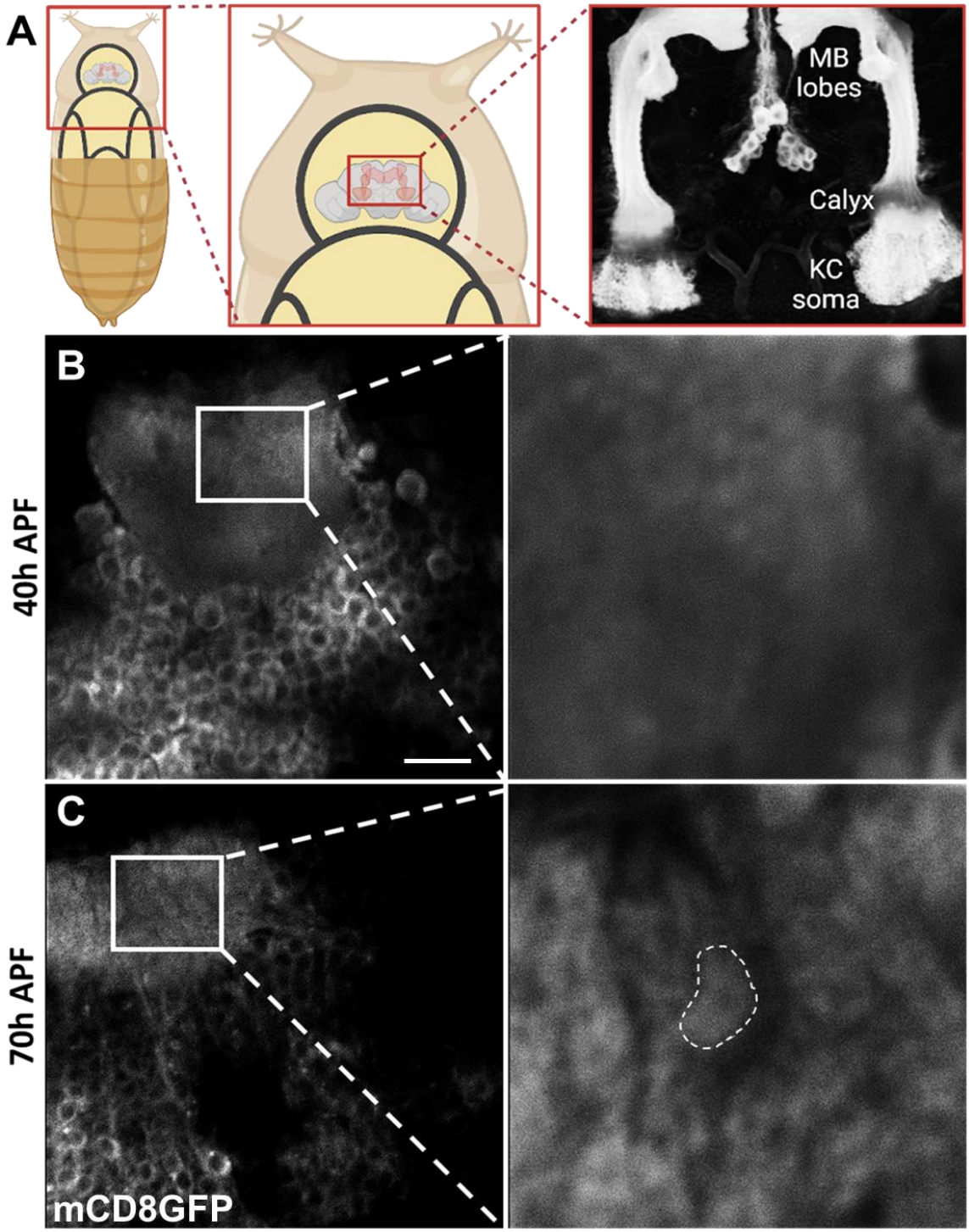

Figure 22. In vivo imaging of pupal calyx development from immature neurites to mature MG structures.

(A) Scheme of pupa mounted with the pupal case open with the MB calyx highlighted. The rightmost panel shows the entire MB imaged with a 3P microscope. (B) At 40h APF, KC dendrites and PN axons are immature and do not display a detectable organisation in the calyx. (C) At 70h APF, the neurites start developing into KC claws and PN boutons and microglomerular structures are visible (outlined with dotted line). Scale bar = 10 µm. Genotypes listed in Table 4.

5 Discussion

5.1 Investigating wiring logic of mushroom body calyx as a non-stereotypical circuit

The combinatorial sensory information from ~50 types of PNs converges on to ~2000 KCs in the mushroom body calyx where there is a 40-fold expansion between olfactory input and the postsynaptic KCs (Laurent, 2002; Litwin-Kumar et al., 2017). An olfactory stimulus activates ~50% of PNs, but only 10%of KCs show responses, displaying a sparse coding of the olfactory input (Perez-Orive et al., 2002; Wang et al., 2004; Turner et al., 2008; Honegger et al., 2011; Lin et al., 2014). The sparsely coded expansion layer plays an important role in pattern separation of incident stimuli by distinguishing between the overlap of their sensory representations (Rolls and Treves, 1990; Fiete et al., 2004; Cayco-Gajic and Silver, 2019). These connectivity motifs are also observed in input regions of cerebellar and dentate gyrus circuits in mammals (Cayco-Gajic et al., 2017; Cayco-Gajic and Silver, 2019). Motifs such as sparse coding and expansion layer networks are seen across different phylogenetic groups, and hence, seem to be conserved across evolution. This indicates the importance of such connectivity patterns in allowing an animal to navigate its environment. However, how these motifs are encoded for and developmentally set up is not understood.

The general consensus in the field has been that the KC-PN connectivity is largely random (Caron et al., 2013; Litwin-Kumar et al., 2017). However, recent mapping of the KC-PN microglomerular connections using the comprehensive EM datasets as well as connectivity analysis using computational models reveal the presence of a cluster of food-responsive PNs that innervate the calyx in consistent patterns across individuals (Zheng et al., 2020). This observed connectivity along with computational models that take into account the KC and PN neurite innervation patterns in the calyx suggests that the organisation of connections might not be fully random (Zheng et al., 2022).

Multiple factors may play a role in the innervation of the calyx and determine PN-KC partner matching. Neuroblast origin and birth order might dictate a timeline of innervation in the calyx for PNs and KCs, such that the neurites innervating simultaneously would preferentially synapse with each other (Li et al., 2018; Wong et al., 2023). Another possibility could be that spontaneous neuronal activity patterns could help neurons make or refine their synaptic connections (McLaughlin et al., 2003; Wan et al., 2019; Akin and Zipursky, 2020). Lastly, the neurons may exhibit cell surface molecules that help them synapse with neurons carrying a complementary cell surface code (Xie et al., 2021; Wong et al., 2023). This study is an initial attempt to decipher what wiring paradigms and fine-scale developmental processes may contribute to the observed network structure.

To date, wiring logic in the fly brain has been elucidated in the context of stereotyped circuits like the optic lobe or the antennal lobe as the connections are consistent across synaptic partners and across different individuals, allowing to examine wiring defects or wiring logic systematically (Barish et al., 2018; Xu et al., 2019; Wong et al., 2023). These approaches have revealed the proficient use of cell surface markers and secreted gradients by neuronal populations to carry out accurate synaptic partner matching (Tan et al., 2015; Ashley et al., 2019; Cheng et al., 2019). To explore and verify whether non-stereotypical systems employ similar wiring rationale to make accurate synaptic connections, I hypothesized that a major role is played by cell surface molecules in KCs and PNs during mid-pupal stages (30-40h APF) that allow for accurate synaptic partner matching and synaptogenesis (Alyagor et al., 2018; Xie et al., 2021). Screening through 215 molecules, yielded 14 interaction pairs/groups of molecules that were classified in 4 phenotypic categories, namely: synaptic organization defect, decreased bouton number, increased bouton number and altered bouton localization. Based on the published literature, interaction analysis as well as genetic constructs and tools available, *alk* and *jeb* were chosen to further probe their role in PN-KC interaction.

5.2 Alk-Jeb signalling is implicated in KCs and PNs

Alk is a receptor tyrosine kinase that interacts exclusively with its secreted ligand Jeb (Englund et al., 2003). In the optic lobe, Alk-Jeb signalling regulates layer-specific expression of cell-adhesion molecules, thereby allowing the photoreceptor cells to shape their environment to achieve accurate dendrite targeting (Bazigou et al., 2007). Alk and Jeb are localized in the mushroom body calyx and Alk-Jeb signalling has also been found to play a role in associative learning and memory formation (Gouzi et al., 2011).

The initial screening with *alk* and *jeb* interestingly produced opposing phenotypes, i.e., an overproduction of boutons in the case of *alk* knockdown but a reduction of boutons when *jeb* is knocked down irrespective of where the knockdown is carried out, i.e. pre- or post- synaptically. This suggests that the *alk* or *jeb* may not be exclusively implicated in either the pre- or the post- synaptic side, which is concurrent with the RNA sequencing analysis that reveals that *alk* and *jeb* are expressed robustly by PNs as well as KCs.The implication of *alk* and *jeb* being expressed in both KCs and PNs was verified using antibodies generated against Alk and Jeb and they revealed an enriched localization of Alk and Jeb in the MG microcircuit of the calyx, in concurrence with findings in a recent study on the role of Alk-Jeb signalling in the calyx in the context of memory formation (Gouzi et al., 2018). In the AL, the antibodies indicated a diffuse localization of Alk and a strong localization of Jeb in most glomeruli.

Interestingly, the use of Alk^{DN} construct phenocopied the reduction of boutons seen with *jeb* knockdown. This difference in phenotype when *alk* is knocked down compared to when the Alk^{DN} construct is expressed needs to be verified with mutant analysis and further evaluated for the differential dynamics employed by the RNAi vs DN construct in both the KCs and the PNs. Research on activation of RTKs puts forward two modes of activation: ligand mediated dimerization or receptor mediated dimerization (Paul and Hristova, 2019; Bae and Schlessinger, 2010; Shen and Maruyama, 2010). Ligand mediated dimerization requires the monomer of the RTK to bind to its ligand, which leads to a conformational change allowing it to dimerize and then be activated.

Receptor mediated dimerization posits that the receptor is capable of dimerizing independently of the ligand binding, while still being inactive. While the activation seems to be dependent on binding of the ligand to the receptor, the self-dimerization may have some effect on downstream process and could perhaps be a viable explanation for the difference in phenotype observed with *alk* knockdown as compared to the expression of Alk^{DN}. This functional difference would be very interesting to resolve to be able to determine the how Alk interacts with its ligand and downstream molecules in the developing KCs and PNs.

5.3 Alk and Jeb localization in the calyx

Utilising the specific antibodies against Alk and Jeb, the relative localization between the two molecules across KCs and PNs was investigated. Alk and Jeb expression in the AL was independent of expression of Alk or Jeb in KCs, however, PN-specific changes of Alk or Jeb had a very clear impact on Alk and Jeb localization in the calyx. Alk seems to be primarily be expressed in the KCs and the localization of Alk in the MGs is dependent on the expression of pre-synaptic Alk and Jeb and also post-synaptic Jeb. Jeb seems to be primarily expressed in the PNs and localization of Jeb in the MGs is dependent on the expression of post-synaptic Alk and Jeb. These observations suggest that the Alk-Jeb interaction may be important for synaptic localization of the molecules at the MG synapse, and that this interaction occurs not only across the PN-KC connection but also within the PNs and KCs. So far, the Alk-Jeb interaction in *Drosophila* has been seen to be only trans-synaptic with one neuronal partner expressing Alk and the other expressing Jeb (Loren et al., 2003; Bazigou et al., 2007).

The calyx-specific interactions found here suggest a new cis-regulatory role of Alk-Jeb interaction. The trans- and cis- interactions may regulate different aspects of PN-KC synaptic matching in the calyx, where the cis- interaction may play a role in synaptogenesis and synaptic differentiation, and the trans- interaction might be required for synaptic partner identification and/or synaptic adhesion. These possible interactions and the mechanisms they activate open up an intriguing new aspect of

Alk-Jeb signalling that needs to be further analysed and delineated. To characterize the cis- and trans- interactions of Alk and Jeb, it will be useful to generate constructs that label Alk and Jeb in the KCs and PNs. These constructs along with super-resolution imaging will help decipher how these molecules may interact intracellularly and across the synapse during development to form the adult calyx to answer some open questions. In addition, different isoforms of both *alk* and *jeb* vary only on the UTR regions, suggesting the isoforms may be differentially regulated and/or trafficked at the mRNA level. Hence, generating isoform specific null mutants and isoform specific GFP tagged lines would allow to explore the different role of the isoforms, if any.

Identifying the type of Alk activation (ligand mediated dimerization or receptor mediated dimerization) and the role of the different *alk* and *jeb* isoforms in the PNs and KCs is vital to understand how the Alk-Jeb signalling regulates different cellular processes during development. In addition, it could help reveal more information on Jeb secretion as well as explore the possibility that there may be an as yet unknown interactor of Alk apart from Jeb that also regulates its downstream pathways. It would also be highly interesting to probe whether the inhibitory interneuron APL also expresses Alk and Jeb and how this expression affects the PN-KC interactions in the developing calyx

5.4 Role of Alk-jeb signalling on neuronal health and survival

Alk-Jeb signalling has been implicated in neuronal cell viability and a recent study in the MB NBs has shown that a strong reduction of Alk-Jeb signalling increased the level of apoptosis and an overactivation of the signalling led to decreased apoptosis in NB progeny (Pfeifer et al., 2022). This study examined how this increase in apoptosis affects the neuronal health of KCs and PNs. Quantification of the cell numbers after disrupting Alk-Jeb signalling demonstrated a 20% loss of PNs as well as KCs, indicating that Alk-Jeb signalling is indeed required for cell survival but only for a fraction of the population. Whether this 20% cell loss affects a particular subset of KCs and PNs or is due to random stochastic cell death remains to be elucidated. Whether

some KC and PN subsets are more susceptible to cell death as a result of disrupted Alk-Jeb signalling needs to be investigated.

Recent work on KC-PN scaling suggests that KCs are the driver of PN innervation in the calyx and loss or alteration of KC cell number or claw numbers directly scales the PN bouton numbers (Elkahlah et al., 2020). However, a loss of PN cell numbers did not affect the number or distribution of MGs in the calyx since the surviving PNs compensated by sprouting more boutons (Elkahlah et al., 2020). To investigate how this compensation mechanism is affected in the context of the role to *alk* and *jeb* in neuronal survival, Alk-Jeb signalling was disrupted in a small subset of food-responsive PNs (VC3, DL2v, VM5v). The PNs showed a ~17% loss in cell numbers but also a 50% of loss in bouton numbers. These findings suggest that disrupting the Alk-Jeb signalling not only affects cell viability to some extent but also drastically affects the boutons produced by the surviving PNs in the calyx. This indicates a possibility of Alk-Jeb signalling to be implicated not only in cell survival but also cell growth such that it affects the ability of PNs to produce or maintain boutons in the calyx.

The role of Alk-Jeb signalling must then be investigated separately in the context of neuronal survival and in the context of bouton production/maintenance in the calyx. The role in neuronal viability can be examined by analysing the expression of apoptotic cascade molecules and cell death markers. Recent research also showed a change in cellular markers on constitutive activation of Alk-Jeb signalling, and hence it would be interesting to observe cellular marker expression pattern in the context of *alk* knockdown for changes in cell fate determination (Pfeifer et al., 2022). To analyse the role of Alk-Jeb signalling in the context of bouton production/maintenance in the calyx, it would be vital to knockdown *alk* or *jeb* acutely in PN subsets that have attained their final cell count but have not yet produced boutons. Larval born PNs that have not yet innerated the calyx during early pupation could be good candidates. This would help in resolving whether the lack of these molecules leads to an inability of the PNs either to produce boutons or to maintain the boutons in the calyx.

5.5 Development of an *in vivo* longitudinal imaging method of developing pupae

To isolate the calyx specific effect of the disruption of Alk-Jeb signalling, developmental dynamics in the calyx need to be investigated during the pupal assembly of the calyx. Developing an *in vivo* method for long term imaging of the assembling of the calycal circuits is an important endeavour that allows for the possibility of imaging deep brain structures *in situ* and with no perturbation to the tissue/animal such that the same pupa can be imaged at different developmental time points to follow the step-wise assembly of the adult specific calyx. Indeed, this study presents the possibility of imaging immature neurites in early pupal stages and. *In vivo* long term imaging is a first step in investigating the detailed dynamics occurring in the calyx during disassembling and re-assembly of the calyx, and can be used to verify the effect of disrupted cellular signalling on developmental programs. For example, investigating the *in vivo* dynamics in the context of an acute pupa-specific disruption of the Alk-Jeb signalling would help elucidate the exact role of *alk* and *jeb* across PNs and KCs during the assembly of the calyx.

This method also allows for the possibility to dissect other hitherto unknown aspects of the calyx rewiring. This includes determining the sequence of pruning and re-innervation of different subsets of KC and PN neurites into the calyx, and investigating the filopodial dynamics involved in microglomerular synaptogenesis. If combined with calcium sensors, one can also investigate the role, if any, neural activity plays in the disassembly or re-assembly of the calyx. Silencing of neural activity in a subset of PNs has been shown to alter the size, number, and active zone density of the MGs formed by these PNs (Kremer et al., 2010). However, it remains to be seen, whether KCs are active spontaneously during development and whether silencing KCs would have any effect on the MG formation and organization. Therefore, this method provides a way to investigate a plethora of open questions regarding the calycal rewiring and the molecules implicated therein. Exploring these questions is vital in understanding how a non-stereotypical circuit like the calyx wires to form a functional circuit.

6 Supplementary Information

Table 4. Genotypes used for figures in the results section

Figure	Genotype
Figure 9	**A:** *Elav^{C155}-GAL4, UAS-Dicer2/+; P{GMR68D02-lexA}, 8xlexAop2-brp-mCherry, MB247-Dα7-GFP/+; UAS-mCD8-GFP/+* **B, C, D:** *Elav^{C155}-GAL4, UAS-Dicer2; P{GMR68D02-lexA}, 8xlexAop2-brp-mCherry, MB247-Dα7-GFP;*
Figure 10	**A:** *Elav^{C155}-GAL4, UAS-Dicer2/+; P{GMR68D02-lexA}, 8xlexAop2-brp-mCherry, MB247-Dα7-GFP/+; UAS-Luciferase RNAi/+ (Control)* **B:** *Elav^{C155}-GAL4, UAS-Dicer2/+; P{GMR68D02-lexA}, 8xlexAop2-brp-mCherry, MB247-Dα7-GFP/+; UAS-Sema1a-RNAi/+* **C:** *Elav^{C155}-GAL4, UAS-Dicer2/+; P{GMR68D02-lexA}, 8xlexAop2-brp-mCherry, MB247-Dα7-GFP/+; UAS-18w-RNAi/+* **D:** *Elav^{C155}-GAL4, UAS-Dicer2/+; P{GMR68D02-lexA}, 8xlexAop2-brp-mCherry, MB247-Dα7-GFP/ UAS-ena-RNAi;*
Figure 11	**A:** *Elav^{C155}-GAL4, UAS-Dicer2/+; P{GMR68D02-lexA}, 8xlexAop2-brp-mCherry, MB247-Dα7-GFP/+; UAS-Luciferase RNAi/+ (Control)* **B:** *Elav^{C155}-GAL4, UAS-Dicer2/+; P{GMR68D02-lexA}, 8xlexAop2-brp-mCherry, MB247-Dα7-GFP/ UAS-Npc2a-RNAi* **C:** *Elav^{C155}-GAL4, UAS-Dicer2/+; P{GMR68D02-lexA}, 8xlexAop2-brp-mCherry, MB247-Dα7-GFP/+; UAS-sns-RNAi/+* **D:** *Elav^{C155}-GAL4, UAS-Dicer2/+; P{GMR68D02-lexA}, 8xlexAop2-brp-mCherry, MB247-Dα7-GFP/ UAS-DPR2-RNAi;*
Figure 12	**Pan neuronal line:** *Elav^{C155}-GAL4, UAS-Dicer2/+; P{GMR68D02-lexA}, 8xlexAop2-brp-mCherry, MB247-Dα7-GFP/+;* **Post-synaptic line:** *;P{GMR68D02-lexA}, 8xlexAop2-brp-mCherry, MB247-Dα7-GFP/CKG;;OK107-GAl4* **Pre-synaptic line:** *Acj6-GAl4/FM7i; P{GMR68D02-lexA}, 8xlexAop2-brp-mCherry, MB247-Dα7-GFP/CKG;;* Each line was crossed to *;;UAS-Luciferase RNAi (control), ;;UAS-Alk RNAi, ;UAS-Jeb-RNAi, or UAS-Alk^{DN};;;*

Figure 13	*;UAS-mCD8-GFP/CyO;;OK107-Gal4*
Figure 14 and 15,	**A-D:** *Elav^{C155}-GAL4, UAS-Dicer2/+; P{GMR68D02-lexA}, 8xlexAop2-brp-mCherry, MB247-Dα7-GFP/+; UAS-Luciferase RNAi/+ (Control)* **E-H:** *Elav^{C155}-GAL4, UAS-Dicer2/+; P{GMR68D02-lexA}, 8xlexAop2-brp-mCherry, MB247-Dα7-GFP/+; UAS-Alk RNAi/+* **I-L**: *Elav^{C155}-GAL4, UAS-Dicer2/+; P{GMR68D02-lexA}, 8xlexAop2-brp-mCherry, MB247-Dα7-GFP/ UAS-Jeb-RNAi*
Figure 16 and 17	**A-D:** *Acj6-GAl4/ UAS-Alk^{DN}; P{GMR68D02-lexA}, 8xlexAop2-brp-mCherry, MB247-Dα7-GFP/+;;* **E-H:** *Acj6-GAl4/ X; P{GMR68D02-lexA}, 8xlexAop2-brp-mCherry, MB247-Dα7-GFP/+; UAS-Alk RNAi/+* **I-L:** *Acj6-GAl4/ X; P{GMR68D02-lexA}, 8xlexAop2-brp-mCherry, MB247-Dα7-GFP/ UAS-Jeb-RNAi*
Figure 18 and 19	**A-D:** *UAS-Alk^{DN} /X; P{GMR68D02-lexA}, 8xlexAop2-brp-mCherry, MB247-Dα7-GFP/+;; OK107-GAl4/+* **E-H:** *;P{GMR68D02-lexA}, 8xlexAop2-brp-mCherry, MB247-Dα7-GFP/+; UAS-Alk RNAi/+; OK107-GAl4/+* **I-L:** *;P{GMR68D02-lexA}, 8xlexAop2-brp-mCherry, MB247-Dα7-GFP/ UAS-Jeb-RNAi;; OK107-GAl4/+*
Figure 20	**PN line:** *Acj6-GAl4/+; UAS-nls-mCherry/+* **KC line:** ;*UAS-nls-mCherry/+;;OK107-Gal4/+* Each line was crossed to *;;UAS-Luciferase RNAi (control), ;;UAS-Alk RNAi, ;UAS-Jeb-RNAi, or UAS-Alk^{DN};;;*
Figure 21	*;UAS-mCD8-GFP;GMR68D02-Gal4; was crossed to ;;UAS-Luciferase RNAi (control), ;;UAS-Alk RNAi, ;UAS-Jeb-RNAi, or UAS-Alk^{DN};;;*
Figure 22	*;UAS-mCD8-GFP/CyO;;OK107-Gal4*

Table 5. RNAi lines used in this study.

Molecule	Source	Line ID	Molecule	Source	Line ID	Molecule	Source	Line ID
18w	BDSC	30498	Dscam1	BDSC	38945	Nrk	BDSC	56936
18w	VDRC	36305	Dscam1	BDSC	29628	Nrt	BDSC	28742
acj6	BDSC	29335	Dscam2	BDSC	51839	Nrt	VDRC	106080
acj6	VDRC	105292	Dscam2	VDRC	107939	Nrx	VDRC	36328
Alk	BDSC	27518	Dscam3	VDRC	6685	ome	VDRC	100077
Alk	VDRC	107083	Dscam4	BDSC	51508	ome	VDRC	110361
Arp6	BDSC	65155	Dscam4	VDRC	42883	otk	BDSC	67966
Arp6	VDRC	108081	dysc	VDRC	109928	otk	BDSC	55869
bdl	BDSC	31974	dysc	VDRC	110019	PlexA	BDSC	67845
beat-Ia	BDSC	54820	E(z)	BDSC	36068	PlexA	BDSC	30483
beat-Ia	BDSC	64938	E(z)	BDSC	33659	PlexB	BDSC	28911
beat-Ib	BDSC	55938	ed	BDSC	38209	PlexB	BDSC	57813
beat-Ic	BDSC	64528	ed	BDSC	38243	pod1	BDSC	41705
beat-IIa	BDSC	28702	Egfr	BDSC	60012	pod1	BDSC	31219
beat-IIb	BDSC	57157	Egfr	BDSC	36773	pot	VDRC	105189
beat-IIb	VDRC	104935	eIF2beta	BDSC	53268	pot	VDRC	8316 (1 off target)
beat-IIIa	BDSC	64526	eIF2beta	VDRC	105291 (2 off targets)	Ppn	VDRC	108005
beat-IIIb	BDSC	56984	ena	BDSC	39034	Ppn	VDRC	16523
beat-IIIc	BDSC	50941	ena	BDSC	31582	Psc	BDSC	35297
beat-IIIc	BDSC	29607	eph	BDSC	41607	Psc	BDSC	38261
beat-IV	BDSC	56981	eph	BDSC	39066	psidin	VDRC	103558
beat-Va	BDSC	60053	ephrin	BDSC	34614	ptc	BDSC	55686
beat-Vb	BDSC	28758	ephrin	BDSC	27039	ptc	BDSC	28795
beat-Vc	BDSC	60067	esn	BDSC	34371	Ptp36E	BDSC	65919
beat-Vc	BDSC	58213	esn	VDRC	32040 (2 off targets)	Ptp4E	BDSC	38369

Molecule	Source	Line ID	Molecule	Source	Line ID	Molecule	Source	Line ID
beat-VI	VDRC	105798	eya	BDSC	90850	Ptp4E	BDSC	60008
beat-VII	BDSC	60056	eya	BDSC	90852	Pvr	BDSC	37520
betaTub60D	BDSC	64856	Fas1	BDSC	41854	Pvr	VDRC	105353
betaTub60D	VDRC	104937	Fas1	BDSC	42887	Rab6	BDSC	27490
brat	BDSC	28590	Fas3	BDSC	77396	Rab6	BDSC	35744
brat	BDSC	34646	Fas3	VDRC	26850	Rac1	BDSC	34910
Cad87A	BDSC	28716	Fdh	BDSC	34937	Rac1	BDSC	28985
Cad87A	VDRC	105901	Fdh	VDRC	110071	Rac2	VDRC	50349 (1 off target)
CadN	BDSC	27503	fog	BDSC	56902	Rac2	VDRC	50350 (1 off target)
CadN	BDSC	41982	fog	BDSC	61917	rdo	VDRC	107213
CadN2	BDSC	27508	fra	BDSC	40826	rho	BDSC	38920
CadN2	BDSC	40889	fra	BDSC	31469	rho	BDSC	41699
capt	BDSC	33010	fru	BDSC	31593	Rho1	BDSC	32383
capt	VDRC	101588 (1 off target)	fru	BDSC	66694	Rho1	VDRC	109420
CD98hc	BDSC	57746	fz2	BDSC	67863	RhoGEF64C	BDSC	77431
CD98hc	VDRC	108365	fz2	BDSC	31390	RhoGEF64C	BDSC	31130
CdGAPr	BDSC	38279	Gat	BDSC	29422	robo1	BDSC	35768
CdGAPr	BDSC	6438	Gat	VDRC	107303	robo1	BDSC	39027
Cdk8	BDSC	67010	Gfrl	BDSC	51505	robo2	BDSC	34589
Cdk8	BDSC	35324	Gfrl	VDRC	103213	robo2	BDSC	27317
CG1504	BDSC	28517	GILT1	BDSC	63015	robo3	BDSC	44539
CG1504	BDSC	66939	GILT1	BDSC	67832	robo3	BDSC	29398
CG1607	BDSC	57797	GluRIA	BDSC	40844	rst	BDSC	28672
CG1607	VDRC	105677(1 off target)	GluRIA	BDSC	40907	scb	BDSC	38959

Molecule	Source	Line ID	Molecule	Source	Line ID	Molecule	Source	Line ID
CG3036	BDSC	43179	gogo	BDSC	65193	scb	BDSC	27545
CG3036	VDRC	108500	gogo	VDRC	43929	SelR	BDSC	52919
CG31075	BDSC	50654	grn	BDSC	34578	SelR	VDRC	110755
CG31075	BDSC	62535	grn	BDSC	33746	Sema1a	BDSC	34320
CG34353	BDSC	58291	gt	BDSC	54471	Sema1a	BDSC	29554
CG34353	VDRC	102326	gt	BDSC	54476	Sema1b	BDSC	28588
CG42346	BDSC	28958	Gyc76C	VDRC	106525 (2 ON targets)	Sema1b	VDRC	107233
CG42346	BDSC	51719	hbs	BDSC	57003	Sema2a	BDSC	29519
CG44153	BDSC	33350	hbs	VDRC	105913	Sema2a	BDSC	35432
CG44153	VDRC	102832	hig	BDSC	42000	Sema2b	BDSC	28932
CG44837	BDSC	65378	hig	BDSC	28376	Sema2b	VDRC	108030
CG44837	BDSC	53032	Hsc70-3	BDSC	32402	Sema5c	BDSC	29436
CG5758	BDSC	57808	Hsc70-3	BDSC	80420	Shc	BDSC	66961
CG5758	VDRC	108061 (1 off target)	ImpL2	BDSC	55855	Shc	VDRC	40464
CG6218	BDSC	28386	ImpL2	BDSC	64936	shf	BDSC	55867
CG6218	VDRC	106638	InR	BDSC	35251	shf	VDRC	105890
CG6867	BDSC	64573	InR	BDSC	51518	shg	BDSC	38207
CG6867	VDRC	37416	ItgaPS4	BDSC	44534	shg	BDSC	32904
CG7381	BDSC	60386	ItgaPS4	BDSC	28535	side	BDSC	50642
CG7381	VDRC	100860	jbug	BDSC	39070	side	VDRC	27049
chb	BDSC	35442	jbug	BDSC	31590	side-III	VDRC	103669
chb	BDSC	34669	jeb	BDSC	56022	side-III	VDRC	22742
chic	BDSC	34523	jeb	VDRC	103047	side-IV	VDRC	16636
chic	VDRC	102759	jing	BDSC	55633	side-IV	VDRC	102563 (1 off target)
Cht2	BDSC	35717	jing	BDSC	35750	side-V	BDSC	61953
Cht2	BDSC	60369	kek1	BDSC	57000	side-VIII	BDSC	62897
ctp	BDSC	44044	kek1	VDRC	101166	side-VIII	VDRC	104814
ctp	VDRC	109084	kek2	BDSC	31874	sli	BDSC	31468

Molecule	Source	Line ID	Molecule	Source	Line ID	Molecule	Source	Line ID
D1	BDSC	33655	kek3	BDSC	77354	sli	BDSC	31467
D1	BDSC	28616	kek3	VDRC	6356	smal	BDSC	55907
Dfmr	VDRC	110800	kek4	BDSC	67206	smal	BDSC	44089
Dg	BDSC	34895	kek4	VDRC	105647	sns	BDSC	64872
Dg	VDRC	100828	kek5	BDSC	40830	sns	VDRC	109442
DIP-gamma	BDSC	80461	kek6	BDSC	61212	spz	BDSC	58499
DIP-gamma	VDRC	104056	kek6	VDRC	109681	spz	BDSC	66924
DIP-lambda	BDSC	41980	kirre	BDSC	64918	Sra-1	VDRC	108876
DIP-zeta	BDSC	38227	kirre	BDSC	67340	Sra-1	VDRC	34907
DIP-zeta	VDRC	107866	klg	BDSC	28746	Src64B	BDSC	51772
DIP-α	BDSC	38965	klg	VDRC	102502	Src64B	BDSC	62157
DIP-β	BDSC	38310	ko	VDRC	31266	Ten-m	BDSC	29390
DIP-ε	BDSC	38936	ko	VDRC	31267	tey	VDRC	106065 (2 off targets)
DIP-η	BDSC	38229	Lac	BDSC	28940	tinc	VDRC	101175 (1 off target)
DIP-θ	BDSC	28654	Lac	BDSC	38895	tinc	VDRC	10208 (1 off target)
DIP-ι	BDSC	38231	LanA	BDSC	28071	Tl	BDSC	35628
DIP-κ	BDSC	31740	LanA	VDRC	18873	Tl	BDSC	31477
dlp	BDSC	50540	LanB2	BDSC	55388	Toll-6	BDSC	64968
dlp	BDSC	34089	LanB2	BDSC	62002	Toll-6	BDSC	56048
dnt	BDSC	37469	Lgr1	BDSC	27509	Toll-7	BDSC	30488
dnt	BDSC	67251	Lgr1	BDSC	51465	Toll-7	VDRC	24473
dpr10	BDSC	27991	Lola	BDSC	26714	Tor	BDSC	35578
dpr10	VDRC	103511	Lola	BDSC	35721	Tor	BDSC	33951
dpr11	VDRC	23243	LRP1	BDSC	44579	trio	BDSC	43549
dpr12	BDSC	28782	LRP1	BDSC	31151	trio	BDSC	27732
dpr12	VDRC	44741	Ltl	BDSC	29527	trn	BDSC	50520

Molecule	Source	Line ID	Molecule	Source	Line ID	Molecule	Source	Line ID
dpr13	VDRC	107676	Ltl	BDSC	44577	trn	BDSC	28525
dpr14	BDSC	29626	Meltrin	BDSC	58331	tutl	BDSC	54850
dpr14	VDRC	102040	Meltrin	VDRC	3702	tutl	VDRC	101900
dpr15	VDRC	46245 (3 off targets)	mew	BDSC	44553	uif	BDSC	38354
dpr15	VDRC	29144 (off targets)	mew	BDSC	27543	uif	BDSC	38365
dpr17	BDSC	41656	Mgstl	BDSC	57472	unc-104	BDSC	58191
dpr17	BDSC	62364	Mgstl	VDRC	109140	unc-104	BDSC	58083
dpr18	BDSC	29604	Mical	BDSC	67846	unc-5	BDSC	33756
dpr18	VDRC	45821	Mical	BDSC	31148	unc-5	VDRC	110155
dpr19	VDRC	110059	mirr	BDSC	65877	unc-51	VDRC	16133
dpr2	VDRC	100169	mirr	BDSC	42960	uzip	BDSC	29558
dpr20	BDSC	28293	Mmp2	BDSC	65935	uzip	VDRC	104208 (1 off target)
dpr20	VDRC	101673	Mmp2	BDSC	61309	Vang	BDSC	34354
dpr3	VDRC	6692	mspo	BDSC	29460	Vang	VDRC	100819
dpr4	VDRC	102905	mspo	VDRC	107608 (2 off targets)	Vmat	BDSC	31257
dpr5	BDSC	29627	Mtl	BDSC	35754	Vmat	BDSC	44471
dpr5	VDRC	102228	Mtl	BDSC	51932	Wnt4	BDSC	29442
dpr6	VDRC	103521	NetA	BDSC	31665	Wnt4	VDRC	104671
dpr7	VDRC	106546	NetA	BDSC	31288	zfh1	BDSC	38929
dpr8	BDSC	28744	NetB	BDSC	34698	zfh1	BDSC	43195
dpr8	VDRC	106791	NetB	BDSC	25861			
dpr9	BDSC	33409	not	BDSC	28725			
dpr9	VDRC	51990 (7 off targets)	Npc2a	VDRC	106771			
drl	BDSC	39002	Npc2a	VDRC	30722			
drl	BDSC	29602	Nrg	BDSC	37496			
Drl-2	BDSC	55893	Nrg	BDSC	38215			
Drl-2	BDSC	25961	Nrk	BDSC	55184			

7 References

- Abdelrahman, N. Y., Vasilaki, E., & Lin, A. C. (2021). Compensatory variability in network parameters enhances memory performance in the Drosophila mushroom body. *Proceedings of the National Academy of Sciences of the United States of America*, 118(49).
- Ache, B. W., & Young, J. M. (2005). Olfaction: diverse species, conserved principles. *Neuron*, 48(3), 417–430.
- Ackman, J. B., & Crair, M. C. (2014). Role of emergent neural activity in visual map development. *Current Opinion in Neurobiology*, 24(1), 166–175.
- Afgan, E., Baker, D., van den Beek, M., Blankenberg, D., Bouvier, D., Čech, M., … Goecks, J. (2016). The Galaxy platform for accessible, reproducible and collaborative biomedical analyses: 2016 update. *Nucleic Acids Research*, 44(W1), W3–W10.
- Agi, E., Kulkarni, A., & Hiesinger, P. R. (2020). Neuronal strategies for meeting the right partner during brain wiring. *Current Opinion in Neurobiology*, 63, 1–8.
- Akin, O., Bajar, B. T., Keles, M. F., Frye, M. A., & Zipursky, S. L. (2019). Cell-Type-Specific Patterned Stimulus-Independent Neuronal Activity in the Drosophila Visual System during Synapse Formation. *Neuron*, 101(5), 894-904.e5.
- Akin, O., & Zipursky, S. L. (2020). Activity regulates brain development in the fly. *Current Opinion in Genetics & Development*, 65, 8–13.
- Alyagor, I., Berkun, V., Keren-Shaul, H., Marmor-Kollet, N., David, E., Mayseless, O., … Schuldiner, O. (2018). Combining Developmental and Perturbation-Seq Uncovers Transcriptional Modules Orchestrating Neuronal Remodeling. *Developmental Cell*, 47(1), 38-52.e6.
- Antón-Bolaños, N., Sempere-Ferràndez, A., Guillamón-Vivancos, T., Martini, F. J., Pérez-Saiz, L., Gezelius, H., … López-Bendito, G. (2019). Prenatal activity from thalamic neurons governs the emergence of functional cortical maps in mice. *Science*, 364(6444), 987–990.

- Aragon, M. J., Mok, A. T., Shea, J., Wang, M., Kim, H., Barkdull, N., … Yapici, N. (2022). Multiphoton imaging of neural structure and activity in Drosophila through the intact cuticle. *ELife*, 11.
- Araújo, S. J., & Tear, G. (2003). Axon guidance mechanisms and molecules: lessons from invertebrates. *Nature Reviews. Neuroscience*, 4(11), 910–922.
- Armstrong, J. D., de Belle, J. S., Wang, Z., & Kaiser, K. (1998). Metamorphosis of the mushroom bodies; large-scale rearrangements of the neural substrates for associative learning and memory in Drosophila. *Learning & Memory*, 5(1–2), 102–114.
- Arroyo, D. A., & Feller, M. B. (2016). Spatiotemporal features of retinal waves instruct the wiring of the visual circuitry. *Frontiers in Neural Circuits*, 10, 54.
- Ashley, J., Sorrentino, V., Lobb-Rabe, M., Nagarkar-Jaiswal, S., Tan, L., Xu, S., … Carrillo, R. A. (2019). Transsynaptic interactions between IgSF proteins DIP-α and Dpr10 are required for motor neuron targeting specificity. *ELife*, 8.
- Aso, Y., Grübel, K., Busch, S., Friedrich, A. B., Siwanowicz, I., & Tanimoto, H. (2009). The mushroom body of adult Drosophila characterized by GAL4 drivers. *Journal of Neurogenetics*, 23(1–2), 156–172.
- Aso, Y., Hattori, D., Yu, Y., Johnston, R. M., Iyer, N. A., Ngo, T.-T. B., … Rubin, G. M. (2014). The neuronal architecture of the mushroom body provides a logic for associative learning. *ELife*, 3, e04577.
- Aso, Y., Ray, R. P., Long, X., Bushey, D., Cichewicz, K., Ngo, T.-T., … Rubin, G. M. (2019). Nitric oxide acts as a cotransmitter in a subset of dopaminergic neurons to diversify memory dynamics. *ELife*, 8.
- Awasaki, T., Saito, M., Sone, M., Suzuki, E., Sakai, R., Ito, K., & Hama, C. (2000). The Drosophila trio plays an essential role in patterning of axons by regulating their directional extension. *Neuron*, 26(1), 119–131.
- Ayaz, D., Leyssen, M., Koch, M., Yan, J., Srahna, M., Sheeba, V., … Hassan, B. A. (2008). Axonal injury and regeneration in the adult brain of Drosophila. *The Journal of Neuroscience*, 28(23), 6010–6021.
- Azevedo, F. A. C., Carvalho, L. R. B., Grinberg, L. T., Farfel, J. M., Ferretti, R. E. L., Leite, R. E. P., … Herculano-Houzel, S. (2009). Equal numbers of

neuronal and nonneuronal cells make the human brain an isometrically scaled-up primate brain. *The Journal of Comparative Neurology*, 513(5), 532–541.

- Bae, J. H., & Schlessinger, J. (2010). Asymmetric tyrosine kinase arrangements in activation or autophosphorylation of receptor tyrosine kinases. *Molecules and Cells*, 29(5), 443–448
- Bai, L., & Sehgal, A. (2015). Anaplastic lymphoma kinase acts in the drosophila mushroom body to negatively regulate sleep. *PLoS Genetics*, 11(11), e1005611.
- Bainbridge, S. P., & Bownes, M. (1981). Staging the metamorphosis of *Drosophila melanogaster*. *Development*, 66(1), 57–80.
- Bajar, B. T., Phi, N. T., Isaacman-Beck, J., Reichl, J., Randhawa, H., & Akin, O. (2022). A discrete neuronal population coordinates brain-wide developmental activity. *Nature*, 602(7898), 639–646.
- Bali, N., Lee, H.-K. P., & Zinn, K. (2022). Sticks and Stones, a conserved cell surface ligand for the Type IIa RPTP Lar, regulates neural circuit wiring in Drosophila. *ELife*, 11.
- Baltruschat, L., Prisco, L., Ranft, P., Lauritzen, J. S., Fiala, A., Bock, D. D., & Tavosanis, G. (2021). Circuit reorganization in the Drosophila mushroom body calyx accompanies memory consolidation. *Cell Reports*, 34(11), 108871.
- Barak, O., Rigotti, M., & Fusi, S. (2013). The sparseness of mixed selectivity neurons controls the generalization-discrimination trade-off. *The Journal of Neuroscience*, 33(9), 3844–3856.
- Bargmann, C. I., & Marder, E. (2013). From the connectome to brain function. *Nature Methods*, 10(6), 483–490.
- Barish, S., Nuss, S., Strunilin, I., Bao, S., Mukherjee, S., Jones, C. D., & Volkan, P. C. (2018). Combinations of DIPs and Dprs control organization of olfactory receptor neuron terminals in Drosophila. *PLoS Genetics*, 14(8), e1007560.
- Bates, A. S., Schlegel, P., Roberts, R. J. V., Drummond, N., Tamimi, I. F. M., Turnbull, R. G., … Jefferis, G. S. X. E. (2020). Complete connectomic reconstruction of olfactory projection neurons in the fly brain. *BioRxiv*.

- Bazigou, E., Apitz, H., Johansson, J., Lorén, C. E., Hirst, E. M. A., Chen, P.-L., … Salecker, I. (2007). Anterograde Jelly belly and Alk receptor tyrosine kinase signaling mediates retinal axon targeting in Drosophila. *Cell*, 128(5), 961–975.
- Bellen, H. J., O'Kane, C. J., Wilson, C., Grossniklaus, U., Pearson, R. K., & Gehring, W. J. (1989). P-element-mediated enhancer detection: a versatile method to study development in Drosophila. *Genes & Development*, 3(9), 1288–1300.
- Bengtsson, F., & Jörntell, H. (2009). Sensory transmission in cerebellar granule cells relies on similarly coded mossy fiber inputs. *Proceedings of the National Academy of Sciences of the United States of America*, 106(7), 2389–2394.
- Benton, R., Sachse, S., Michnick, S. W., & Vosshall, L. B. (2006). Atypical membrane topology and heteromeric function of Drosophila odorant receptors in vivo. *PLoS Biology*, 4(2), e20.
- Benzer, S. (1967). BEHAVIORAL MUTANTS OF drosophila ISOLATED BY COUNTERCURRENT DISTRIBUTION. *Proceedings of the National Academy of Sciences of the United States of America*, 58(3), 1112–1119.
- Berdnik, D., Favaloro, V., & Luo, L. (2012). The SUMO protease Verloren regulates dendrite and axon targeting in olfactory projection neurons. *The Journal of Neuroscience*, 32(24), 8331–8340.
- Betkiewicz, R., Lindner, B., & Nawrot, M. P. (2020). Circuit and Cellular Mechanisms Facilitate the Transformation from Dense to Sparse Coding in the Insect Olfactory System. *ENeuro*, 7(2).
- Blockus, H., & Polleux, F. (2021). Developmental mechanisms underlying circuit wiring: Novel insights and challenges ahead. *Current Opinion in Neurobiology*, 66, 205–211.
- Bloss, E. B., Cembrowski, M. S., Karsh, B., Colonell, J., Fetter, R. D., & Spruston, N. (2016). Structured Dendritic Inhibition Supports Branch-Selective Integration in CA1 Pyramidal Cells. *Neuron*, 89(5), 1016–1030.
- Bornstein, B., Alyagor, I., Berkun, V., Meltzer, H., Reh, F., Keren-Shaul, H., … Schuldiner, O. (2019). Transneuronal interactions facilitate axonal compartment formation. *BioRxiv.*

- Boto, T., Stahl, A., & Tomchik, S. M. (2020). Cellular and circuit mechanisms of olfactory associative learning in Drosophila. *Journal of Neurogenetics*, 34(1), 36–46.
- Boto, T., Stahl, A., Zhang, X., Louis, T., & Tomchik, S. M. (2019). Independent contributions of discrete dopaminergic circuits to cellular plasticity, memory strength, and valence in drosophila. *Cell Reports*, 27(7), 2014-2021.e2.
- Bouchard, M. B., Voleti, V., Mendes, C. S., Lacefield, C., Grueber, W. B., Mann, R. S., … Hillman, E. M. C. (2015). Swept confocally-aligned planar excitation (SCAPE) microscopy for high speed volumetric imaging of behaving organisms. *Nature Photonics*, 9(2), 113–119.
- Brand, A. H., & Perrimon, N. (1993). Targeted gene expression as a means of altering cell fates and generating dominant phenotypes. *Development*, 118(2), 401–415.
- Brandt, W. N., Flamm, W. G., & Bernheim, N. J. (1972). The value of hydroxyurea in assessing repair synthesis of DNA in HeLa cells. *Chemico-Biological Interactions*, 5(5), 327–339.
- Briggman, K. L., & Bock, D. D. (2012). Volume electron microscopy for neuronal circuit reconstruction. *Current Opinion in Neurobiology*, 22(1), 154–161.
- Briggman, K. L., Helmstaedter, M., & Denk, W. (2011). Wiring specificity in the direction-selectivity circuit of the retina. *Nature*, 471(7337), 183–188
- Butcher, N. J., Friedrich, A. B., Lu, Z., Tanimoto, H., & Meinertzhagen, I. A. (2012). Different classes of input and output neurons reveal new features in microglomeruli of the adult Drosophila mushroom body calyx. *The Journal of Comparative Neurology*, 520(10), 2185–2201.
- Cafferty, P., Yu, L., Long, H., & Rao, Y. (2006). Semaphorin-1a functions as a guidance receptor in the Drosophila visual system. *The Journal of Neuroscience*, 26(15), 3999–4003.
- Campbell, R. A. A., Honegger, K. S., Qin, H., Li, W., Demir, E., & Turner, G. C. (2013). Imaging a population code for odor identity in the Drosophila mushroom body. *The Journal of Neuroscience*, 33(25), 10568–10581.

- Caron, S. J. C., Ruta, V., Abbott, L. F., & Axel, R. (2013). Random convergence of olfactory inputs in the Drosophila mushroom body. *Nature*, 497(7447), 113–117.
- Cayco-Gajic, N. A., Clopath, C., & Silver, R. A. (2017). Sparse synaptic connectivity is required for decorrelation and pattern separation in feedforward networks. *Nature Communications*, 8(1), 1116.
- Cayco-Gajic, N. A., & Silver, R. A. (2019). Re-evaluating Circuit Mechanisms Underlying Pattern Separation. *Neuron*, 101(4), 584–602.
- Cheng, L. Y., Bailey, A. P., Leevers, S. J., Ragan, T. J., Driscoll, P. C., & Gould, A. P. (2011). Anaplastic lymphoma kinase spares organ growth during nutrient restriction in Drosophila. *Cell*, 146(3), 435–447.
- Cheng, S., Ashley, J., Kurleto, J. D., Lobb-Rabe, M., Park, Y. J., Carrillo, R. A., & Özkan, E. (2019). Molecular basis of synaptic specificity by immunoglobulin superfamily receptors in Drosophila. *ELife*, 8.
- Cho, J. H., Prince, J. E. A., & Cloutier, J.-F. (2009). Axon guidance events in the wiring of the mammalian olfactory system. *Molecular Neurobiology*, 39(1), 1–9.
- Christiansen, F., Zube, C., Andlauer, T. F. M., Wichmann, C., Fouquet, W., Owald, D., … Sigrist, S. J. (2011). Presynapses in Kenyon cell dendrites in the mushroom body calyx of Drosophila. *The Journal of Neuroscience*, 31(26), 9696–9707.
- Colón-Ramos, D. A., Margeta, M. A., & Shen, K. (2007). Glia promote local synaptogenesis through UNC-6 (netrin) signaling in C. elegans. *Science*, 318(5847), 103–106.
- Connolly, J. B., Roberts, I. J., Armstrong, J. D., Kaiser, K., Forte, M., Tully, T., & O'Kane, C. J. (1996). Associative learning disrupted by impaired Gs signaling in Drosophila mushroom bodies. *Science*, 274(5295), 2104–2107.
- Consalez, G. G., Goldowitz, D., Casoni, F., & Hawkes, R. (2020). Origins, development, and compartmentation of the granule cells of the cerebellum. *Frontiers in Neural Circuits*, 14, 611841.

- Crittenden, J. R., Skoulakis, E. M., Han, K. A., Kalderon, D., & Davis, R. L. (1998). Tripartite mushroom body architecture revealed by antigenic markers. *Learning & Memory*, 5(1–2), 38–51.
- Danielsen, E. T., Moeller, M. E., & Rewitz, K. F. (2013). Nutrient signaling and developmental timing of maturation. *Current Topics in Developmental Biology*, 105, 37–67.
- Davie, K., Janssens, J., Koldere, D., De Waegeneer, M., Pech, U., Kreft, Ł., … Aerts, S. (2018). A Single-Cell Transcriptome Atlas of the Aging *Drosophila* Brain. *Cell*, 174(4).
- de Belle, J. S., & Heisenberg, M. (1994). Associative odor learning in Drosophila abolished by chemical ablation of mushroom bodies. *Science*, 263(5147), 692–695.
- De Belle, J. S., & Heisenberg, M. (1996). Expression of Drosophila mushroom body mutations in alternative genetic backgrounds: A case study of the mushroom body miniature gene. *Proceedings of the National Academy of Sciences of the United States of America*, 93, 9875–9880.
- de Wit, J., & Ghosh, A. (2016). Specification of synaptic connectivity by cell surface interactions. *Nature Reviews. Neuroscience*, 17(1), 22–35.
- Dhar, M., Hantman, A. W., & Nishiyama, H. (2018). Developmental pattern and structural factors of dendritic survival in cerebellar granule cells in vivo. *Scientific Reports*, 8(1), 17561.
- Dietzl, G., Chen, D., Schnorrer, F., Su, K.-C., Barinova, Y., Fellner, M., … Dickson, B. J. (2007). A genome-wide transgenic RNAi library for conditional gene inactivation in Drosophila. *Nature*, 448(7150), 151–156
- DISSERTATIONS.SE: Deciphering the Alk signaling pathway in Drosophila. (n.d.). Retrieved February 7, 2024,
- Doll, C. A., & Broadie, K. (2015). Activity-dependent FMRP requirements in development of the neural circuitry of learning and memory. *Development*, 142(7), 1346–1356.
- Doll, C. A., Vita, D. J., & Broadie, K. (2017). Fragile X Mental Retardation Protein Requirements in Activity-Dependent Critical Period Neural Circuit Refinement. *Current Biology*, 27(15).

- Dombrovski, M., & Condron, B. (2021). Critical periods shaping the social brain: A perspective from Drosophila. *Bioessays: News and Reviews in Molecular, Cellular and Developmental Biology*, 43(1).
- Donà, E., & Jefferis, G. S. X. E. (2021). Neurodevelopment: Comparative connectomics and the study of circuit assembly. *Current Biology*, 31(9), R452–R454.
- Dubnau, J., Grady, L., Kitamoto, T., & Tully, T. (2001). Disruption of neurotransmission in Drosophila mushroom body blocks retrieval but not acquisition of memory. *Nature*, 411(6836), 476–480.
- Dudai, Y., Jan, Y. N., Byers, D., Quinn, W. G., & Benzer, S. (1976). dunce, a mutant of Drosophila deficient in learning. *Proceedings of the National Academy of Sciences of the United States of America*, 73(5), 1684–1688.
- Dunn, F. A., & Wong, R. O. L. (2012). Diverse strategies engaged in establishing stereotypic wiring patterns among neurons sharing a common input at the visual system's first synapse. *The Journal of Neuroscience*, 32(30), 10306–10317.
- Durkin, J., Poe, A. R., Belfer, S. J., Rodriguez, A., Tang, S. H., Walker, J. A., & Kayser, M. S. (2023). Neurofibromin 1 regulates early developmental sleep in Drosophila. *Neurobiology of Sleep and Circadian Rhythms*, 15, 100101.
- Eichler, K., Li, F., Litwin-Kumar, A., Park, Y., Andrade, I., Schneider-Mizell, C. M., … Cardona, A. (2017). The complete connectome of a learning and memory centre in an insect brain. *Nature*, 548(7666), 175–182.
- Elkahlah, N. A., Rogow, J. A., Ahmed, M., & Clowney, E. J. (2020). Presynaptic developmental plasticity allows robust sparse wiring of the Drosophila mushroom body. *ELife*, 9.
- Endo, K., & Kazama, H. (2022). Central organization of a high-dimensional odor space. *Current Opinion in Neurobiology*, 73, 102528.
- Englund, C., Lorén, C. E., Grabbe, C., Varshney, G. K., Deleuil, F., Hallberg, B., & Palmer, R. H. (2003). Jeb signals through the Alk receptor tyrosine kinase to drive visceral muscle fusion. *Nature*, 425(6957), 512–516.
- Enriquez, J., Venkatasubramanian, L., Baek, M., Peterson, M., Aghayeva, U., & Mann, R. S. (2015). Specification of individual adult motor neuron

morphologies by combinatorial transcription factor codes. *Neuron*, 86(4), 955–970.

- Erö, C., Gewaltig, M.-O., Keller, D., & Markram, H. (2018). A cell atlas for the mouse brain. *Frontiers in Neuroinformatics*, 12, 84.
- Eschbach, C., Fushiki, A., Winding, M., Afonso, B., Andrade, I. V., Cocanougher, B. T., … Zlatic, M. (2020). Circuits for integrating learnt and innate valences in the fly brain. *BioRxiv*.
- Escobet-Montalbán, A., Gasparoli, F. M., Nylk, J., Liu, P., Yang, Z., & Dholakia, K. (2018). Three-photon light-sheet fluorescence microscopy. *Optics Letters*, 43(21), 5484–5487.
- Favuzzi, E., Deogracias, R., Marques-Smith, A., Maeso, P., Jezequel, J., Exposito-Alonso, D., … Rico, B. (2019). Distinct molecular programs regulate synapse specificity in cortical inhibitory circuits. *Science*, 363(6425), 413–417.
- Feldheim, D. A., & O'Leary, D. D. M. (2010). Visual map development: bidirectional signaling, bifunctional guidance molecules, and competition. *Cold Spring Harbor Perspectives in Biology*, 2(11), a001768.
- Fischbach, K.-F., & Hiesinger, P. R. (2008). Optic lobe development. *Advances in Experimental Medicine and Biology*, 628, 115–136.
- Fischbach, K.-F., Linneweber, G. A., Andlauer, T. F. M., Hertenstein, A., Bonengel, B., & Chaudhary, K. (2009). The irre cell recognition module (IRM) proteins. *Journal of Neurogenetics*, 23(1–2), 48–67.
- Fischer, J. A., Giniger, E., Maniatis, T., & Ptashne, M. (1988). GAL4 activates transcription in Drosophila. *Nature*, 332(6167), 853–856.
- Furrer, M.-P., Kim, S., Wolf, B., & Chiba, A. (2003). Robo and Frazzled/DCC mediate dendritic guidance at the CNS midline. *Nature Neuroscience*, 6(3), 223–230.
- Furrer, M.-P., Vasenkova, I., Kamiyama, D., Rosado, Y., & Chiba, A. (2007). Slit and Robo control the development of dendrites in Drosophila CNS. *Development*, 134(21), 3795–3804.
- Galy, A., Schenck, A., Sahin, H. B., Qurashi, A., Sahel, J.-A., Diebold, C., & Giangrande, A. (2011). CYFIP dependent actin remodeling controls specific

aspects of Drosophila eye morphogenesis. *Developmental Biology*, 359(1), 37–46.

- Gao, Q., Yuan, B., & Chess, A. (2000). Convergent projections of Drosophila olfactory neurons to specific glomeruli in the antennal lobe. *Nature Neuroscience*, 3(8), 780–785.
- Gardeux, V., David, F. P. A., Shajkofci, A., Schwalie, P. C., & Deplancke, B. (2017). ASAP: a web-based platform for the analysis and interactive visualization of single-cell RNA-seq data. *Bioinformatics*, 33(19), 3123–3125.
- Gayko, U., Cleghon, V., Copeland, T., Morrison, D. K., & Perrimon, N. (1999). Synergistic activities of multiple phosphotyrosine residues mediate full signaling from the Drosophila Torso receptor tyrosine kinase. *Proceedings of the National Academy of Sciences of the United States of America*, 96(2), 523–528.
- Georganta, E.-M., Moressis, A., & Skoulakis, E. M. C. (2021). Associative learning requires neurofibromin to modulate gabaergic inputs to drosophila mushroom bodies. *The Journal of Neuroscience*, 41(24), 5274–5286.
- Gerhard, S., Andrade, I., Fetter, R. D., Cardona, A., & Schneider-Mizell, C. M. (2017). Conserved neural circuit structure across Drosophila larval development revealed by comparative connectomics. *ELife*, 6.
- Gibbs, S. M., & Truman, J. W. (1998). Nitric oxide and cyclic GMP regulate retinal patterning in the optic lobe of Drosophila. *Neuron*, 20(1), 83–93.
- Godenschwege, T. A., Hu, H., Shan-Crofts, X., Goodman, C. S., & Murphey, R. K. (2002). Bi-directional signaling by Semaphorin 1a during central synapse formation in Drosophila. *Nature Neuroscience*, 5(12), 1294–1301.
- Godenschwege, T. A., Simpson, J. H., Shan, X., Bashaw, G. J., Goodman, C. S., & Murphey, R. K. (2002). Ectopic expression in the giant fiber system of Drosophila reveals distinct roles for roundabout (Robo), Robo2, and Robo3 in dendritic guidance and synaptic connectivity. *The Journal of Neuroscience*, 22(8), 3117–3129.
- Golic, K. G. (1991). Site-specific recombination between homologous chromosomes in Drosophila. *Science*, 252(5008), 958–961.

- Golic, K. G., & Lindquist, S. (1989). The FLP recombinase of yeast catalyzes site-specific recombination in the Drosophila genome. *Cell*, 59(3), 499–509.
- Gomez, A. M., Traunmüller, L., & Scheiffele, P. (2021). Neurexins: molecular codes for shaping neuronal synapses. *Nature Reviews. Neuroscience*, 22(3), 137–151.
- Gouzi, J. Y., Bouraimi, M., Roussou, I. G., Moressis, A., & Skoulakis, E. M. C. (2018). The Drosophila Receptor Tyrosine Kinase Alk Constrains Long-Term Memory Formation. *The Journal of Neuroscience*, 38(35), 7701–7712.
- Gouzi, J. Y., Moressis, A., Walker, J. A., Apostolopoulou, A. A., Palmer, R. H., Bernards, A., & Skoulakis, E. M. C. (2011). The receptor tyrosine kinase Alk controls neurofibromin functions in Drosophila growth and learning. *PLoS Genetics*, 7(9), e1002281.
- Grabe, V., Baschwitz, A., Dweck, H. K. M., Lavista-Llanos, S., Hansson, B. S., & Sachse, S. (2016). Elucidating the neuronal architecture of olfactory glomeruli in the drosophila antennal lobe. *Cell Reports*, 16(12), 3401–3413.
- Grabe, V., Strutz, A., Baschwitz, A., Hansson, B. S., & Sachse, S. (2015). Digital in vivo 3D atlas of the antennal lobe of *Drosophila melanogaster*. *The Journal of Comparative Neurology*, 523(3), 530–544.
- Grimaud, J., Dorrell, W., Pehlevan, C., & Murthy, V. (2020). Bilateral Alignment of Receptive Fields in the Olfactory Cortex Points to Non-Random Connectivity. *BioRxiv*.
- Groh, C., & Rössler, W. (2020). Analysis of synaptic microcircuits in the mushroom bodies of the honeybee. *Insects*, 11(1).
- Groschner, L. N., Chan Wah Hak, L., Bogacz, R., DasGupta, S., & Miesenböck, G. (2018). Dendritic Integration of Sensory Evidence in Perceptual Decision-Making. *Cell*, 173(4), 894-905.e13.
- Groschner, L. N., & Miesenböck, G. (2019). Mechanisms of Sensory Discrimination: Insights from Drosophila Olfaction. *Annual Review of Biophysics*, 48, 209–229.
- Gruntman, E., & Turner, G. C. (2013). Integration of the olfactory code across dendritic claws of single mushroom body neurons. *Nature Neuroscience*, 16(12), 1821–1829.

- Haenicke, J., Yamagata, N., Zwaka, H., Nawrot, M., & Menzel, R. (2018). Neural correlates of odor learning in the presynaptic microglomerular circuitry in the honeybee mushroom body calyx. *ENeuro*, 5(3).
- Hallberg, B., & Palmer, R. H. (2013). Mechanistic insight into ALK receptor tyrosine kinase in human cancer biology. *Nature Reviews. Cancer*, 13(10), 685–700.
- Hamid, A., Gutierrez, A., Munroe, J., & Syed, M. H. (2023). The Drivers of Diversity: Integrated genetic and hormonal cues regulate neural diversity. *Seminars in Cell & Developmental Biology*, 142, 23–35.
- Hao, J. C., Yu, T. W., Fujisawa, K., Culotti, J. G., Gengyo-Ando, K., Mitani, S., Bargmann, C. I. (2001). C. elegans slit acts in midline, dorsal-ventral, and anterior-posterior guidance via the SAX-3/Robo receptor. *Neuron*, 32(1), 25–38.
- Hao, J., Wang, X., Dan, Y., Poo, M., & Zhang, X. (2009). An arithmetic rule for spatial summation of excitatory and inhibitory inputs in pyramidal neurons. *Proceedings of the National Academy of Sciences of the United States of America*, 106(51), 21906–21911.
- Hartenstein, V., Omoto, J. J., & Lovick, J. K. (2021). The role of cell lineage in the development of neuronal circuitry and function. *Developmental Biology*, 475, 165–180.
- Hayashi, T. T., MacKenzie, A. J., Ganguly, I., Ellis, K. E., Smihula, H. M., Jacob, M. S., … Caron, S. J. C. (2022). Mushroom body input connections form independently of sensory activity in Drosophila melanogaster. *Current Biology*, 32(18), 4000-4012.e5.
- Hebb, D. O. (1949). The organization of behavior; A neuropsychological theory. *The American Journal of Psychology*, 63(4), 633.
- Heckman, E. L., & Doe, C. Q. (2021). Establishment and maintenance of neural circuit architecture. *The Journal of Neuroscience*, 41(6), 1119–1129
- Heisenberg, M, Borst, A., Wagner, S., & Byers, D. (1985). Drosophila mushroom body mutants are deficient in olfactory learning. *Journal of Neurogenetics*, 2(1), 1–30.

- Heisenberg, Martin. (2003). Mushroom body memoir: from maps to models. *Nature Reviews. Neuroscience*, 4(4), 266–275.
- Hell, S. W., Bahlmann, K., Schrader, M., Soini, A., Malak, H. M., Gryczynski, I., & Lakowicz, J. R. (1996). Three-photon excitation in fluorescence microscopy. *Journal of Biomedical Optics*, 1(1), 71–74.
- Hellerman, M. B., Choe, R. H., & Johnson, R. I. (2015). Live-imaging of the Drosophila pupal eye. *Journal of Visualized Experiments*, (95), 52120.
- Hiesinger, P. R., & Hassan, B. A. (2018). The evolution of variability and robustness in neural development. *Trends in Neurosciences*, 41(9), 577–586.
- Honegger, K. S., Campbell, R. A. A., & Turner, G. C. (2011). Cellular-resolution population imaging reveals robust sparse coding in the Drosophila mushroom body. *The Journal of Neuroscience*, 31(33), 11772–11785.
- Huang, C., Maxey, J. R., Sinha, S., Savall, J., Gong, Y., & Schnitzer, M. J. (2018). Long-term optical brain imaging in live adult fruit flies. *Nature Communications*, 9(1), 872.
- Huang, X., Warren, J. T., Buchanan, J., Gilbert, L. I., & Scott, M. P. (2007). Drosophila Niemann-Pick type C-2 genes control sterol homeostasis and steroid biosynthesis: a model of human neurodegenerative disease. *Development*, 134(20), 3733–3742.
- Huang, Z. J. (2006). Subcellular organization of GABAergic synapses: role of ankyrins and L1 cell adhesion molecules. *Nature Neuroscience*, 9(2), 163–166.
- Hubbard, S. R., & Till, J. H. (2000). Protein tyrosine kinase structure and function. *Annual Review of Biochemistry*, 69, 373–398.
- Huber, A. B., Kolodkin, A. L., Ginty, D. D., & Cloutier, J.-F. (2003). Signaling at the growth cone: ligand-receptor complexes and the control of axon growth and guidance. *Annual Review of Neuroscience*, 26, 509–563.
- Hugosson, F. (n.d.). Deciphering the Alk signaling pathway in Drosophila.
- Ichinose, T., Kanno, M., Wu, H., Yamagata, N., Sun, H., Abe, A., & Tanimoto, H. (2021). Mushroom body output differentiates memory processes and distinct memory-guided behaviors. *Current Biology*, 31(6), 1294-1302.e4.
- Inoue, Y. H., do Carmo Avides, M., Shiraki, M., Deak, P., Yamaguchi, M., Nishimoto, Y., … Glover, D. M. (2000). Orbit, a novel microtubule-associated

protein essential for mitosis in Drosophila melanogaster. *The Journal of Cell Biology*, 149(1), 153–166.

- Ishikawa, T., Shimuta, M., & Häusser, M. (2015). Multimodal sensory integration in single cerebellar granule cells in vivo. *ELife*, 4.
- Ito, I., Ong, R. C.-Y., Raman, B., & Stopfer, M. (2008). Sparse odor representation and olfactory learning. *Nature Neuroscience*, 11(10), 1177–1184.
- Ito, K., Awano, W., Suzuki, K., Hiromi, Y., & Yamamoto, D. (1997). The Drosophila mushroom body is a quadruple structure of clonal units each of which contains a virtually identical set of neurones and glial cells. *Development*, 124(4), 761–771.
- Ito, K., & Hotta, Y. (1992). Proliferation pattern of postembryonic neuroblasts in the brain of Drosophila melanogaster. *Developmental Biology*, 149(1), 134–148.
- Ito, K., Suzuki, K., Estes, P., Ramaswami, M., Yamamoto, D., & Strausfeld, N. J. (1998). The organization of extrinsic neurons and their implications in the functional roles of the mushroom bodies in Drosophila melanogaster Meigen. *Learning & Memory*, 5(1–2), 52–77.
- Jain, S., Lin, Y., Kurmangaliyev, Y. Z., Valdes-Aleman, J., LoCascio, S. A., Mirshahidi, P., … Zipursky, S. L. (2022). A global timing mechanism regulates cell-type-specific wiring programmes. *Nature*, 603(7899), 112–118.
- Jarecki, J., & Keshishian, H. (1995). Role of neural activity during synaptogenesis in Drosophila. *The Journal of Neuroscience*, 15(12), 8177–8190.
- Jefferis, G. S., Marin, E. C., Stocker, R. F., & Luo, L. (2001). Target neuron prespecification in the olfactory map of Drosophila. *Nature*, 414(6860), 204–208.
- Jefferis, G. S. X. E., Potter, C. J., Chan, A. M., Marin, E. C., Rohlfing, T., Maurer, C. R., & Luo, L. (2007). Comprehensive maps of Drosophila higher olfactory centers: spatially segregated fruit and pheromone representation. *Cell*, 128(6), 1187–1203.

- Jefferis, G. S. X. E., Vyas, R. M., Berdnik, D., Ramaekers, A., Stocker, R. F., Tanaka, N. K., … Luo, L. (2004). Developmental origin of wiring specificity in the olfactory system of Drosophila. *Development*, 131(1), 117–130.
- Jenett, A., Rubin, G. M., Ngo, T.-T. B., Shepherd, D., Murphy, C., Dionne, H., … Zugates, C. T. (2012). A GAL4-driver line resource for Drosophila neurobiology. *Cell Reports*, 2(4), 991–1001.
- Johard, H. A. D., Enell, L. E., Gustafsson, E., Trifilieff, P., Veenstra, J. A., & Nässel, D. R. (2008). Intrinsic neurons of Drosophila mushroom bodies express short neuropeptide F: relations to extrinsic neurons expressing different neurotransmitters. *The Journal of Comparative Neurology*, 507(4), 1479–1496.
- Kania, A., & Klein, R. (2016). Mechanisms of ephrin-Eph signalling in development, physiology and disease. *Nature Reviews. Molecular Cell Biology*, 17(4), 240–256.
- Kaupp, U. B. (2010). Olfactory signalling in vertebrates and insects: differences and commonalities. *Nature Reviews. Neuroscience*, 11(3), 188–200.
- Keroles, M. B., Dusseault, S. K., Liu, C., Mohammed, M. R., Vadakkan, C. M., Amiel, J. H., … Baker, J. (2014). Imaging through the pupal case of Drosophila melanogaster. *Journal of Visualized Experiments*, (83), e51239.
- Kidd, T., Bland, K. S., & Goodman, C. S. (1999). Slit is the midline repellent for the robo receptor in Drosophila. *Cell*, 96(6), 785–794.
- Kiral, F. R., Dutta, S. B., Linneweber, G. A., Hilgert, S., Poppa, C., Duch, C., … Hiesinger, P. R. (2021). Brain connectivity inversely scales with developmental temperature in Drosophila. *Cell Reports*, 37(12), 110145.
- Klassen, M. P., & Shen, K. (2007). Wnt signaling positions neuromuscular connectivity by inhibiting synapse formation in C. elegans. *Cell*, 130(4), 704–716.
- Kolodkin, A. L., & Tessier-Lavigne, M. (2011). Mechanisms and molecules of neuronal wiring: a primer. *Cold Spring Harbor Perspectives in Biology*, 3(6).
- Komiyama, T., & Luo, L. (2007). Intrinsic control of precise dendritic targeting by an ensemble of transcription factors. *Current Biology*, 17(3), 278–285.

- Komiyama, T., Sweeney, L. B., Schuldiner, O., Garcia, K. C., & Luo, L. (2007). Graded expression of semaphorin-1a cell-autonomously directs dendritic targeting of olfactory projection neurons. *Cell*, 128(2), 399–410.
- Kondo, S., Takahashi, T., Yamagata, N., Imanishi, Y., Katow, H., Hiramatsu, S., … Tanimoto, H. (2020). Neurochemical organization of the drosophila brain visualized by endogenously tagged neurotransmitter receptors. *Cell Reports*, 30(1), 284-297.e5.
- Kossio, Y. F. K., Goedeke, S., Klos, C., & Memmesheimer, R.-M. (2021). Drifting assemblies for persistent memory: Neuron transitions and unsupervised compensation. *Proceedings of the National Academy of Sciences of the United States of America*, 118(46).
- Kremer, M. C., Christiansen, F., Leiss, F., Paehler, M., Knapek, S., Andlauer, T. F. M., … Tavosanis, G. (2010). Structural long-term changes at mushroom body input synapses. *Current Biology*, 20(21), 1938–1944.
- Krishnaswamy, A., Yamagata, M., Duan, X., Hong, Y. K., & Sanes, J. R. (2015). Sidekick 2 directs formation of a retinal circuit that detects differential motion. *Nature*, 524(7566), 466–470.
- Kumar, S., Tunc, I., Tansey, T. R., Pirooznia, M., & Harbison, S. T. (2021). Identification of genes contributing to a long circadian period in drosophila melanogaster. *Journal of Biological Rhythms*, 36(3), 239–253.
- Kunz, T., Kraft, K. F., Technau, G. M., & Urbach, R. (2012). Origin of Drosophila mushroom body neuroblasts and generation of divergent embryonic lineages. *Development*, 139(14), 2510–2522.
- Kurusu, M., Cording, A., Taniguchi, M., Menon, K., Suzuki, E., & Zinn, K. (2008). A screen of cell-surface molecules identifies leucine-rich repeat proteins as key mediators of synaptic target selection. *Neuron*, 59(6), 972–985.
- Lai, S.-L., Awasaki, T., Ito, K., & Lee, T. (2008). Clonal analysis of Drosophila antennal lobe neurons: diverse neuronal architectures in the lateral neuroblast lineage. *Development*, 135(17), 2883–2893.
- Laissue, P. P., Reiter, C., Hiesinger, P. R., Halter, S., Fischbach, K. F., & Stocker, R. F. (1999). Three-dimensional reconstruction of the antennal lobe in Drosophila melanogaster. *Journal of Comparative Neurology*.

- Langley, J. N. (1895). Note on Regeneration of Prae-Ganglionic Fibres of the Sympathetic. *The Journal of Physiology*, 18(3), 280–284.
- Lasek, A. W., Lim, J., Kliethermes, C. L., Berger, K. H., Joslyn, G., Brush, G., … Heberlein, U. (2011). An evolutionary conserved role for anaplastic lymphoma kinase in behavioral responses to ethanol. *Plos One*, 6(7), e22636.
- Laurent, G., Stopfer, M., Friedrich, R. W., Rabinovich, M. I., Volkovskii, A., & Abarbanel, H. D. (2001). Odor encoding as an active, dynamical process: experiments, computation, and theory. *Annual Review of Neuroscience*, 24, 263–297.
- Lee, H.-H., Norris, A., Weiss, J. B., & Frasch, M. (2003). Jelly belly protein activates the receptor tyrosine kinase Alk to specify visceral muscle pioneers. *Nature*, 425(6957), 507–512.
- Lee, T., Lee, A., & Luo, L. (1999). Development of the Drosophila mushroom bodies: sequential generation of three distinct types of neurons from a neuroblast. *Development*, 126(18), 4065–4076.
- Lee, T., & Luo, L. (2001). Mosaic analysis with a repressible cell marker (MARCM) for Drosophila neural development. *Trends in Neurosciences*, 24(5), 251–254.
- Lee, T., Marticke, S., Sung, C., Robinow, S., & Luo, L. (2000). Cell-autonomous requirement of the USP/EcR-B ecdysone receptor for mushroom body neuronal remodeling in Drosophila. *Neuron*, 28(3), 807–818.
- Lee, T., Winter, C., Marticke, S. S., Lee, A., & Luo, L. (2000). Essential roles of Drosophila RhoA in the regulation of neuroblast proliferation and dendritic but not axonal morphogenesis. *Neuron*, 25(2), 307–316.
- Lee, W.-C. A., Bonin, V., Reed, M., Graham, B. J., Hood, G., Glattfelder, K., & Reid, R. C. (2016). Anatomy and function of an excitatory network in the visual cortex. *Nature*, 532(7599), 370–374.
- Leinwand, S. G., & Scott, K. (2021). Juvenile hormone drives the maturation of spontaneous mushroom body neural activity and learned behavior. *Neuron*, 109(11), 1836-1847.e5.

- Leiss, F., Groh, C., Butcher, N. J., Meinertzhagen, I. A., & Tavosanis, G. (2009). Synaptic organization in the adult Drosophila mushroom body calyx. *The Journal of Comparative Neurology*, 517(6), 808–824.
- Lemke, S. B., & Schnorrer, F. (2018). In Vivo Imaging of Muscle-tendon Morphogenesis in Drosophila Pupae. *Journal of Visualized Experiments*, (132).
- Lewis, L. P. C., Siju, K. P., Aso, Y., Friedrich, A. B., Bulteel, A. J. B., Rubin, G. M., & Grunwald Kadow, I. C. (2015). A higher brain circuit for immediate integration of conflicting sensory information in drosophila. *Current Biology*, 25(17), 2203–2214.
- Li, F., Lindsey, J., Marin, E., Otto, N., Dreher, M., Dempsey, G., … Rubin, G. M. (2020). The connectome of the adult Drosophila mushroom body: implications for function. *BioRxiv*.
- Li, Hao, Li, Y., Lei, Z., Wang, K., & Guo, A. (2013). Transformation of odor selectivity from projection neurons to single mushroom body neurons mapped with dual-color calcium imaging. *Proceedings of the National Academy of Sciences of the United States of America*, 110(29), 12084–12089.
- Li, Hongjie, Horns, F., Wu, B., Xie, Q., Li, J., Li, T., … Luo, L. (2017). Classifying Drosophila Olfactory Projection Neuron Subtypes by Single-Cell RNA Sequencing. *Cell*, 171(5), 1206-1220.e22.
- Li, Hongjie, Janssens, J., De Waegeneer, M., Kolluru, S. S., Davie, K., Gardeux, V., … Zinzen, R. P. (2022). Fly Cell Atlas: A single-nucleus transcriptomic atlas of the adult fruit fly. *Science*, 375(6584), eabk2432.
- Li, Hongjie, Li, T., Horns, F., Li, J., Xie, Q., Xu, C., … Luo, L. (2020). Single-Cell Transcriptomes Reveal Diverse Regulatory Strategies for Olfactory Receptor Expression and Axon Targeting. *Current Biology*, 30(7), 1189-1198.e5.
- Li, Hongjie, Shuster, S. A., Li, J., & Luo, L. (2018). Linking neuronal lineage and wiring specificity. *Neural Development*, 13(1), 5.
- Li, Jiefu, Han, S., Li, H., Udeshi, N. D., Svinkina, T., Mani, D. R., … Luo, L. (2020). Cell-Surface Proteomic Profiling in the Fly Brain Uncovers Wiring Regulators. *Cell*, 180(2), 373-386.e15.

- Li, Jinzhi, Mahoney, B. D., Jacob, M. S., & Caron, S. J. C. (2020). Visual Input into the Drosophila melanogaster Mushroom Body. *Cell Reports*, 32(11), 108138.
- Li, T., Fu, T.-M., Li, H., Xie, Q., Luginbuhl, D. J., Betzig, E., & Luo, L. (2021). Cellular Bases of Olfactory Circuit Assembly Revealed by Systematic Time-lapse Imaging. *BioRxiv*.
- Li, T., & Luo, L. (2021). An Explant System for Time-Lapse Imaging Studies of Olfactory Circuit Assembly in Drosophila. *Journal of Visualized Experiments*, (176).
- Lichtneckert, R., & Reichert, H. (2005). Insights into the urbilaterian brain: conserved genetic patterning mechanisms in insect and vertebrate brain development. *Heredity*, 94(5), 465–477.
- Lin, C.-C., & Potter, C. J. (2016). Editing Transgenic DNA Components by Inducible Gene Replacement in Drosophila melanogaster. *Genetics*, 203(4), 1613–1628.
- Lin, C.-C., Prokop-Prigge, K. A., Preti, G., & Potter, C. J. (2015). Food odors trigger Drosophila males to deposit a pheromone that guides aggregation and female oviposition decisions. *ELife*, 4.
- Lin, S. (2023a). Internal-state-dependent modulation of olfactory responses: a tale of dopamine neurons in the adult Drosophila mushroom body. *Current Opinion in Insect Science*, 59, 101104.
- Lin, S. (2023b). The making of the Drosophila mushroom body. *Frontiers in Physiology*, 14, 1091248.
- Linneweber, G. A., Andriatsilavo, M., Dutta, S. B., Bengochea, M., Hellbruegge, L., Liu, G., … Hassan, B. A. (2020). A neurodevelopmental origin of behavioral individuality in the Drosophila visual system. *Science*, 367(6482), 1112–1119.
- Littleton, J. T., & Ganetzky, B. (2000). Ion channels and synaptic organization: analysis of the Drosophila genome. *Neuron*, 26(1), 35–43.
- Litwin-Kumar, A., & Doiron, B. (2014). Formation and maintenance of neuronal assemblies through synaptic plasticity. *Nature Communications*, 5, 5319.
- Litwin-Kumar, A., Harris, K. D., Axel, R., Sompolinsky, H., & Abbott, L. F. (2017). Optimal degrees of synaptic connectivity. *Neuron*, 93(5), 1153-1164.e7.

- Liu, Z., Steward, R., & Luo, L. (2000). Drosophila Lis1 is required for neuroblast proliferation, dendritic elaboration and axonal transport. *Nature Cell Biology*, 2(11), 776–783.
- Lorén, C E, Scully, A., Grabbe, C., Edeen, P. T., Thomas, J., McKeown, M., … Palmer, R. H. (2001). Identification and characterization of DAlk: a novel Drosophila melanogaster RTK which drives ERK activation in vivo. *Genes To Cells*, 6(6), 531–544.
- Lorén, Christina E, Englund, C., Grabbe, C., Hallberg, B., Hunter, T., & Palmer, R. H. (2003). A crucial role for the Anaplastic lymphoma kinase receptor tyrosine kinase in gut development in Drosophila melanogaster. *EMBO Reports*, 4(8), 781–786.
- Lowery, L. A., Lee, H., Lu, C., Murphy, R., Obar, R. A., Zhai, B., … Zhan, Y. (2010). Parallel genetic and proteomic screens identify Msps as a CLASP-Abl pathway interactor in Drosophila. *Genetics*, 185(4), 1311–1325.
- Luschnig, S., Krauss, J., Bohmann, K., Desjeux, I., & Nüsslein-Volhard, C. (2000). The Drosophila SHC adaptor protein is required for signaling by a subset of receptor tyrosine kinases. *Molecular Cell*, 5(2), 231–241.
- Marin, E. C., Jefferis, G. S. X. E., Komiyama, T., Zhu, H., & Luo, L. (2002). Representation of the glomerular olfactory map in the Drosophila brain. *Cell*, 109(2), 243–255.
- Marin, E. C., Roberts, R. J. V., Büld, L., Theiss, M., Pleijzier, M. W., Sarkissian, T., … Jefferis, G. S. X. E. (2020). Connectomics analysis reveals first, second, and third order thermosensory and hygrosensory neurons in the adult *Drosophila* brain. *BioRxiv*.
- Marin, E. C., Watts, R. J., Tanaka, N. K., Ito, K., & Luo, L. (2005). Developmentally programmed remodeling of the Drosophila olfactory circuit. *Development*, 132(4), 725–737.
- Mark, B., Lai, S.-L., Zarin, A. A., Manning, L., Pollington, H. Q., Litwin-Kumar, A., … Doe, C. Q. (2021). A developmental framework linking neurogenesis and circuit formation in the Drosophila CNS. *ELife*, 10.
- Masland, R. H. (1977). Maturation of function in the developing rabbit retina. *The Journal of Comparative Neurology*, 175(3), 275–286.

- Masse, N. Y., Turner, G. C., & Jefferis, G. S. X. E. (2009). Olfactory information processing in Drosophila. *Current Biology*, 19(16), R700-13.
- Masuda-Nakagawa, L. M., Tanaka, N. K., & O'Kane, C. J. (2005). Stereotypic and random patterns of connectivity in the larval mushroom body calyx of Drosophila. *Proceedings of the National Academy of Sciences of the United States of America*, 102(52), 19027–19032.
- Mayseless, O., Berns, D. S., Yu, X. M., Riemensperger, T., Fiala, A., & Schuldiner, O. (2018). Developmental Coordination during Olfactory Circuit Remodeling in Drosophila. *Neuron*, 99(6), 1204-1215.e5.
- Mayseless, O., Shapira, G., Rachad, E. Y., Fiala, A., & Schuldiner, O. (2023). Neuronal excitability as a regulator of circuit remodeling. *Current Biology*, 33(5), 981-989.e3.
- McCormick, L. E., & Gupton, S. L. (2020). Mechanistic advances in axon pathfinding. *Current Opinion in Cell Biology*, 63, 11–19.
- McGuire, S. E., Le, P. T., & Davis, R. L. (2001). The role of Drosophila mushroom body signaling in olfactory memory. *Science*, 293(5533), 1330–1333.
- McLaughlin, T., Torborg, C. L., Feller, M. B., & O'Leary, D. D. M. (2003). Retinotopic map refinement requires spontaneous retinal waves during a brief critical period of development. *Neuron*, 40(6), 1147–1160.
- Medioni, C., Ephrussi, A., & Besse, F. (2015). Live imaging of axonal transport in Drosophila pupal brain explants. *Nature Protocols*, 10(4), 574–584.
- Meier, M., & Borst, A. (2019). Extreme compartmentalization in a drosophila amacrine cell. *Current Biology*, 29(9), 1545-1550.e2.
- Mele, S., & Johnson, T. K. (2019). Receptor Tyrosine Kinases in Development: Insights from Drosophila. *International Journal of Molecular Sciences*, 21(1).
- Meltzer, H., Marom, E., Alyagor, I., Mayseless, O., Berkun, V., Segal-Gilboa, N., … Schuldiner, O. (2019). Tissue-specific (ts)CRISPR as an efficient strategy for in vivo screening in Drosophila. *Nature Communications*, 10(1), 2113.
- Mendoza-Garcia, P., Basu, S., Sukumar, S. K., Arefin, B., Wolfstetter, G., Anthonydhason, V., … Palmer, R. H. (2021). DamID transcriptional profiling

identifies the Snail/Scratch transcription factor Kahuli as an Alk target in the Drosophila visceral mesoderm. *Development*, 148(23).

- Mittal, A. M., Gupta, D., Singh, A., Lin, A. C., & Gupta, N. (2020). Multiple network properties overcome random connectivity to enable stereotypic sensory responses. *Nature Communications*, 11(1), 1023.
- Mochizuki, H., Toda, H., Ando, M., Kurusu, M., Tomoda, T., & Furukubo-Tokunaga, K. (2011). Unc-51/ATG1 controls axonal and dendritic development via kinesin-mediated vesicle transport in the Drosophila brain. *Plos One*, 6(5), e19632.
- Modi, M. N., Shuai, Y., & Turner, G. C. (2020). The drosophila mushroom body: from architecture to algorithm in a learning circuit. *Annual Review of Neuroscience*, 43, 465–484.
- Morey, M., Yee, S. K., Herman, T., Nern, A., Blanco, E., & Zipursky, S. L. (2008). Coordinate control of synaptic-layer specificity and rhodopsins in photoreceptor neurons. *Nature*, 456(7223), 795–799.
- Murthy, M., Fiete, I., & Laurent, G. (2008). Testing odor response stereotypy in the Drosophila mushroom body. *Neuron*, 59(6), 1009–1023.
- Nakashima, A., Ihara, N., Shigeta, M., Kiyonari, H., Ikegaya, Y., & Takeuchi, H. (2019). Structured spike series specify gene expression patterns for olfactory circuit formation. *Science*, 365(6448).
- Ng, J., Nardine, T., Harms, M., Tzu, J., Goldstein, A., Sun, Y., … Luo, L. (2002). Rac GTPases control axon growth, guidance and branching. *Nature*, 416(6879), 442–447.
- Ni, J.-Q., Markstein, M., Binari, R., Pfeiffer, B., Liu, L.-P., Villalta, C., … Perrimon, N. (2008). Vector and parameters for targeted transgenic RNA interference in Drosophila melanogaster. *Nature Methods*, 5(1), 49–51.
- Nieus, T. R., Mapelli, L., & D'Angelo, E. (2014). Regulation of output spike patterns by phasic inhibition in cerebellar granule cells. *Frontiers in Cellular Neuroscience*, 8, 246.
- O'Connor, J. T., Shannon, E. K., Hutson, M. S., & Page-McCaw, A. (2022). Mounting Drosophila pupae for laser ablation and live imaging of the dorsal thorax. *STAR Protocols*, 3(2), 101396.

- Oliva, C., Soldano, A., Mora, N., De Geest, N., Claeys, A., Erfurth, M.-L., … Hassan, B. A. (2016). Regulation of Drosophila Brain Wiring by Neuropil Interactions via a Slit-Robo-RPTP Signaling Complex. *Developmental Cell*, 39(2), 267–278.
- Ou, Y., Chwalla, B., Landgraf, M., & van Meyel, D. J. (2008). Identification of genes influencing dendrite morphogenesis in developing peripheral sensory and central motor neurons. *Neural Development*, 3, 16.
- Özkan, E., Carrillo, R. A., Eastman, C. L., Weiszmann, R., Waghray, D., Johnson, K. G., … Garcia, K. C. (2013). An extracellular interactome of immunoglobulin and LRR proteins reveals receptor-ligand networks. *Cell*, 154(1), 228–239.
- Pan, L., Zhang, Y. Q., Woodruff, E., & Broadie, K. (2004). The Drosophila fragile X gene negatively regulates neuronal elaboration and synaptic differentiation. *Current Biology*, 14(20), 1863–1870.
- Pan, X., & O'Connor, M. B. (2021). Coordination among multiple receptor tyrosine kinase signals controls Drosophila developmental timing and body size. *Cell Reports*, 36(9), 109644.
- Park, H., Yamamoto, Y., & Tanaka-Yamamoto, K. (2020). Refinement of cerebellar network organization by extracellular signaling during development. *Neuroscience*.
- Pauls, D., Selcho, M., Gendre, N., Stocker, R. F., & Thum, A. S. (2010). Drosophila larvae establish appetitive olfactory memories via mushroom body neurons of embryonic origin. *The Journal of Neuroscience*, 30(32), 10655–10666.
- Pech, U., Dipt, S., Barth, J., Singh, P., Jauch, M., Thum, A. S., … Riemensperger, T. (2013). Mushroom body miscellanea: transgenic Drosophila strains expressing anatomical and physiological sensor proteins in Kenyon cells. *Frontiers in Neural Circuits*, 7, 147.
- Pech, U., Revelo, N. H., Seitz, K. J., Rizzoli, S. O., & Fiala, A. (2015). Optical dissection of experience-dependent pre- and postsynaptic plasticity in the Drosophila brain. *Cell Reports*, 10(12), 2083–2095.

- Pecot, M. Y., Chen, Y., Akin, O., Chen, Z., Tsui, C. Y. K., & Zipursky, S. L. (2014). Sequential axon-derived signals couple target survival and layer specificity in the Drosophila visual system. *Neuron*, 82(2), 320–333.
- Perez-Orive, J., Mazor, O., Turner, G. C., Cassenaer, S., Wilson, R. I., & Laurent, G. (2002). Oscillations and sparsening of odor representations in the mushroom body. *Science*, 297(5580), 359–365.
- Perisse, E., Yin, Y., Lin, A. C., Lin, S., Huetteroth, W., & Waddell, S. (2013). Different kenyon cell populations drive learned approach and avoidance in Drosophila. *Neuron*, 79(5), 945–956.
- Perkins, L. A., Holderbaum, L., Tao, R., Hu, Y., Sopko, R., McCall, K., … Perrimon, N. (2015). The transgenic rnai project at harvard medical school: resources and validation. *Genetics*, 201(3), 843–852.
- Peters, A., & Feldman, M. L. (1976). The projection of the lateral geniculate nucleus to area 17 of the rat cerebral cortex. I. General description. *Journal of Neurocytology*, 5(1), 63–84.
- Pfeifer, K., Wolfstetter, G., Anthonydhason, V., Masudi, T., Arefin, B., Bemark, M., … Palmer, R. H. (2022). Patient-associated mutations in Drosophila Alk perturb neuronal differentiation and promote survival. *Disease Models & Mechanisms*, 15(8).
- Pitman, J. L., Huetteroth, W., Burke, C. J., Krashes, M. J., Lai, S.-L., Lee, T., & Waddell, S. (2011). A pair of inhibitory neurons are required to sustain labile memory in the Drosophila mushroom body. *Current Biology*, 21(10), 855–861.
- Plazaola-Sasieta, H., Fernández-Pineda, A., Zhu, Q., & Morey, M. (2017). Untangling the wiring of the Drosophila visual system: developmental principles and molecular strategies. *Journal of Neurogenetics*, 31(4), 231–249.
- Poon, V. Y., Klassen, M. P., & Shen, K. (2008). UNC-6/netrin and its receptor UNC-5 locally exclude presynaptic components from dendrites. *Nature*, 455(7213), 669–673.
- Pouille, F., Watkinson, O., Scanziani, M., & Trevelyan, A. J. (2013). The contribution of synaptic location to inhibitory gain control in pyramidal cells. *Physiological Reports*, 1(5), e00067.

- Puñal, V. M., Ahmed, M., Thornton-Kolbe, E. M., & Clowney, E. J. (2021). Untangling the wires: development of sparse, distributed connectivity in the mushroom body calyx. *Cell and Tissue Research*, 383(1), 91–112.
- Qiu, Q., Wu, Y., Ma, L., & Yu, C. R. (2021). Encoding innately recognized odors via a generalized population code. *Current Biology*, 31(9), 1813-1825.e4.
- Quinn, W. G., Harris, W. A., & Benzer, S. (1974). Conditioned behavior in Drosophila melanogaster. *Proceedings of the National Academy of Sciences of the United States of America*, 71(3), 708–712.
- Rabinovich, D., Mayseless, O., & Schuldiner, O. (2015). Long term ex vivo culturing of Drosophila brain as a method to live image pupal brains: insights into the cellular mechanisms of neuronal remodeling. *Frontiers in Cellular Neuroscience*, 9, 327.
- Ramaekers, A., Magnenat, E., Marin, E. C., Gendre, N., Jefferis, G. S. X. E., Luo, L., & Stocker, R. F. (2005). Glomerular maps without cellular redundancy at successive levels of the Drosophila larval olfactory circuit. *Current Biology*, 15(11), 982–992.
- Rees, C. L., Moradi, K., & Ascoli, G. A. (2017). Weighing the evidence in peters' rule: does neuronal morphology predict connectivity? *Trends in Neurosciences*, 40(2), 63–71.
- Robinow, S., & White, K. (1988). The locus elav of Drosophila melanogaster is expressed in neurons at all developmental stages. *Developmental Biology*, 126(2), 294–303.
- Rohrbough, J., & Broadie, K. (2010). Anterograde Jelly belly ligand to Alk receptor signaling at developing synapses is regulated by Mind the gap. *Development*, 137(20), 3523–3533.
- Rohrbough, J., Kent, K. S., Broadie, K., & Weiss, J. B. (2013). Jelly Belly trans-synaptic signaling to anaplastic lymphoma kinase regulates neurotransmission strength and synapse architecture. *Developmental Neurobiology*, 73(3), 189–208.
- Rubin, G. M., & Spradling, A. C. (1982). Genetic transformation of Drosophila with transposable element vectors. *Science*, 218(4570), 348–353.

- Sabado, V., & Nagoshi, E. (2018). Single-cell Resolution Fluorescence Live Imaging of Drosophila Circadian Clocks in Larval Brain Culture. *Journal of Visualized Experiments*, (131).
- Sabandal, J. M., Berry, J. A., & Davis, R. L. (2021). Dopamine-based mechanism for transient forgetting. *Nature*, 591(7850), 426–430.
- Sabatier, C., Plump, A. S., Le Ma, Brose, K., Tamada, A., Murakami, F., … Tessier-Lavigne, M. (2004). The divergent Robo family protein rig-1/Robo3 is a negative regulator of slit responsiveness required for midline crossing by commissural axons. *Cell*, 117(2), 157–169.
- Sahay, A., Wilson, D. A., & Hen, R. (2011). Pattern separation: a common function for new neurons in hippocampus and olfactory bulb. *Neuron*, 70(4), 582–588.
- Sales, E. C., Heckman, E. L., Warren, T. L., & Doe, C. Q. (2019). Regulation of subcellular dendritic synapse specificity by axon guidance cues. *ELife*, 8.
- Sanderson, J. (2023). Multi-Photon Microscopy. *Current Protocols*, 3(1), e634.
- Sanes, J. R., & Yamagata, M. (2009). Many paths to synaptic specificity. *Annual Review of Cell and Developmental Biology*, 25, 161–195.
- Sanes, J. R., & Zipursky, S. L. (2020). Synaptic specificity, recognition molecules, and assembly of neural circuits. *Cell*, 181(3), 536–556.
- Scheffer, L. K., Xu, C. S., Januszewski, M., Lu, Z., Takemura, S.-Y., Hayworth, K. J., … Plaza, S. M. (2020). A connectome and analysis of the adult Drosophila central brain. *ELife*, 9.
- Schenck, A., Bardoni, B., Langmann, C., Harden, N., Mandel, J. L., & Giangrande, A. (2003). CYFIP/Sra-1 controls neuronal connectivity in Drosophila and links the Rac1 GTPase pathway to the fragile X protein. *Neuron*, 38(6), 887–898.
- Schenck, A., Qurashi, A., Carrera, P., Bardoni, B., Diebold, C., Schejter, E., … Giangrande, A. (2004). WAVE/SCAR, a multifunctional complex coordinating different aspects of neuronal connectivity. *Developmental Biology*, 274(2), 260–270.

- Schindelin, J., Arganda-Carreras, I., Frise, E., Kaynig, V., Longair, M., Pietzsch, T., … Cardona, A. (2012). Fiji: an open-source platform for biological-image analysis. *Nature Methods*, 9(7), 676–682.
- Schneider-Mizell, C. M., Gerhard, S., Longair, M., Kazimiers, T., Li, F., Zwart, M. F., … Cardona, A. (2016). Quantitative neuroanatomy for connectomics in Drosophila. *ELife*, 5.
- Schoonover, C. E., Ohashi, S. N., Axel, R., & Fink, A. J. P. (2021). Representational drift in primary olfactory cortex. *Nature*, 594(7864), 541–546.
- Séjourné, J., Plaçais, P.-Y., Aso, Y., Siwanowicz, I., Trannoy, S., Thoma, V., … Preat, T. (2011). Mushroom body efferent neurons responsible for aversive olfactory memory retrieval in Drosophila. *Nature Neuroscience*, 14(7), 903–910.
- Seki, Y., Rybak, J., Wicher, D., Sachse, S., & Hansson, B. S. (2010). Physiological and morphological characterization of local interneurons in the Drosophila antennal lobe. *Journal of Neurophysiology*, 104(2), 1007–1019.
- Sergeeva, A. P., Katsamba, P. S., Cosmanescu, F., Brewer, J. J., Ahlsen, G., Mannepalli, S., … Honig, B. (2020). DIP/Dpr interactions and the evolutionary design of specificity in protein families. *Nature Communications*, 11(1), 2125.
- Serizawa, S., Miyamichi, K., Takeuchi, H., Yamagishi, Y., Suzuki, M., & Sakano, H. (2006). A neuronal identity code for the odorant receptor-specific and activity-dependent axon sorting. *Cell*, 127(5), 1057–1069.
- Shanbhag, S. R., Müller, B., & Steinbrecht, R. A. (2000). Atlas of olfactory organs of Drosophila melanogaster. *Arthropod Structure & Development*, 29(3), 211–229.
- Shatz, C. J., & Stryker, M. P. (1978). Ocular dominance in layer IV of the cat's visual cortex and the effects of monocular deprivation. *The Journal of Physiology*, 281, 267–283.
- Shen, J., & Maruyama, I. N. (2011). Nerve growth factor receptor TrkA exists as a preformed, yet inactive, dimer in living cells. *FEBS Letters*, 585(2), 295–299.

- Shen, K., & Bargmann, C. I. (2003). The immunoglobulin superfamily protein SYG-1 determines the location of specific synapses in C. elegans. *Cell*, 112(5), 619–630.
- Shen, K., Fetter, R. D., & Bargmann, C. I. (2004). Synaptic specificity is generated by the synaptic guidepost protein SYG-2 and its receptor, SYG-1. *Cell*, 116(6), 869–881.
- Shih, M.-F. M., Davis, F. P., Henry, G. L., & Dubnau, J. (2019). Nuclear transcriptomes of the seven neuronal cell types that constitute the drosophila mushroom bodies. *G3 (Bethesda, Md.)*, 9(1), 81–94.
- Shuster, A., Wagner, M., Pan-Doh, N., Ren, J., Grutzner, S., Beier, K., … Luo, L. (2021). The Relationship between Birth Timing, Circuit Wiring, and Physiological Response Properties of Cerebellar Granule Cells. *BioRxiv*.
- Smith, M. A.-Y., Honegger, K. S., Turner, G., & de Bivort, B. (2022). Idiosyncratic learning performance in flies. *Biology Letters*, 18(2), 20210424.
- Sood, C., Doyle, S. E., & Siegrist, S. E. (2021). Steroid hormones, dietary nutrients, and temporal progression of neurogenesis. *Current Opinion in Insect Science*, 43, 70–77.
- Sopko, R., & Perrimon, N. (2013). Receptor tyrosine kinases in Drosophila development. *Cold Spring Harbor Perspectives in Biology*, 5(6).
- Sperry, A. E., & Sen, S. E. (2001). Farnesol oxidation in insects: evidence that the biosynthesis of insect juvenile hormone is mediated by a specific alcohol oxidase. *Insect Biochemistry and Molecular Biology*, 31(2), 171–178.
- Sperry, R. W. (1963). CHEMOAFFINITY IN THE ORDERLY GROWTH OF NERVE FIBER PATTERNS AND CONNECTIONS. *Proceedings of the National Academy of Sciences of the United States of America*, 50, 703–710.
- Spletter, M. L., Liu, J., Liu, J., Su, H., Giniger, E., Komiyama, T., … Luo, L. (2007). Lola regulates Drosophila olfactory projection neuron identity and targeting specificity. *Neural Development*, 2, 14.
- Stocker, R F. (1994). The organization of the chemosensory system in Drosophila melanogaster: a review. *Cell and Tissue Research*, 275(1), 3–26.

- Stocker, R F, Lienhard, M. C., Borst, A., & Fischbach, K. F. (1990). Neuronal architecture of the antennal lobe in Drosophila melanogaster. *Cell and Tissue Research*, 262(1), 9–34.
- Stocker, Reinhard F., Heimbeck, G., Gendre, N., & de Belle, J. S. (1997). Neuroblast ablation in Drosophila P[GAL4] lines reveals origins of olfactory interneurons. *Journal of Neurobiology*.
- Stopfer, M., Jayaraman, V., & Laurent, G. (2003). Intensity versus identity coding in an olfactory system. *Neuron*, 39(6), 991–1004.
- Strausfeld, N. J., Sinakevitch, I., & Vilinsky, I. (2003). The mushroom bodies of Drosophila melanogaster: an immunocytological and golgi study of Kenyon cell organization in the calyces and lobes. *Microscopy Research and Technique*, 62(2), 151–169.
- Stute, C., Schimmelpfeng, K., Renkawitz-Pohl, R., Palmer, R. H., & Holz, A. (2004). Myoblast determination in the somatic and visceral mesoderm depends on Notch signalling as well as on milliways(mili(Alk)) as receptor for Jeb signalling. *Development*, 131(4), 743–754.
- Su, C.-Y., Menuz, K., & Carlson, J. R. (2009). Olfactory perception: receptors, cells, and circuits. *Cell*, 139(1), 45–59.
- Subach, O. M., Gundorov, I. S., Yoshimura, M., Subach, F. V., Zhang, J., Grüenwald, D., … Verkhusha, V. V. (2008). Conversion of red fluorescent protein into a bright blue probe. *Chemistry & Biology*, 15(10), 1116–1124.
- Sugie, A., Marchetti, G., & Tavosanis, G. (2018). Structural aspects of plasticity in the nervous system of Drosophila. *Neural Development*, 13(1), 14.
- Sullivan, K. G., & Bashaw, G. J. (2023). Intracellular Trafficking Mechanisms that Regulate Repulsive Axon Guidance. *Neuroscience*, 508, 123–136.
- Sweeney, L. B., Chou, Y.-H., Wu, Z., Joo, W., Komiyama, T., Potter, C. J., … Luo, L. (2011). Secreted semaphorins from degenerating larval ORN axons direct adult projection neuron dendrite targeting. *Neuron*, 72(5), 734–747.
- Sweeney, L. B., Couto, A., Chou, Y.-H., Berdnik, D., Dickson, B. J., Luo, L., & Komiyama, T. (2007). Temporal target restriction of olfactory receptor neurons by Semaphorin-1a/PlexinA-mediated axon-axon interactions. *Neuron*, 53(2), 185–200.

- Sweeney, S. T., Hidalgo, A., de Belle, J. S., & Keshishian, H. (2012). Hydroxyurea ablation of mushroom bodies in Drosophila. *Cold Spring Harbor Protocols*, 2012(2), 231–234.
- Tan, L., Zhang, K. X., Pecot, M. Y., Nagarkar-Jaiswal, S., Lee, P.-T., Takemura, S.-Y., … Zipursky, S. L. (2015). Ig superfamily ligand and receptor pairs expressed in synaptic partners in drosophila. *Cell*, 163(7), 1756–1769.
- Tanaka, N. K., Awasaki, T., Shimada, T., & Ito, K. (2004). Integration of chemosensory pathways in the Drosophila second-order olfactory centers. *Current Biology*, 14(6), 449–457.
- Tanaka, N. K., Endo, K., & Ito, K. (2012). Organization of antennal lobe-associated neurons in adult Drosophila melanogaster brain. *The Journal of Comparative Neurology*, 520(18), 4067–4130.
- Tanaka, N. K., Ito, K., & Stopfer, M. (2009). Odor-evoked neural oscillations in Drosophila are mediated by widely branching interneurons. *The Journal of Neuroscience*, 29(26), 8595–8603.
- Tanaka, N. K., Tanimoto, H., & Ito, K. (2008). Neuronal assemblies of the Drosophila mushroom body. *The Journal of Comparative Neurology*, 508(5), 711–755.
- Technau, G. M. (1984). Fiber Number in the Mushroom Bodies of Adult*Drosophila melanogaster* depends on Age, Sex and Experience. *Journal of Neurogenetics*, 1(2), 113–126.
- Tempel, B. L., Bonini, N., Dawson, D. R., & Quinn, W. G. (1983). Reward learning in normal and mutant Drosophila. *Proceedings of the National Academy of Sciences of the United States of America*, 80(5), 1482–1486.
- Thum, A. S., & Gerber, B. (2019). Connectomics and function of a memory network: the mushroom body of larval Drosophila. *Current Opinion in Neurobiology*, 54, 146–154.
- Thum, A. S., Jenett, A., Ito, K., Heisenberg, M., & Tanimoto, H. (2007). Multiple memory traces for olfactory reward learning in Drosophila. *The Journal of Neuroscience*, 27(41), 11132–11138.

- Truman, J W, & Bate, M. (1988). Spatial and temporal patterns of neurogenesis in the central nervous system of Drosophila melanogaster. *Developmental Biology*, 125(1), 145–157.
- Truman, James W, Price, J., Miyares, R. L., & Lee, T. (2023). Metamorphosis of memory circuits in Drosophila reveals a strategy for evolving a larval brain. *ELife*, 12.
- Tully, T., & Quinn, W. G. (1985). Classical conditioning and retention in normal and mutant Drosophila melanogaster. *Journal of Comparative Physiology. A, Sensory, Neural, and Behavioral Physiology*, 157(2), 263–277.
- Turner, G. C., Bazhenov, M., & Laurent, G. (2008). Olfactory representations by Drosophila mushroom body neurons. *Journal of Neurophysiology*, 99(2), 734–746.
- Tyrrell, T., & Willshaw, D. (1992). Cerebellar cortex: its simulation and the relevance of Marr's theory. *Philosophical Transactions of the Royal Society of London. Series B, Biological Sciences*, 336(1277), 239–257.
- Uçkun, E., Wolfstetter, G., Anthonydhason, V., Sukumar, S. K., Umapathy, G., Molander, L., … Palmer, R. H. (2021). In vivo Profiling of the Alk Proximitome in the Developing Drosophila Brain. *Journal of Molecular Biology*, 433(23), 167282.
- Valdes-Aleman, J., Fetter, R. D., Sales, E. C., Heckman, E. L., Venkatasubramanian, L., Doe, C. Q., … Zlatic, M. (2021). Comparative connectomics reveals how partner identity, location, and activity specify synaptic connectivity in drosophila. *Neuron*, 109(1), 105-122.e7.
- Vogt, K., Aso, Y., Hige, T., Knapek, S., Ichinose, T., Friedrich, A. B., … Tanimoto, H. (2016). Direct neural pathways convey distinct visual information to Drosophila mushroom bodies. *ELife*, 5.
- Vosshall, L B, Wong, A. M., & Axel, R. (2000). An olfactory sensory map in the fly brain. *Cell*, 102(2), 147–159.
- Vosshall, Leslie B, & Stocker, R. F. (2007). Molecular architecture of smell and taste in Drosophila. *Annual Review of Neuroscience*, 30, 505–533.

- Wan, Y., Wei, Z., Looger, L. L., Koyama, M., Druckmann, S., & Keller, P. J. (2019). Single-Cell Reconstruction of Emerging Population Activity in an Entire Developing Circuit. *Cell*, 179(2), 355-372.e23.
- Wang, Y., Guo, H.-F., Pologruto, T. A., Hannan, F., Hakker, I., Svoboda, K., & Zhong, Y. (2004). Stereotyped odor-evoked activity in the mushroom body of Drosophila revealed by green fluorescent protein-based Ca2+ imaging. *The Journal of Neuroscience*, 24(29), 6507–6514.
- Weiss, J. B., Weber, S., Marzulla, T., & Raber, J. (2017). Pharmacological inhibition of Anaplastic Lymphoma Kinase rescues spatial memory impairments in Neurofibromatosis 1 mutant mice. *Behavioural Brain Research*, 332, 337–342.
- White, J. G., Southgate, E., Thomson, J. N., & Brenner, S. (1986). The structure of the nervous system of the nematode Caenorhabditis elegans. *Philosophical Transactions of the Royal Society of London. Series B, Biological Sciences*, 314(1165), 1–340.
- Williams, M. E., de Wit, J., & Ghosh, A. (2010). Molecular mechanisms of synaptic specificity in developing neural circuits. *Neuron*, 68(1), 9–18.
- Witvliet, D., Mulcahy, B., Mitchell, J. K., Meirovitch, Y., Berger, D. R., Wu, Y., … Zhen, M. (2021). Connectomes across development reveal principles of brain maturation. *Nature*, 596(7871), 257–261.
- Wolfstetter, G., Pfeifer, K., Backman, M., Masudi, T. A., Mendoza-García, P., Chen, S., … Palmer, R. H. (2020). Identification of the Wallenda JNKKK as an Alk suppressor reveals increased competitiveness of Alk-expressing cells. *Scientific Reports*, 10(1), 14954.
- Wong, A. M., Wang, J. W., & Axel, R. (2002). Spatial representation of the glomerular map in the Drosophila protocerebrum. *Cell*, 109(2), 229–241.
- Wong, K. K. L., Li, T., Fu, T.-M., Liu, G., Lyu, C., Kohani, S., … Luo, L. (2023). Origin of wiring specificity in an olfactory map revealed by neuron type-specific, time-lapse imaging of dendrite targeting. *ELife*, 12.
- Woodling, N. S., Aleyakpo, B., Dyson, M. C., Minkley, L. J., Rajasingam, A., Dobson, A. J., … Partridge, L. (2020). The neuronal receptor tyrosine kinase Alk is a target for longevity. *Aging Cell*, 19(5), e13137.

- Xiao, Y., Deng, P., Zhao, Y., Yang, S., & Li, B. (2023). Three-photon excited fluorescence imaging in neuroscience: From principles to applications. *Frontiers in Neuroscience*, 17, 1085682.
- Xie, Q., Brbic, M., Horns, F., Kolluru, S. S., Jones, R. C., Li, J., … Li, H. (2021). Temporal evolution of single-cell transcriptomes of Drosophila olfactory projection neurons. *ELife*, 10.
- Xie, Q., Li, J., Li, H., Udeshi, N. D., Svinkina, T., Orlin, D., … Luo, L. (2022). Transcription factor Acj6 controls dendrite targeting via a combinatorial cell-surface code. *Neuron*, 110(14), 2299-2314.e8.
- Xie, Q., Wu, B., Li, J., Xu, C., Li, H., Luginbuhl, D. J., … Luo, L. (2019). Transsynaptic Fish-lips signaling prevents misconnections between nonsynaptic partner olfactory neurons. *Proceedings of the National Academy of Sciences of the United States of America*, 116(32), 16068–16073.
- Xu, C. S., Januszewski, M., Lu, Z., Takemura, S., Hayworth, K., Huang, G., … Plaza, S. M. (2020). A connectome of the adult drosophila central brain. *BioRxiv*.
- Xu, C., Theisen, E., Maloney, R., Peng, J., Santiago, I., Yapp, C., … Pecot, M. Y. (2019). Control of synaptic specificity by establishing a relative preference for synaptic partners. *Neuron*, 103(5), 865-877.e7.
- Yao, S., Cheng, M., Zhang, Q., Wasik, M., Kelsh, R., & Winkler, C. (2013). Anaplastic lymphoma kinase is required for neurogenesis in the developing central nervous system of zebrafish. *Plos One*, 8(5), e63757.
- Yasuyama, K., Meinertzhagen, I. A., & Schürmann, F.-W. (2002). Synaptic organization of the mushroom body calyx in Drosophila melanogaster. *The Journal of Comparative Neurology*, 445(3), 211–226.
- Yogev, S., & Shen, K. (2014). Cellular and molecular mechanisms of synaptic specificity. *Annual Review of Cell and Developmental Biology*, 30, 417–437.
- Zavitz, D., Amematsro, E., Borisyuk, A., & Caron, S. J. C. (2021). Connectivity patterns shape sensory representation in a cerebellum-like network. *BioRxiv*.
- Zheng, Z., Lauritzen, J. S., Perlman, E., Robinson, C. G., Nichols, M., Milkie, D., … Bock, D. D. (2018). A Complete Electron Microscopy Volume of the Brain of Adult Drosophila melanogaster. *Cell*, 174(3), 730-743.e22.

- Zhu, H., & Luo, L. (2004). Diverse functions of N-cadherin in dendritic and axonal terminal arborization of olfactory projection neurons. *Neuron*, 42(1), 63–75.
- Zhu, S., Chiang, A.-S., & Lee, T. (2003). Development of the Drosophila mushroom bodies: elaboration, remodeling and spatial organization of dendrites in the calyx. *Development*, 130(12), 2603–2610.
- Zhu, S., Lin, S., Kao, C.-F., Awasaki, T., Chiang, A.-S., & Lee, T. (2006). Gradients of the Drosophila Chinmo BTB-zinc finger protein govern neuronal temporal identity. *Cell*, 127(2), 409–422.
- Zwarts, L., Goossens, T., Clements, J., Kang, Y. Y., & Callaerts, P. (2016). Axon Branch-Specific Semaphorin-1a Signaling in Drosophila Mushroom Body Development. *Frontiers in Cellular Neuroscience*, 10, 210.

Acknowledgements

This thesis and the work involved in it would not be possible without the help and support of numerous people. First and foremost, I would like to thank my supervisor, Prof Dr. Tavosanis, who gave me the opportunity to conduct this work in her laboratory, guided the presented work through this Ph.D. thesis. I am greatful for all the support and guidance I have received from her during my PhD. I would also like to thank the whole Tavosanis lab for their help and support. In particular, thanks to Lukas and Karo for encouraging as well as sufferring through many lively discussions in and out of the lab. Thanks to Gigi and Anna for giving me clarity of thought when I was confused.

I would also like to thank Nastaran, Debbie and Rita, for their unwavering support and for helping me through quite a few personal and work crises. I am thankful for Aynur and Melas, for heavily contributing towards my mental health. Lastly but definitely not the least, a massive thank you to my parents, sister and dear friends for their constant loving support and help in navigating the ups and downs of life during the course of this chapter of my life.